AN EXPERIMENTAL INVESTIGATION OF TAYLOR'S HYPOTHESIS FOR ATMOSPHERIC BOUNDARY LAYER FLOW

by

Rodney L. Duncan

Thesis submitted to the Graduate Faculty of the

Virginia Polytechnic Institute

in partial fulfillment for the degree of

MASTER OF SCIENCE

in

MECHANICAL ENGINEERING

APPROVED:

Chairman Dr. J. B. Jones

Dr. H. L. Wood

Prof. F. J. Maher

June 1969

Blacksburg, Virginia

TABLE OF CONTENTS

LIST OF FIGURES

FIGURE PAGE

LIST OF TABLES

LIST OF SYMBOLS

$C_{\xi_1}(\tau)$	autocovariance, (feet per second)^2
$C_{\xi_1, \xi_2}(\tau)$	cross-covariance, (feet per second)^2
d	horizontal separation distance, feet
f	frequency, cycles per second
F	force, pounds
k	von Karman constant (0.4)
K	kurtosis or "flatness factor," $\sigma^4/(\sigma^2)^2$
L	scale of turbulence, feet
n	integer
p( )	probability distribution function
q	dynamic pressure, pounds per feet^2
$R_{\xi_1}(\tau)$	time correlation function
$R_{\xi_1, \xi_2}(d)$	spatial correlation function
$R_{\xi_1, \xi_2}(\tau)$	cross-correlation function
R_N	Reynolds number
S	skewness, $\sigma^3/(\sigma^2)^{3/2}$
t	time, seconds
U	longitudinal component of velocity, feet per second
$\bar{U}$	time averaged mean wind velocity, feet per second
u	longitudinal component of the turbulent velocity, feet per second
u^*	friction velocity, feet per second
V	lateral component of velocity, feet per second

v	lateral component of the turbulent velocity, feet per second
w	vertical component of the turbulent velocity, feet per second
z	height, feet
z_o	roughness length. feet
θ	wind azimuth, degrees
ν	kinematic viscosity, feet^2 per second
ξ	dummy variable
π	pi
ρ	density, pounds per feet^3
σ	standard deviation, feet per second
τ	time lag, second

Subscripts:

ew	east-west component
i	instantaneous value
ns	north-south component
p	portable tower
z	height
1	measuring station 1
2	measuring station 2

$\lvert\ \rvert$	absolute value
$\vec{\ }$	vector quantity

INTRODUCTION

Atmospheric turbulence in surface and low-altitude winds results in a number of important structural design problems to the engineer. This is especially true for the case of tall, thin structures such as smokestacks, towers and launch vehicles. This ground-wind loads problem on launch vehicles has been investigated almost totally using aeroelastic models in wind tunnels and applying techniques for predicting the full-scale load values. This approach was necessitated because of conflicting prelaunch operation requirements and by considerations for the actual flight vehicle.

Because of characteristic differences between wind-tunnel flow and atmospheric surface winds, it was uncertain that the wind-tunnel results were accurately indicative of the full-scale loads. The wind tunnel presents a uniform velocity profile and a very low-turbulence environment for the model. Atmospheric winds near the ground present a nonuniform velocity profile, due to shear flow, and turbulence values much greater than those found in wind-tunnel flow. To study and evaluate the effects of turbulence and shear flow on the response of launch vehicles, a research program utilizing a full-scale missile was initiated.

A surplus Jupiter vehicle was erected at Wallops Island, Virginia, in an attempt to correlate wind-tunnel predicted loads with the measured full-scale values. The vehicle was instrumented to obtain base bending moments and tip deflection data on the freestanding launch vehicle while it was subjected to a range of atmospheric

surface winds. The full-scale ground-wind loads program is described and initial data are presented in reference 1.

A photograph of the Jupiter vehicle on the pad at the Wallops Island site is shown in Figure 1. The missile is approximately 60 feet in length and has a base diameter of 8.75 feet. Two wind sensors, capable of sensing orthogonal horizontal wind components and following gust frequencies up to 5 cps, were installed on a mast near the Jupiter to help define the characteristics of the wind impinging on the missile. These two wind sensors were placed at heights of 13 and 53 feet above the ground and can be seen in this figure. The instruments were located upstream of the vehicle for the prevailing wind direction at Wallops Island and far enough away from the vehicle to avoid perturbed flow — on the order of five vehicle diameters. Since the wind sensors were this distance from the vehicle, the question arose as to a change in wind characteristics between measurement and impingement on the missile. One can extrapolate remote measurement along the mean wind direction using Taylor's hypothesis which considers the turbulent velocities as a fixed field transported by and at the mean wind velocity.

Under Taylor's hypothesis, a space correlation function in the direction of the mean wind can be determined from the time correlation function using the transformation $d = \bar{U}\tau$. The spatial separation, d, is measured in the direction of the mean wind, $\bar{U}$. The necessary condition for the validity of this hypothesis is that the turbulent velocities have to be much smaller than the mean wind speed; i.e.,

$u/\bar{U} \ll 1$. It was felt that this hypothesis required experimental examination for these atmospheric ground wind studies.

Along with this investigation of Taylor's hypothesis, a significant amount of information on the statistical nature of low-level atmospheric turbulence was obtained. Some of this information is presented for its own merit and some is presented for comparison with values obtained in other investigations.

Experience has shown that the local air velocities are continuous and random in nature and definable only in a statistical sense. The usefulness of expressing the properties of turbulence in statistical terms was first suggested by G. I. Taylor in 1921 (ref. 2) with three principal quantities of interest. They are (1) the relative frequency with which certain velocities occur, which is given by the probability distribution, (2) the frequency distribution of the energy contained in the wind, which is given by the power spectral density of the velocity fluctuations, and (3) the spatial correlation of the velocity fluctuations. The Gaussian distribution — a probability distribution identical to the Normal Law of Errors —generally gives an adequate description of the velocity distribution in atmospheric turbulence. On a log-log plot the spectrum of atmospheric turbulence shows no periodic motion and decreases linearly with frequency at a $-\frac{5}{3}$ slope. These properties are examined for the wind data recorded at Wallops Island. The primary area of investigation, however, concerns the spatial correlation of the gust velocities as they are being transported along by the mean wind.

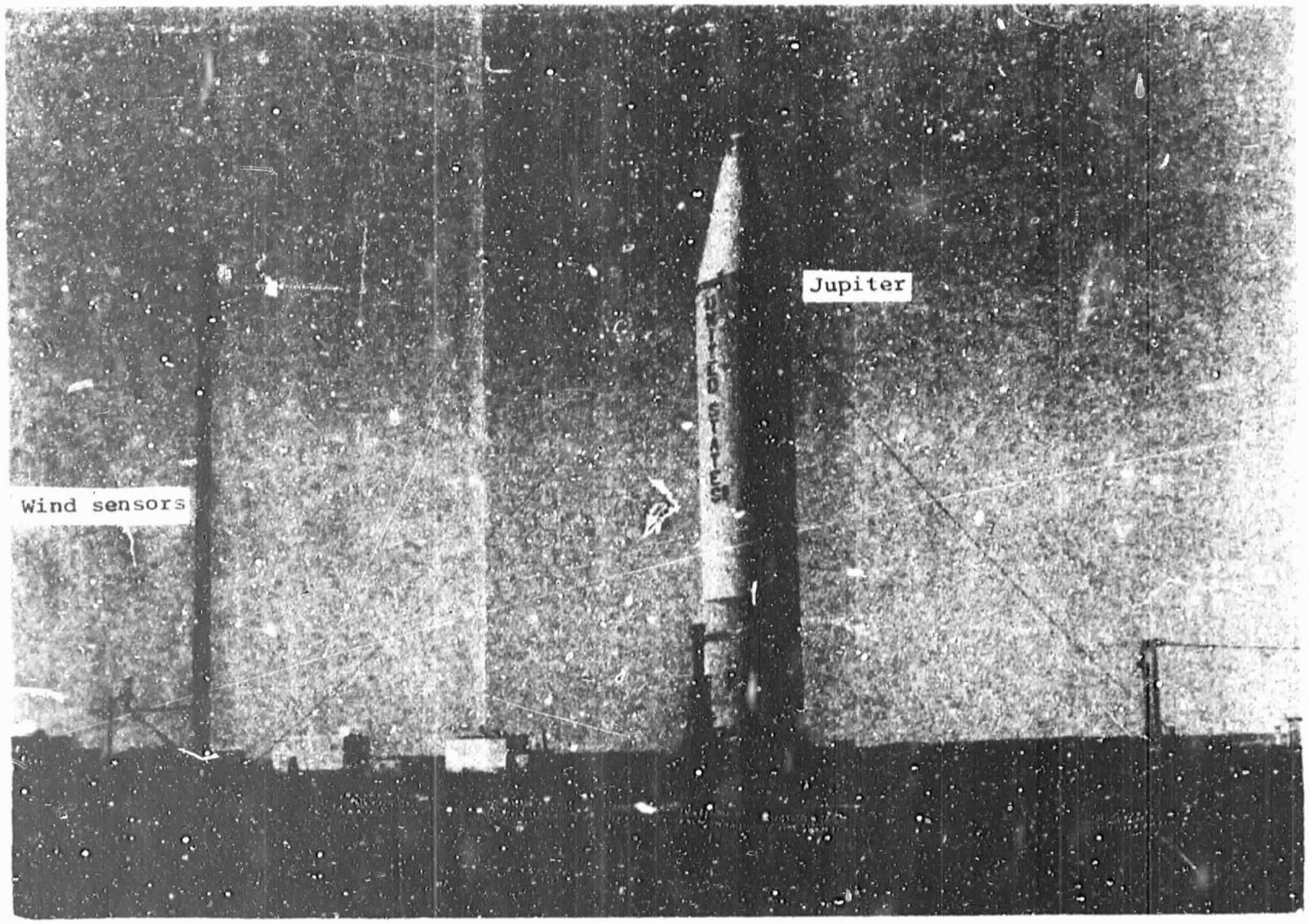

Figure 1.- Jupiter launch vehicle erected at Wallops Island.

THE REVIEW OF LITERATURE

The earliest attempts to provide a mathematical model to define turbulent flow assumed that the turbulent fluctuations consisted of discrete independent masses of fluid in random motion. The theories of this nature were developed mainly by Prandtl and resulted in the well-known mixing-length theory. It is now obvious that it was not realistic to consider discrete fluid particles which retain their identity over a certain distance. The discontinuous action implied by this theory was quite artificial, and the modern treatment of turbulence considers instead the continuous nature of the motion.

The break from the theories that represented a discontinuous motion in turbulent flow was provided by G. I. Taylor in 1921 (ref. 2). The fundamental idea lay in the recognition that the velocity should be varying continuously with time along the path of the particle.

Taylor again provided the next important advancement to the theory of the continuous nature of turbulent motion when in 1935 he considered the spatial structure of turbulence (ref. 3). This work introduced the correlation of velocities at two points as one of the describing quantities of turbulence. The statistical expression of this idea is provided by the cross-correlation function between the velocities at two points a given distance apart.

$$R_{u_1,u_2}(d) \propto \frac{\overline{u_1 u_2}}{\overline{u^2}}$$

In this expression, homogeneous turbulence is implied in that the statistical properties $R(d)$ and $\overline{u^2}$ are taken to be independent of position $(\overline{u_1^2} = \overline{u_2^2} = \overline{u^2})$.

A time correlation, $R(\tau)$, usually referred to as an auto-correlation function, may be defined in terms of the fluctuations measured at a point at instants separated by τ. If the turbulence pattern passing over a point is unchanging and is being transported by the mean wind, it follows that

$$R(\tau) = R(d)$$

when $d = \bar{U}\tau$. This relationship was provided by Taylor in 1938 in the next important advance and is known as Taylor's hypothesis (ref. 4). The necessary condition for this equivalence of time and space correlation functions through the transformation $\tau = d/\bar{U}$ is that the turbulence level in the flow be sufficiently low. The physical realization of this hypothesis is that, if the mean wind velocity is much greater than the turbulent components, the fluctuations at a point in space may be assumed to be the result of the whole turbulent field passing through that point at the velocity of the mean wind. The record of these fluctuations at a point will be nearly identical when measured along the axis of the mean wind.

In wind-tunnel studies, under the necessary condition of $\overline{u^2}/\bar{U} \ll 1$, the validity of Taylor's hypothesis has been demonstrated. The measurements of Favre, Gaviglio and Dumas (ref. 5) in a homogeneous flow indicate excellent agreement using the transformation $\tau = d/\bar{U}$ for a comparison between time and spatial correlation functions.

For atmospheric boundary layer flow the validity of the hypothesis is not quite so clear. The earliest observational data are available from an investigation by Giblett, et al., in 1932 at Cardington, England (ref. 6). These measurements were made at a height of 50 feet and provided some examples of simultaneous auto-correlations and space correlations from instruments approximately in line with the mean wind. Agreement between time and space correlation functions from these data is poor.

A comparison of measurements taken from tower and airplane recordings at heights of 90 and 120 meters, respectively, conducted by Lappe, Davidson and Notess indicated the hypothesis to be valid for the horizontal fluctuating components (ref. 7).

An examination of Taylor's hypothesis at a height of two meters over smooth unobstructed grassland was reported by Panofsky, Cramer and Rao (ref. 8). The data considered for this study was recorded when the mean wind direction was within 10° of the line of wind sensors. Their work concluded that the hypothesis is valid at this height for horizontal separation distances up to 90 meters and intensity of turbulence levels as large as 0.26.

THE EXPERIMENT

Site Description

Wallops Island, the launch site for Wallops Station, a facility of the National Aeronautics and Space Administration, is located on the Atlantic coast approximately 10 miles south of the Virginia-Maryland state line near Chincoteague, Virginia. It is comparatively flat, sparsely wooded, and sandy. The stationary tower used for measurements in this investigation was located about 300 feet from the shoreline and almost 500 feet from the nearest buildings. The surface surrounding this tower was flat and consisted of sandy soil with short grass as the only vegetation. For the high wind samples analyzed the wind came from the sea. A map of Wallops Island showing the shoreline, location of the stationary tower, and prevailing wind direction for the analyzed data is given in Figure 2.

Apparatus

The Wallops Island program obtained information on the statistical nature of atmospheric surface winds in general and the correlation of gust velocities along the mean wind vector in particular using the two-tower arrangement shown in Figure 3. A stationary tower on which four wind sensors were mounted at heights of 13 26, 39 and 53 feet above the ground was used in conjunction with a movable tower. The portable tower contained two wind sensors at heights comparable to the heights of the lower two sensors on the stationary tower (13 and 26 feet). It was desirable to cover a greater range of heights, but to do so severely limited the capability of moving the smaller tower.

Fast-response drag-sphere anemometers are shown mounted at each level.

The stationary tower is a vertical mast, circular in cross-section, approximately 75 feet in length, with a base diameter of 20 inches and a diameter of 12 inches at the highest wind sensor level. The four wind sensors alined vertically on this tower are mounted on 6-foot horizontal booms which extend from the pole toward the northwest, as illustrated in Figure 4(a). Each sensor was located three feet above its supporting boom. Nineteen markers for locating the portable tower were placed at 10° increments on an arc with a 40-foot radius from a marker directly beneath the wind sensors on the stationary tower. Each marker was identified as to its location relative to the marker below the wind sensors. For example, the marker located directly south of the reference marker was labeled 180° and the one west 270°. A diagram of this arrangement is shown in Figure 4(b).

The portable tower, shown in Figure 5, consisted of a 6-foot-square flatbed, two-wheel trailer on which a triangular structure was installed to support two wind sensors. The heights of the wind sensors on this tower were 13 and 26 feet above the surface. The trailer contained adjustable jacks and levels by which it was assured the tower was vertical and the instruments level.

The drag sphere is a Langley-developed fast response wind sensor which is able to follow gust frequencies up to 5 cps. The instrument consists of a 7-inch-diameter perforated hollow sphere mounted on a two-component force balance that senses orthogonal horizontal

components of wind force. This instrument is described more fully in references 9 and 10. In addition to fast response, the drag sphere anemometer has several other important characteristics: (1) the natural frequency of the balance (60 cps) is high compared to the gust frequencies of interest; (2) the coefficient of drag is constant and independent of Reynolds number for both steady and unsteady flow in the R_N range incurred for moderate atmospheric winds; (3) the drag force vector remains alined with the wind direction — a result of the perforations which stabilize the separation point for the flow about the sphere. Some results from measurements taken using this instrument are presented in references 10 and 11.

A Bendix-Friez Aerovane wind transmitter was located approximately 400 feet from the stationary tower and at a height of 65 feet above the ground. This instrument provided a continuous record of wind speed and direction on a Bendix-Friez strip chart recorder.

The output signals of the drag spheres were amplified, FM multiplexed, and recorded on analog magnetic tape. The multiplexing enables one to record up to five separate signals onto one tape track. To recover the data the multiplexed signals are reproduced through discriminator units which convert the frequency modulated signals back to discrete voltages.

Procedure

A typical data sampling interval was initiated by determining the prevailing wind direction from the continuous strip chart record of the Aerovane anemometer, placing the portable tower a known distance downstream of the stationary tower and recording data from all wind sensors on analog magnetic tape for a time interval of 15 minutes. The placement of the portable tower was accomplished using the markers for direction and a measuring tape for distance. Instantaneous gust velocities at two stations along the mean wind vector were thus simultaneously recorded.

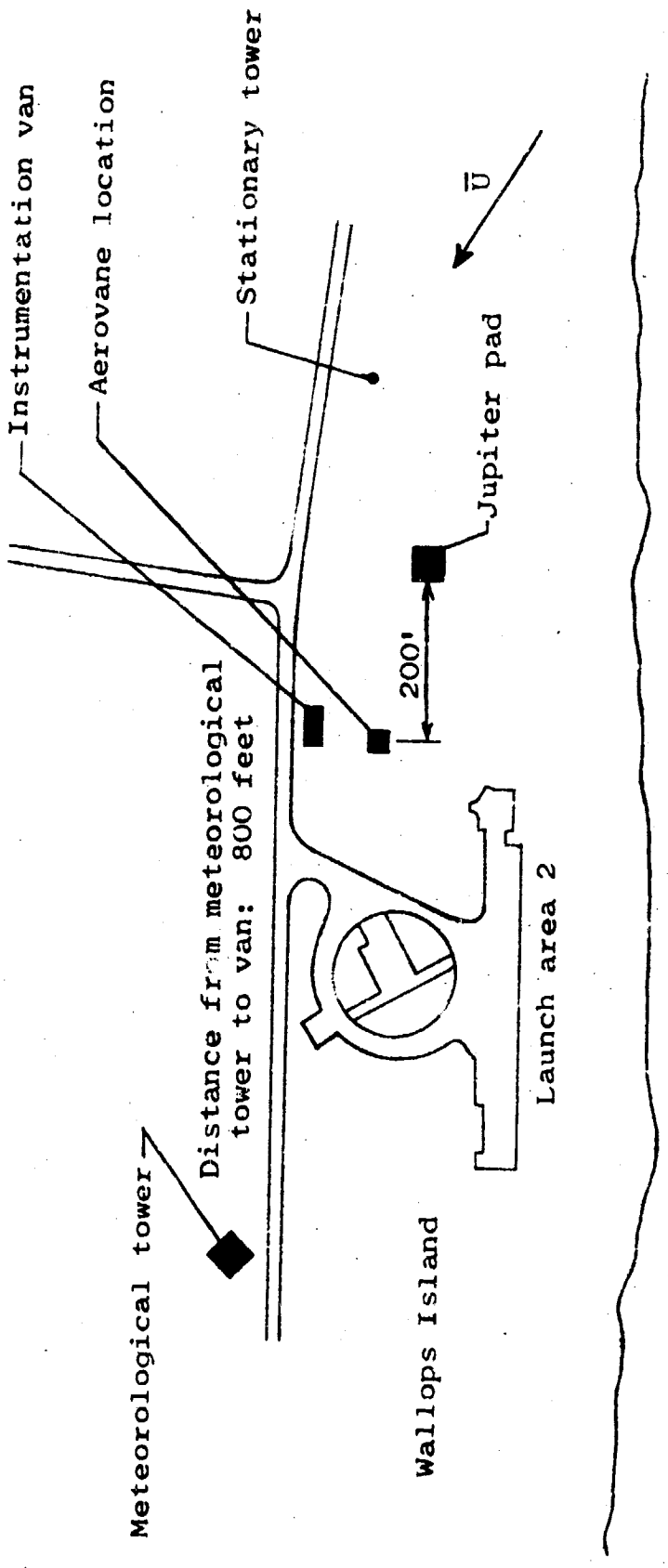

Figure 2.- Wallops Island test site.

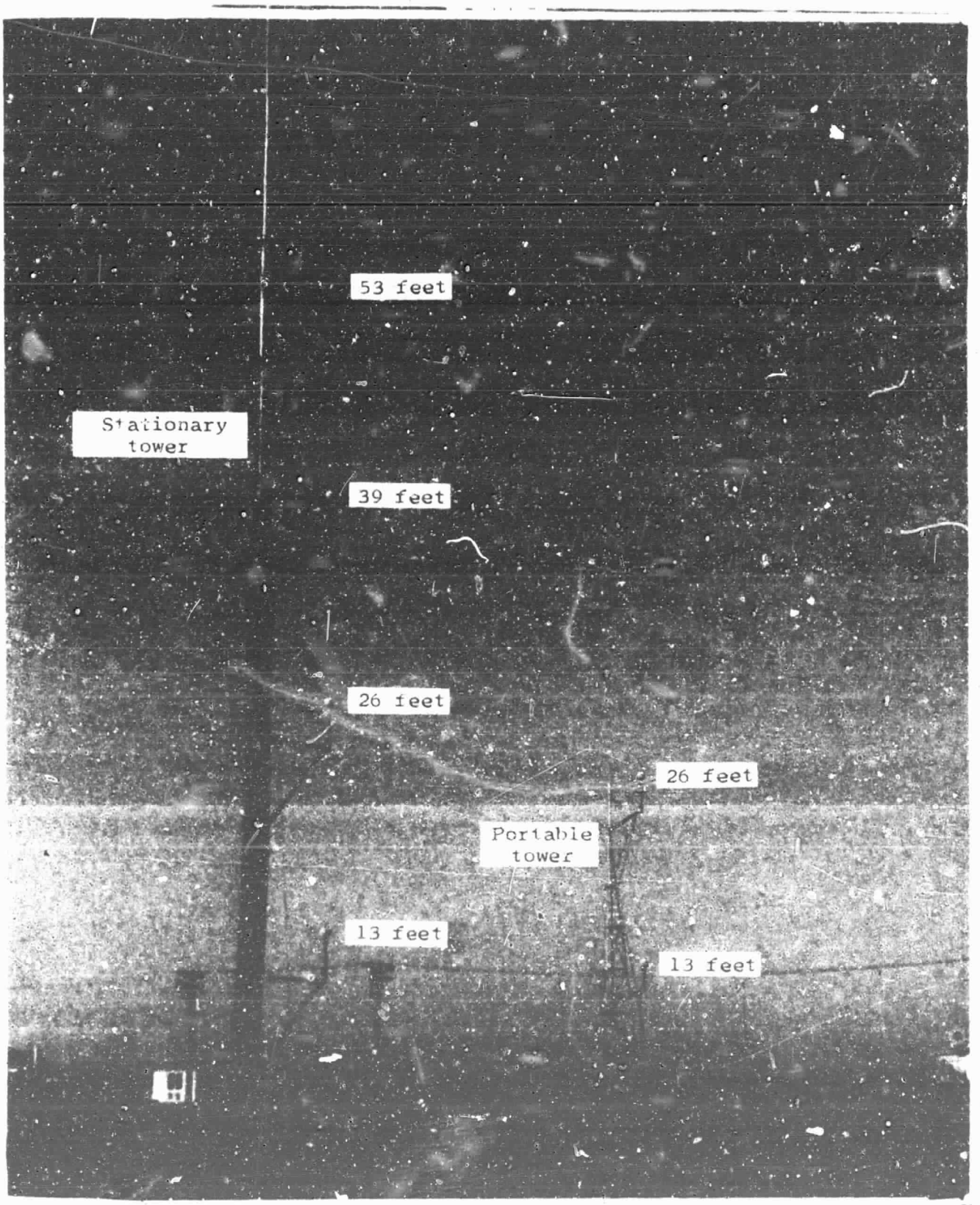

Figure 3.- Two tower arrangement for low-level turbulence measurements.

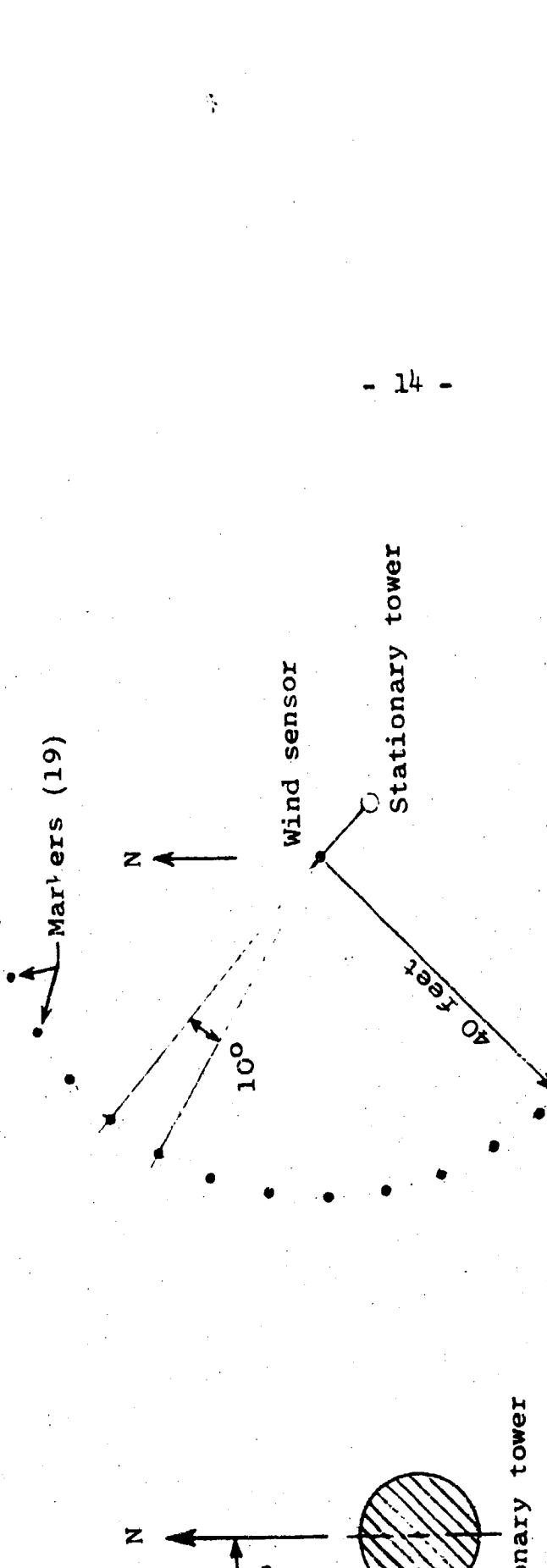

(b) Location of markers for placement of portable tower.

(a) Orientation of support boom on stationary tower.

Figure 4.- Test site description.

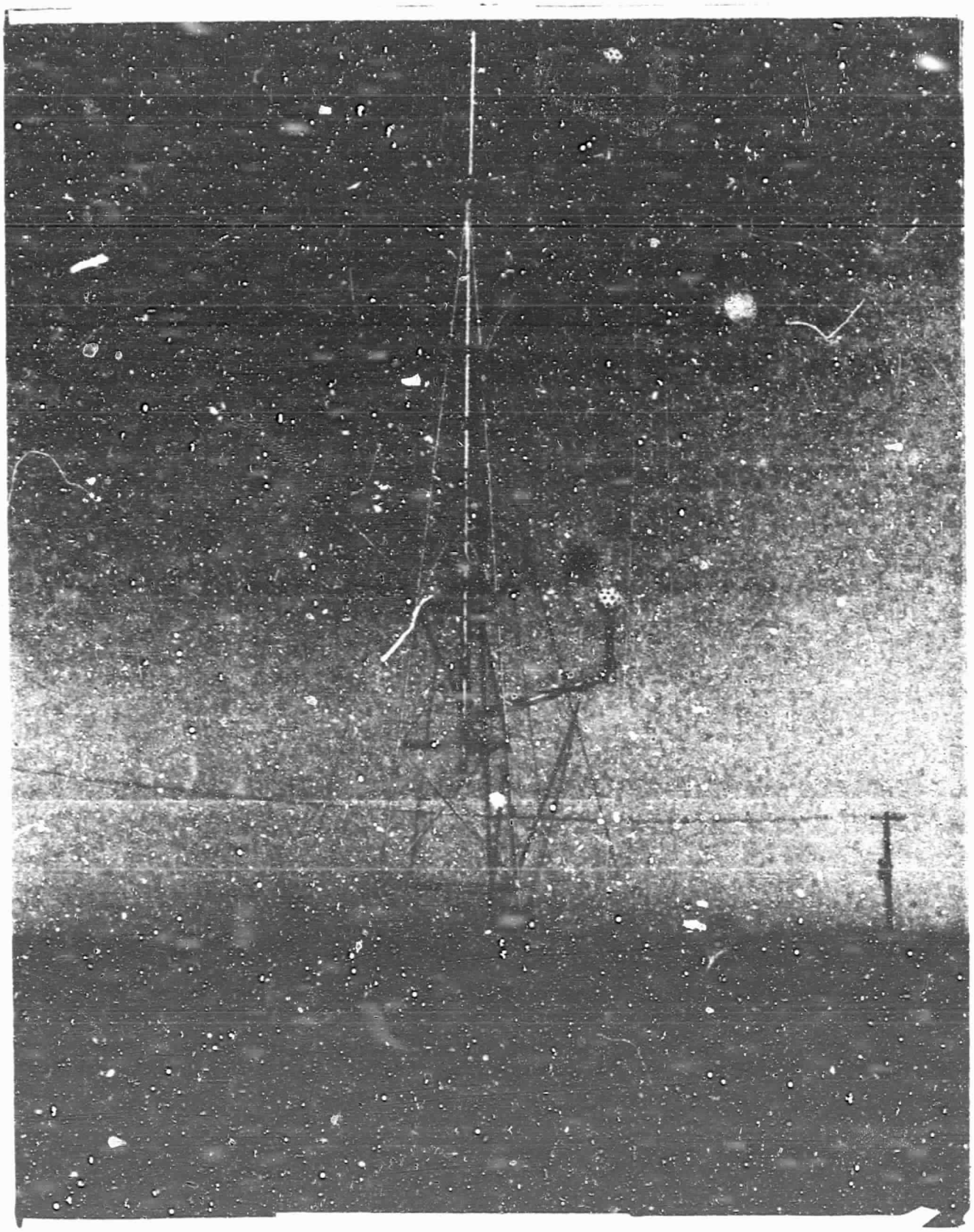

Figure 5.- Portable tower.

DATA ANALYSIS

The drag sphere anemometer measures orthogonal horizontal components of the dynamic pressures of the atmospheric winds. To determine wind direction from this instrument the orientation of the orthogonal axes has to be known. It is recommended that these sensing axes be alined north-south and east-west for field operation, and this was the orientation used at Wallops Island.

Consider an instantaneous wind vector, U_i, striking the drag sphere. U_i is made up of a time-averaged mean value, $\bar{U}$, and an instantaneous value of the fluctuations about the mean, u_i.

$$U_i = \bar{U} + u_i$$

This instantaneous wind vector strikes the drag sphere at some angle, θ_i, relative to one of its sensing axes.

A time history record of the output of the sensor gives a trace of orthogonal components of dynamic pressure, q_{ns} and q_{ew}. Before each sampling interval a zero level signal and known calibrate signal were recorded to determine the scale for the recorded wind data that followed. The procedure for laboratory calibration and field use of the drag sphere anemometer

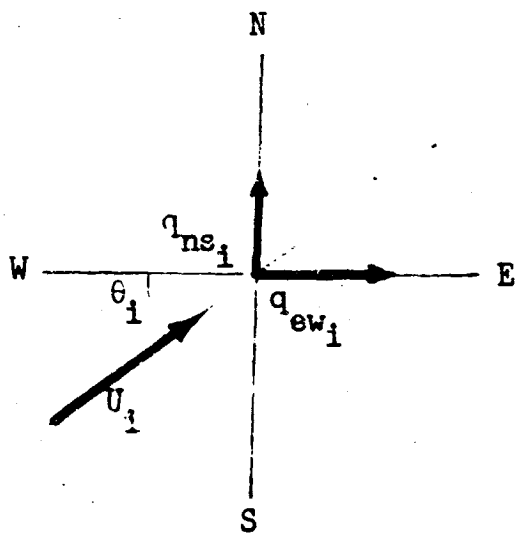

is given in the Appendix. These data were recorded on analog tape and had to be converted to digital values for computer analysis.

Analog-to-digital transformation:

analog tape sample rate = 10 samples/sec

(10 samples/sec)(15 min)(60 sec/min) = 9000 points

Thus, for q_{ns_i} and q_{ew_i}, $i = 1$ to 9000

Dynamic pressure converted to velocity:

At each sample time, t_i, there are values of q_{ns_i} and q_{ew_i} from which the magnitude and direction of the vector quantity, $\vec{q}_i$, is obtained using the following relationships:

$$|q_i| = \sqrt{q_{ns_i}^2 + q_{ew_i}^2}$$

$$\theta_i = \tan^{-1}\left(q_{ns_i}/q_{ew_i}\right)$$

$$\vec{q}_i = |q_i| \angle\theta_i$$

The conversion from dynamic pressure to velocity is given by the following equations:

$$|U_i| = \sqrt{2/\rho}\sqrt{|q_i|}$$

$$\vec{U}_i = |U_i| \angle\theta_i$$

$$U_{ns_i} = |U_i| \sin\theta_i$$

$$U_{ew_i} = |U_i| \cos\theta_i$$

The above steps are done for $i = 1 \rightarrow 9000$. The 15-minute time-average values of U and θ are given by

$$\bar{U} = \sqrt{\bar{U}_{ns}^2 + \bar{U}_{ew}^2}$$

$$\bar{\theta} = \tan^{-1}(\bar{U}_{ns}/\bar{U}_{ew})$$

where

$$\bar{U}_{ns} = \frac{1}{N} \sum_{i=1}^{N} U_{ns_i}$$

$$\bar{U}_{ew} = \frac{1}{N} \sum_{i=1}^{N} U_{ew_i}$$

and

$$N = 9000$$

The values now available are the mean wind speed, $\bar{U}$, the angle, $\bar{\theta}$, and 9000 instantaneous values of the north-south and east-west components of velocity. The objective is to determine the instantaneous values of longitudinal (inwind) and lateral (crosswind) components of velocity.

An axis rotation program using the following equations was used to give the longitudinal and lateral velocity components.

Longitudinal, U:

$$U_i = U_{ew_i} \cos \bar{\theta} + U_{ns_i} \sin \bar{\theta}$$

Lateral, V:

$$V_i = - U_{ew_i} \sin \bar{\theta} + U_{ns_i} \cos \bar{\theta}$$

This essentially creates two new time history records in units of velocity (feet per sec) with the U component alined with, and the V component 90^{o} from, the mean wind vector. From these,

$$\bar{U} = \frac{1}{N} \sum_{i=1}^{N} U_i$$

This value should be equal to $\bar{U}$ as given before axis rotation.

$$\bar{V} = \frac{1}{N} \sum_{i=1}^{N} V_i$$

The value of $\bar{V}$ should be zero when the correct $\bar{\theta}$ is used.

$$u_i = U_i - \bar{U}$$

$$v_i = V_i - \bar{V} \qquad v_i = V_i$$

u_i and v_i are the instantaneous values of the fluctuations about the mean in the longitudinal and lateral directions, respectively. The instantaneous values of these created time histories are then used for the statistical information obtained and presented in this thesis.

RESULTS

Seventeen sample intervals of 15 minutes duration each were recorded during the summer and fall of 1966 using the stationary and movable tower arrangement at Wallops Island. Seven of these sample intervals were chosen for extensive data analysis and are labeled data points one through seven for reference. The mean wind velocity as given by the Aerovane anemometer for each point is given in Figure 6(a), while the wind direction and location of the portable tower relative to the stationary tower is shown in Figure 6(b). The mean wind speeds for the seven points were between 37 (point 5) and 48.5 (point 2) fps, so a large range of mean wind speeds was not covered. These points were all recorded the same day and covered a total time interval of approximately four hours, during which time the weather did not change significantly. Therefore, the data were not influenced by changes in meteorological conditions.

The ten other recorded samples were not statistically analyzed because the wind speeds encountered while recording them were less than 20 mph. The sensitivity of the drag sphere instrument is considerably reduced at low mean wind velocities. One reason for this reduced sensitivity at low wind speeds is that the drag sphere is, as its name implies, a drag-measuring instrument and its output is thus linearly related to the square of the velocity. Because of this reduced sensitivity at low wind speeds, it was decided to analyze extensively only the samples that were recorded when the mean wind speed was above 20 mph.

The mean wind speed values as measured by the six drag sphere sensors for the seven data points are given in Table I. The letter P on the height value signifies the instruments on the portable tower. The maximum mean wind velocity measured at the 53-foot height was 49.56 fps (point 2) while the minimum was 37.84 fps (point 5). The maximum value recorded at the lowest height was 39.87 fps (point 2) and the minimum was 28.19 fps (point 5). The values in parentheses in the 53-foot level column were obtained from the strip chart recording of the Aerovane anemometer output.

The intensity of turbulence for each level is also given in Table I for the seven data points. This parameter is obtained as the ratio of the root-mean-square value (or standard deviation, σ) of the longitudinal component fluctuations to the mean wind speed. It is a numerical measure of the amount of turbulence or gustiness contained in the flow. For the Wallops Island investigation, the maximum and minimum values of this parameter were 0.183 and 0.084, respectively.

The mean wind speeds and intensities are presented as functions of height above ground in Figures 7(a) through 7(g). These plots indicate an increase in mean velocity and a decrease in intensity of turbulence with an increase in height.

There are a number of analytical representations of the atmospheric wind profile available that are valid for certain meteorological conditions (refs. 12 and 13). In the lower part of the boundary layer of the atmosphere, an exponential approximation for the mean wind speed profile is frequently used. This power law approximation is given by

$$\bar{U}_z = \bar{U}_{z_1}(z/z_1)^n$$

where

$\bar{U}_z$ = mean wind velocity at height z

$\bar{U}_{z_1}$ = mean wind velocity at height z_1

n = nondimensional quantity which depends on surface roughness and meteorological parameters

The apparent reasons for the popularity of this power law representation are that it applies over a wide variety of meteorological conditions and that it is much easier to apply than the others that are more theoretically acceptable.

Singer and Nagle (ref. 14) studied the variation of the exponent n with certain meteorological parameters such as wind speed, cloud amount, gustiness, lapse rate, time of day, and wind direction differences. They found that the values of n show a general decrease with increased wind speed up to about 20 ft/sec and then remain relatively constant. The Wallops Island data were all above this value of wind speed. Also, since the Wallops Island data were recorded in a relatively short total elapsed time, it is felt that the other meteorological parameters did not change, and therefore the value of n should be constant. This is verified by the data. A curve with the exponent $n = 0.17$ best fitted the measured values of $\bar{U}_z$ for points 1, 2, 4 and 6, while $n = 0.16$ for points 3, 5 and 7 provided the best fit. This is in agreement with other investigations of the boundary-layer profile over flat, unobstructed grassland (ref. 22).

The mean wind speeds as measured from the stationary tower are plotted along with the mean wind speed values obtained from Aerovane anemometers located on a 250-foot meteorological tower on the island in Figure 8 for points one through four. These plots are interesting for two reasons: (1) the combined data show a continuous curve, and (2) the mean wind speed is still increasing with height at the 250-foot level. A photograph of this meteorological tower, which has Aerovanes located at 50-foot intervals up to 250 feet, is shown in Figure 9.

Another form of presenting the velocity distribution in the outer region of the boundary layer is the velocity defect, $\bar{U} - \bar{U}_z$. This is the difference between the free-stream velocity, $\bar{U}$, and the velocity at a distance z above the surface. This velocity defect is normalized by u^*, the friction velocity, and presented as a function of position in the boundary layer. This form is given in reference 15 for turbulent flow in circular tubes and in reference 16 for turbulent flow over both smooth and rough plates. The form presented in reference 16 is reproduced along with the Wallops Island data in Figure 10. The distance above the surface is normalized by the boundary layer thickness. For $z/\delta < 0.15$ the data presented in reference 16 are grouped around the logarithmic relation given by

$$\frac{\bar{U} - \bar{U}_z}{u^*} = - 2.44 \ln \frac{z}{\delta} + 2.5$$

For $\frac{z}{\delta} > 0.15$ the following empirical formula describes the experimental data

$$\frac{\bar{U} - \bar{U}_z}{u^*} = 9.6 \left(1 - \frac{z}{\delta}\right)^2$$

Hinze states that apparently a value of $z/\delta = 0.15$ roughly indicates the boundary between the wall region and the outer region.

The Wallops Island data were put in this form using a boundary layer thickness of 253 feet and a free-stream mean velocity as the value measured at this height. The Wallops Island data for points one through four are closely grouped and are given by the dashed curve. The slope of this curve is in agreement with that of the other experimental data presented, but the values of the Wallops Island data are consistently lower by approximately 40 percent.

The friction velocity, u^*, mentioned previously is given by

$$u^* = \sqrt{\tau_w / \rho}$$

where

τ_w = wall stress

ρ = density

This parameter is used in the logarithmic profile approximation (ref. 17) which is given by

$$U_z = \frac{u^*}{k} \ln \frac{z + z_o}{z_o}$$

where

k = von Karman constant (0.4)

z_o = roughness length

The roughness length, z_o, is a parameter characterizing the surface roughness. It can be described as the average height of the surface roughness projections and can vary from 0.001 cm over ice (ref. 18) to several meters over cities. Using mean wind speed values from two levels on the stationary tower and solving for u^* and z_o, average values of $u^* = 3$ fps and $z_o = 5$ cm were determined for the seven data points. These values for the Wallops Island site are in agreement with the range of values for z_o given in reference 18. A $z_o = 5$ cm places it in the long grass type of surface which is characteristic of the area on and around Wallops Island.

The preceding information on profiles of wind and intensity and surface conditions was presented to describe the wind regime and environment from which the statistical parameters that follow were obtained.

Any observed sequence of values that cannot be described by an explicit mathematical relationship which gives the value of the quantity at some instant is called a random process. Therefore, since it cannot be described analytically, it must be studied and described in terms of probability statements and statistical averages. To analyze random data properly from sample time history records of finite length, it is necessary to establish three characteristics of the data. They are normality, stationarity, and randomness. All three characteristics were examined for the turbulence data recorded at Wallops Island and will be discussed at the appropriate time during the presentation of the results.

Normality.- The probability distribution defines the relative frequency with which certain values of velocity occur. The Gaussian distribution, i.e., a probability distribution identical to the Normal Law of Errors, generally gives an adequate description of the velocity distribution in atmospheric turbulence. A comparison of the Gaussian form of distribution given by

$$p(\xi) = \left(\sigma_{\xi}\sqrt{2\pi}\right)^{-1} e^{-\xi^2/2\sigma_{\xi}}$$

and the distribution of the recorded data is given in Figure 11. A comparison is made for both the longitudinal, u, and lateral, v, component of velocity for a typical sample interval. The means, $\bar{U}$ and $\bar{V}$, have been subtracted from the data so a mean value of zero on these curves corresponds to the appropriate mean value of the signal. Since the mean has been subtracted from the data, the rms value is

equal to the standard deviation and the mean-square value is equal to the variance.

$$\sqrt{\overline{u^2}} = \sigma_u$$

$$\overline{u^2} = \sigma_u{}^2$$

A visual examination of these curves shows close agreement between the measured distribution and the computed Gaussian distribution.

The moments about the mean describe the shape of the distribution and provide another check on the normality of the data. The fourth central moment when nondimensionalized by the square of the second (σ^2) is called the kurtosis, or flatness factor, and has a value of 3 for a Gaussian distribution.

$$K = \sigma^4/(\sigma^2)^2$$

The nondimensionalized third central moment is called the skewness, and if the distribution is symmetric about the mean, its value is zero.

$$\text{skewness} = \sigma^3/(\sigma^2)^{3/2}$$

The values of these moments are given in Table II and generally meet the requirements for the data to follow a normal distribution. Therefore, an assumption of a Gaussian distribution, normality of the data, for the u and v turbulent velocities appears to be valid. These values are in agreement with those obtained by Townsend and reported by Batchelor in reference 19. Townsend's work was with the u-component turbulence generated by a wire-mesh grid in a wind tunnel.

If a process is shown to be Gaussian, then the mean, the mean square, and the autocovariance function completely determine its statistical properties. The autocovariance function defined by the equation

$$C_\xi(\tau) = \lim_{T\to\infty} \frac{1}{2T} \int_{-T}^{T} \xi(t)\xi(t+\tau)\, dt$$

describes the general dependence of the values of the data at one time, t, on the values at another time, $t + \tau$. The autocovariance, $C_\xi(\tau)$, is always a real-valued, even function with a maximum value at $\tau = 0$, and may be either positive or negative. The maximum value at $\tau = 0$ is the mean-square value of the signal

$$\sigma^2 = C_\xi(\tau = 0) = \lim_{T\to\infty} \frac{1}{2T} \int_{-T}^{T} \xi(t)^2 dt$$

The autocovariance is normalized by the mean-square value to give the autocorrelation function with maximum value of unity at $\tau = 0$.

$$R_\xi(\tau) = C_\xi(\tau)/C_\xi(0)$$

The autocorrelation functions for the four levels on the stationary tower are presented in Figure 12(a) through 12(g). These correlation functions were obtained using increments of lag time, τ, of 0.1 sec and with a maximum lag time of 12 seconds. These plots exhibit a dependence on height, with the breakdown in correlation occurring more rapidly at the lower levels. This is in accordance with the "long memory" and "short memory" regions of a wind-tunnel

boundary layer as concluded from experiments by Clauser and reported in reference 21. Clauser measured the wake generated by a rod placed at two distances from the wall, but still within the boundary layer. The disturbance decayed faster at the station nearer the wall and consequently a correlation value would be less at this station for all distances downstream of the initial disturbance.

This height dependence of the autocorrelation function is also evident in a characteristic length of the atmospheric winds called the "scale of turbulence." This scale of turbulence may be considered to be a rough measure of the largest distance that two points in a turbulent field may be separated before the correlation between gust velocities becomes zero. The autocorrelation function can be used to determine this characteristic length parameter. It is given by the product of the mean wind speed and the area under the autocorrelation function curve to where the curve crosses zero. This is given by

$$L = \bar{U} \int_0^{T_0} R_u(\tau)\, d\tau$$

where T_0 = lag time at which $R_u(\tau)$ crosses zero.

Since the autocorrelation functions presented do not cross zero for the maximum lag time (12 sec), "semiscales" were computed to determine the scale of turbulence. "Semiscales," as explained in reference 17, are defined as the lag distance at which the autocorrelation function dropped to a value of 0.6. Using the approximation of integral scales as twice the semiscales, the integral scales so defined were computed by

$$L = 2\bar{U} \int_0^{T_{0.6}} R_u(\tau)\, d\tau$$

where $T_{0.6}$ = lag time at which $R_u(\tau)$ drops to a value of 0.6. The scales of turbulence are given in Table III and plotted in Figure 13.

This characteristic length appears as a parameter in a mathematical description of turbulence (ref. 20) and reference 17 reports evidence that for altitude below 1000 feet, its value is approximately equal to the altitude. For a linear approximation the scales computed from the Wallops Island data give a $L = (4 \times \text{height})$ variation for the range of heights investigated.

Homogeneity.- Figure 14 gives a comparison of the autocorrelation function at the same level as given by the instruments on both the stationary tower and the portable tower. The data are for points 5 and 6 for which the instruments were separated horizontally by 70 and 80 feet, respectively. The correlation functions for the stationary tower compare favorably with the corresponding function on the portable tower at the same height. This fact that the autocorrelation functions are essentially identical when measured at two points in space at the same height indicates homogeneity in the turbulence. Homogeneous turbulence is implied in that the statistical properties $R_u(\tau)$ and $\overline{u^2}$ are taken to be independent of position. A complete test for horizontal homogeneity would involve measurements with the portable tower located at stations about the stationary tower other than those stations directly upstream or downstream of the stationary

tower. However, for the data presented it is shown that an assumption of homogeneous turbulence along the mean wind vector is valid for bounds on distance of at least 80 feet.

Stationarity.- Another characteristic of the data to be established is to determine whether it is stationary or not. For a signal to be stationary, its probability distribution and statistical averages are not functions of the time measured. A complete proof of stationarity would involve verification that all statistical properties are invariant with time. A practical test would be to divide a single sample and examine the mean, standard deviation, and autocorrelation functions for the parts. This has been done for a representative sample interval with the time history being divided into halves. The autocorrelation functions along with the corresponding mean and standard deviation values are given in Figure 15(a) through 15(f). An examination of these functions and values indicates that the data are reasonably stationary.

Randomness.- The spectrum of the velocity fluctuations defines the frequency-wise distribution of the energy in the wind. The power spectral density function and the autocorrelation function are Fourier transform pairs for a stationary, random fluctuating quantity. These relationships are given by

$$PSD_u(f) = \frac{2}{\pi} \int_0^\infty R_u(t) \cos 2\pi f t \, dt$$

and the inverse

$$R_u(t) = \int_0^\infty PSD_u(f) \cos 2\pi ft \, df$$

The autocorrelation function and the power spectral density function provide similar information in the time domain and the frequency domain, respectively. A test for randomness in the Wallops Island data would require a check for periodic or almost periodic components in the data. The most effective procedure for detecting periodic components in the data is an examination of the power spectral density function. A periodic component would be evidenced on such a plot by a noticeable spike at a given frequency.

The power spectral density function is generally normalized by the mean-square value and this is the form presented in Figure 16(a) through 16(g). An examination of these curves shows no periodic or almost periodic components in the frequency range investigated — 0 to 5 cps. Thus, the data are random in nature. The normalized power spectra as plotted in these figures show a decrease in energy content with frequency at a slope of $-\frac{5}{3}$. This value of the slope is recognized as being valid for atmospheric turbulence spectra representations. The figures also exhibit no dependence on height for the spectra at the four levels on the stationary tower presented.

Isotropy.- Isotropic turbulence is the condition for which certain statistical properties such as the rms values of the orthogonal components, u, v, w, of the gust velocities are unaffected by rotation of the reference axes, i.e., they are equal and show no preference for

direction. The rms values of the orthogonal components measured at Wallops Island, longitudinal u and lateral v, are given in Table IV. In general, the longitudinal component is greater than the corresponding lateral component with the differences in values being on the order of 20 percent of their mean values.

The primary area of investigation during this program was, as stated previously, to examine the characteristics of the turbulent velocities of the wind as they are transported by the mean wind. A comparison of a fluctuating component at one station with its corresponding like component at another station along the mean wind vector is made by use of the cross-correlation function.

Following the same procedure as in defining the autocorrelation function, we define the cross-covariance by

$$C_{\xi_1,\xi_2}(\tau) = \lim_{T\to\infty} \frac{1}{2T} \int_{-T}^{T} \xi_1(t)\xi_2(t+\tau)\, dt$$

This relationship describes the general dependence of the values of one set of data, ξ_1, on the other, ξ_2. The cross-covariance, $C_{\xi_1,\xi_2}(\tau)$, is always a real-valued function which may be either positive or negative. Also, $C_{\xi_1,\xi_2}(\tau)$ does not necessarily have a maximum value at $\tau = 0$ as does the autocorrelation function, or is it an even function. The cross-covariance is normalized by the product of the rms values of the individual signals to give the cross-correlation function

$$R_{\xi_1,\xi_2}(\tau) = C_{\xi_1,\xi_2}(\tau)/\sqrt{\overline{\xi_1^2}\ \overline{\xi_2^2}}$$

with a maximum value of unity at some time lag. When the cross-correlation function does assume a value of unity at, for example, τ_1, it indicates that the two signals, ξ_1 and ξ_2, are perfectly correlated — identical — with one lagging the other on the time scale by τ_1. When $R_{\xi_1,\xi_2}(\tau) = 0$, the two signals are uncorrelated, and are statistically independent if this is true for all values of τ.

The cross-correlation functions were computed using the Wallops Island wind data for similar components measured at two stations along the mean wind direction. In other words, $R_{u_1,u_2}(\tau)$ and $R_{v_1,v_2}(\tau)$, where 1 and 2 refer to the stationary tower and portable tower, respectively, were computed for both the 13-foot and the 26-foot heights. The convection time, i.e., the time it requires for the mean wind to convect the fluctuating velocities, u and v, the distance between the towers, is given by $d/\overline{U}$. The maximum correlation value should occur when the lag time is equal to this convection time ($\tau = d/\overline{U}$).

The cross-correlation functions for the u component are presented in Figures 17(a) through 17(g). Figures 17(a) through 17(g) are in order of increasing separation distance between the two towers — from $d = 20$ feet to $d = 100$ feet. Each exhibits a lag time at which the correlation value peaks and this lag time to maximum correlation, τ_{max}, is compared to the convection time delay, $d/\overline{U}$, in

Figure 18. The values used to obtain this convection time delay are given in Table V. An examination of these figures indicates that the downstream signal does show a dependence on the signal measured at the upstream station which reaches a maximum at the appropriate convection time delay and this maximum dependence — or correlation — decreases with separation distance between the two measuring stations. Figures 17(a) through 17(g) also show that the correlation values are greater at the higher level instrument. This is to be expected since the intensity of turbulence profiles show a decrease with height. This is also in agreement with Clauser's "long memory" and "short memory" regions of the boundary layer.

A comparison of the time and spatial correlation values is given in Figure 19. The time correlation

$$R_{u_1}(\tau) \propto u_1(t)u_1(t+\tau)$$

is given by a representative autocorrelation function for the appropriate height. The space correlation is given by

$$R_{u_1,u_2}(d)\Big|_{\tau=0} \propto u_1(t)u_2(t)$$

where u_1 and u_2 are recorded at two stations separated by a horizontal longitudinal distance d. The spatial correlation values, as represented by the circle symbols in this figure, were obtained from the cross-correlation curves (Fig. 17) at zero lag time. Although the space correlation values are in all cases less than the corresponding time correlation value, the data show good agreement between the two functions. These figures appear quite similar to data presented by

Panofsky, Cramer and Rao in reference 8. From such data Panofsky, Cramer and Rao concluded that Taylor's hypothesis, $d = \bar{U}\tau$, is valid within the limits of their investigation.

From the Wallops Island data it appears that Taylor's hypothesis on the equivalence of time and spatial correlation functions does have some validity. The limits on the Wallops Island investigation are a horizontal separation distance of 100 feet, a height range up to 26 feet above the surface, and the intensity of turbulence in all sample intervals of less than 0.175.

A more stringent interpretation of Taylor's hypothesis would be to assume that the time history of a fluctuating velocity component does not change as it is being convected at the mean wind speed. A cross-correlation function between like components at two stations along the mean wind vector would be identical to the autocorrelation function but shifted on the time lag scale by the appropriate convection time delay. In other words, the maximum value of the cross-correlation function would be unity and it would occur on the time lag scale at $\tau = d/\bar{U}$. One would not expect this rigid interpretation of Taylor's hypothesis to be the case in atmospheric boundary layer flow. The maximum cross-correlation values from Figure 17 are plotted in Figure 20 against the appropriate separation distance. If the time histories measured at the two stations were identical, the maximum cross-correlation value would be unity and independent of separation distance. This is given by the horizontal line at a correlation value of one. The experimental data should approach unity as the separation distance goes to zero. These curves do exhibit this

characteristic with the values recorded at the 26-foot height greater in all cases than those recorded at the 13-foot height. The correlation values at a separation distance of 50 feet are low and apparently in error. The other data do decrease from unity as the separation distance increases. Therefore, this interpretation of Taylor's hypothesis, as expected, is not valid.

TABLE I.- MEAN WIND VELOCITY AND INTENSITY OF TURBULENCE.

Point	Quantity	Height, feet					
		13	26	39	53	13P	26P
1	$\bar{U}$, fps →	36.82	40.94	48.43	47.07(47.0)	38.03	40.71
	$\sigma/\bar{U}$ →	0.152	0.151	0.097	0.104	0.164	0.130
2	$\bar{U}$	39.87	43.77	50.27	49.56(48.5)	39.03	40.79
	$\sigma/\bar{U}$	.128	.113	.086	.090	.146	.114
3	$\bar{U}$	38.45	42.64	48.82	47.99(47.0)	37.53	39.52
	$\sigma/\bar{U}$	.135	.112	.084	.090	.157	.122
4	$\bar{U}$	34.90	38.68	44.83	44.64(44.0)	33.42	34.50
	$\sigma/\bar{U}$	.152	.130	.096	.103	.160	.126
5	$\bar{U}$	28.19	30.47	37.72	37.84(37.0)	28.69	29.15
	$\sigma/\bar{U}$	.160	.167	.100	.093	.163	.151
6	$\bar{U}$	30.93	34.75	41.81	42.68(42.5)	31.66	34.16
	$\sigma/\bar{U}$	.170	.162	.106	.09[illegible]	.167	.151
7	$\bar{U}$	31.19	34.26	40.91	42.60(42.5)	33.92	34.88
	$\sigma/\bar{U}$	.179	.183	.115	.101	.159	.156

TABLE II.- CENTRAL MOMENTS OF THE PROBABILITY DISTRIBUTION
FOR GAUSSIAN DISTRIBUTION: S = 0, K = 3.0

Point	Quantity	Height, feet											
		13		26		39		53		13P		26P	
		u	v	u	v	u	v	u	v	u	v	u	v
1	Skewness	-.40	0.16	-0.42	0.58	-0.20	0.20	-0.04	0.08	-0.14	0.29	-0.22	0.14
	Kurtosis	3.58	3.11	3.25	3.35	2.99	3.45	2.96	3.38	2.66	3.28	2.63	2.97
2	S	- .13	.07	- .09	.02	- .13	.21	- .24	.10	- .03	.09	.06	- .16
	K	2.96	2.93	2.87	2.95	3.21	3.52	3.25	3.21	2.81	3.60	2.82	3.02
3	S	- .10	- .08	- .16	- .07	- .15	.03	- .15	.08	.05	- .06	.10	- .32
	K	2.64	3.50	2.69	3.16	2.83	3.98	2.79	2.91	2.67	4.10	2.71	3.46
4	S	.12	- .14	- .04	.32	- .08	- .28	- .17	.01	.12	- .12	.05	- .06
	K	2.86	3.34	2.63	3.70	2.66	3.03	2.70	3.35	2.98	2.86	2.71	2.36
5	S	.03	- .19	- .25	.06	- .50	.19	- .30	- .26	.20	- .10	10	.14
	K	2.48	3.01	2.58	3.37	2.98	2.66	2.74	3.28	2.53	3.12	57	3.24
6	S	.23	- .31	- .08	- .0001	- .25	.01	.03	.13	.23	- .22	.11	.14
	K	2.67	3.08	2.52	3.47	3.24	2.62	2.98	3.82	2.74	3.29	2.52	3.16
7	S	- .03	- .23	- .13	.08	- .48	.11	- .19	- .10	- .18	.03	- .18	.34
	K	2.47	2.59	2.39	2.81	3.13	2.74	2.72	3.04	2.80	3.13	2.53	3.12

TABLE III.- SCALE OF TURBULENCE.

Point	Height, feet					
	13	26	39	53	13P	26P
1	38.28	18.22	144.89	208.67	56.45	112.34
2	47.60	79.23	119.47	146.52	29.91	42.29
3	51.50	99.37	115.85	155.07	38.93	51.87
4	57.12	151.74	254.82	240.60	29.80	58.16
5	44.34	74.13	132.71	227.51	43.41	54.52
6	47.16	62.95	122.33	170.06	43.02	65.96
7	56.00	72.45	103.19	184.14	64.97	117.02

TABLE IV.- RMS VALUES OF THE LONGITUDINAL AND LATERAL FLUCTUATING VELOCITIES
(VALUES IN TABLE IN UNITS OF FPS)

Height		Data points						
		1	2	3	4	5	6	7
13'	u	5.59	5.12	5.19	5.29	4.52	5.27	5.59
	v	4.49	4.01	4.03	3.72	3.42	3.50	4.23
26'	u	6.18	4.93	4.77	5.03	5.10	5.64	6.29
	v	5.03	4.24	4.15	3.43	2.86	3.11	3.79
39'	u	4.69	4.34	4.11	4.29	3.77	4.43	4.69
	v	3.66	3.47	3.38	3.57	3.61	3.87	4.64
53'	u	4.92	4.45	4.31	4.59	3.53	4.03	4.32
	v	3.31	3.51	3.75	3.19	2.67	2.96	3.66
13'P	u	6.23	5.72	5.91	5.34	4.68	5.30	5.41
	v	3.85	3.79	3.71	3.88	3.14	3.80	4.04
26'P	u	5.28	4.64	4.83	4.34	4.41	5.16	5.44
	v	4.07	4.31	4.51	5.08	3.45	3.73	4.26

TABLE V.- COMPARISON OF CONVECTION TIME WITH TIME LAG TO MAXIMUM CORRELATION.

Point	Height, feet	$\bar{U}_z$	$\frac{\bar{U}_z + \bar{U}_{zp}}{2}$	$d/\bar{U}$, sec	$\tau_{max.}$	$R_{u_1,u_2}(\tau_{max.})$
1 (d = 50')	13	36.82	37.42	1.34	1.6	0.499
	13P	38.03				
	26	40.94	40.82	1.25	1.2	.548
	26P	40.71				
2 (d = 40')	13	39.87	39.45	1.01	1.0	.727
	13P	39.03				
	26	43.77	42.28	.94	.9	.755
	26P	40.79				
3 (d = 30')	13	38.45	37.99	.79	.8	.763
	13P	37.53				
	26	42.64	41.06	.73	.7	.785
	26P	39.52				
4 (d = 20')	13	34.90	34.16	.59	.6	.739
	13P	33.42				
	26	38.42	36.50	.55	.6	.796
	26P	34.58				
5 (d = 70')	13	28.19	28.44	2.46	2.4	.545
	13P	28.69				
	26	30.47	29.81	2.34	2.3	.681
	26P	29.15				
6 (d = 80')	13	30.93	31.30	2.56	2.9	.475
	13P	31.66				
	26	34.75	34.46	2.32	2.4	.672
	26P	34.16				
7 (d = 100')	13	31.19	32.60	3.06	4.3	.350
	13P	33.92				
	26	33.62	34.25	2.92	2.7	.565
	26P	34.88				

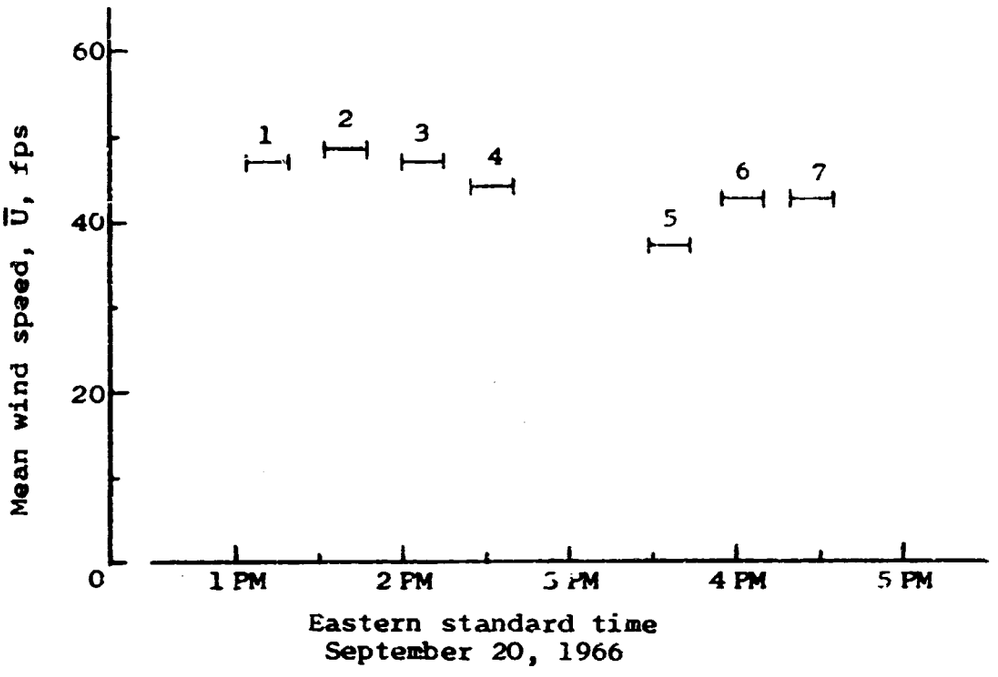

(a) Mean wind speed variation during time interval in which points 1-7 were recorded.

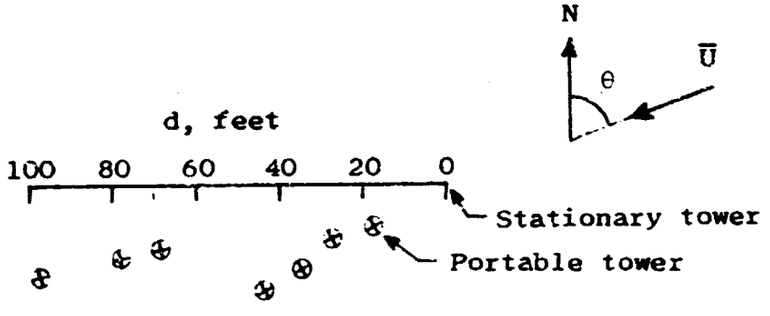

Point	θ, deg	d, ft
1	65	50
2	65	40
3	70	30
4	65	20
5	80	70
6	80	80
7	80	100

(b) Location of portable tower relative to stationary tower.

Figure 6.- Test conditions.

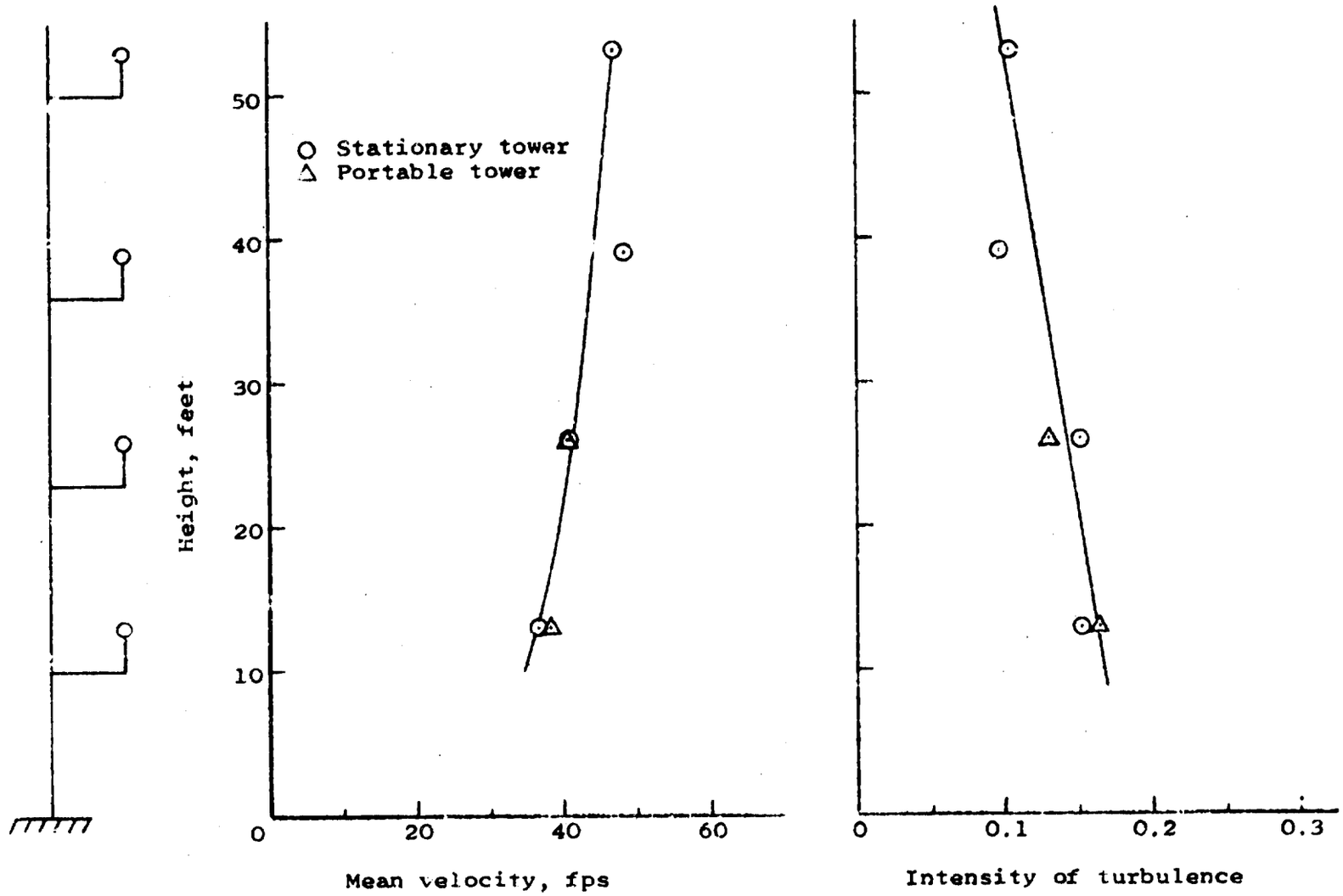

(a) Point 1.

Figure 7.- Profiles of mean wind velocity and intensity of turbulence up to 53 feet above the ground.

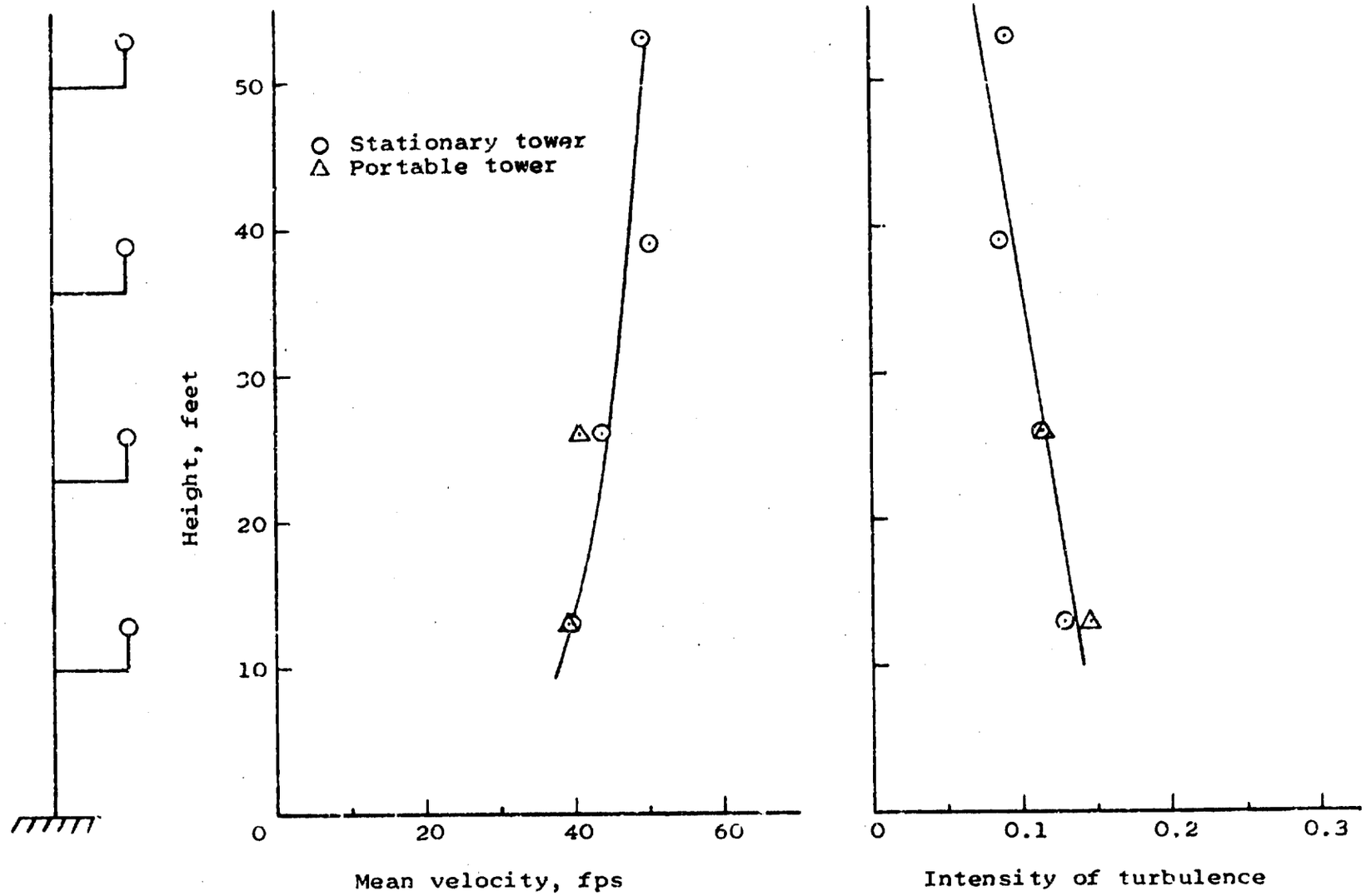

(b) Point 2.

Figure 7.- Continued.

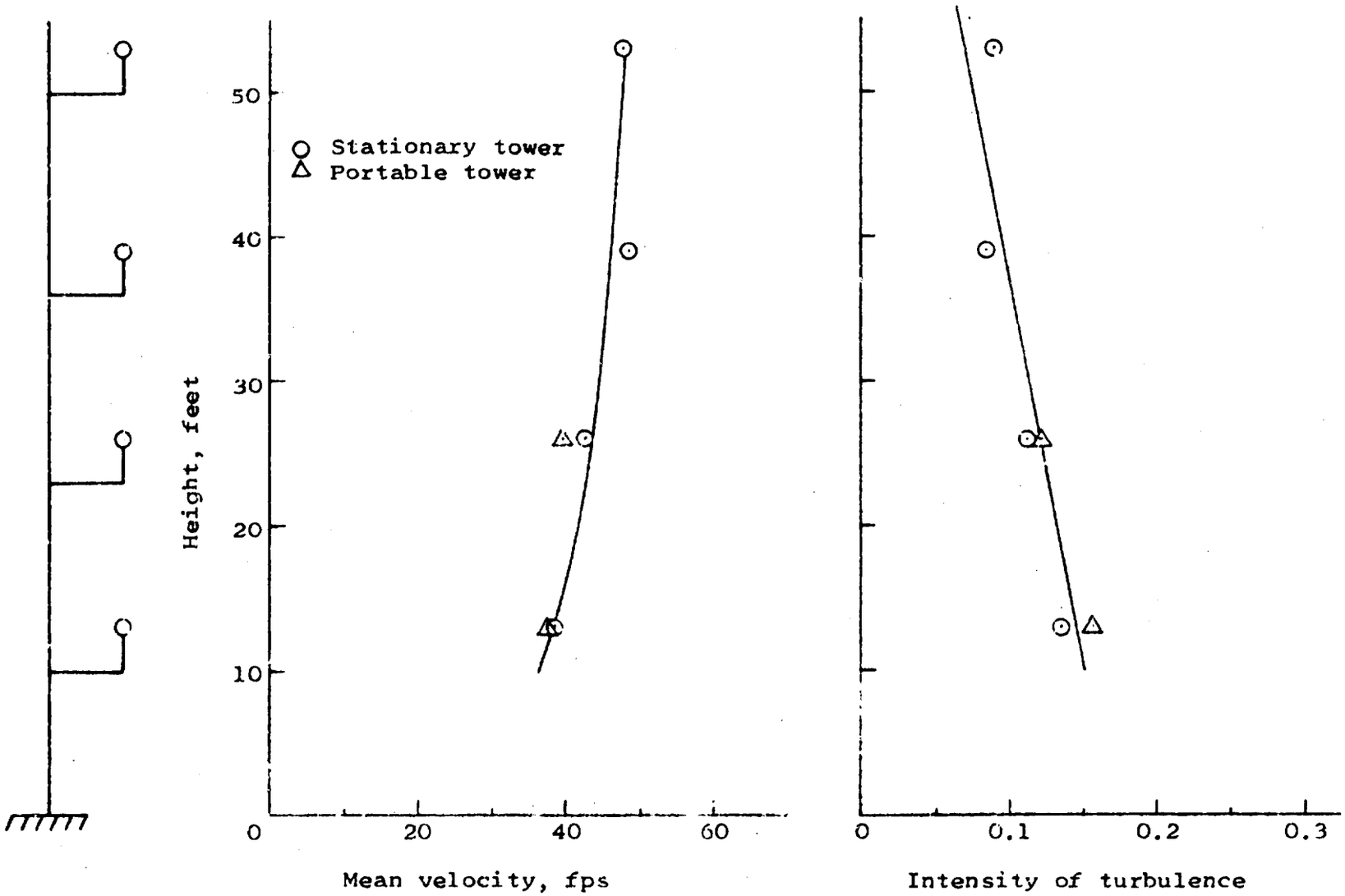

(c) Point 3.

Figure 7.- Continued.

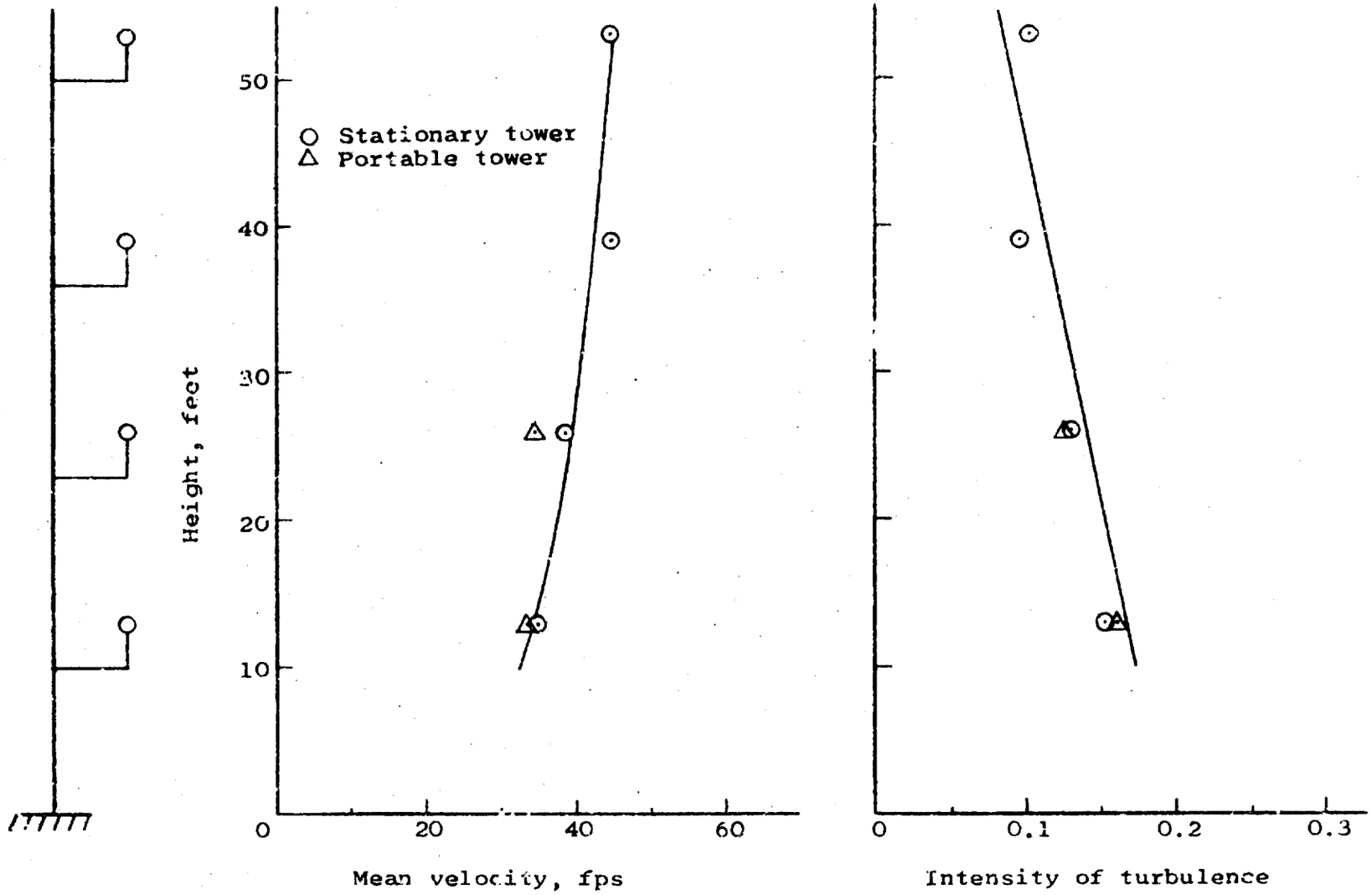

(d) Point 4.

Figure 7.- Continued.

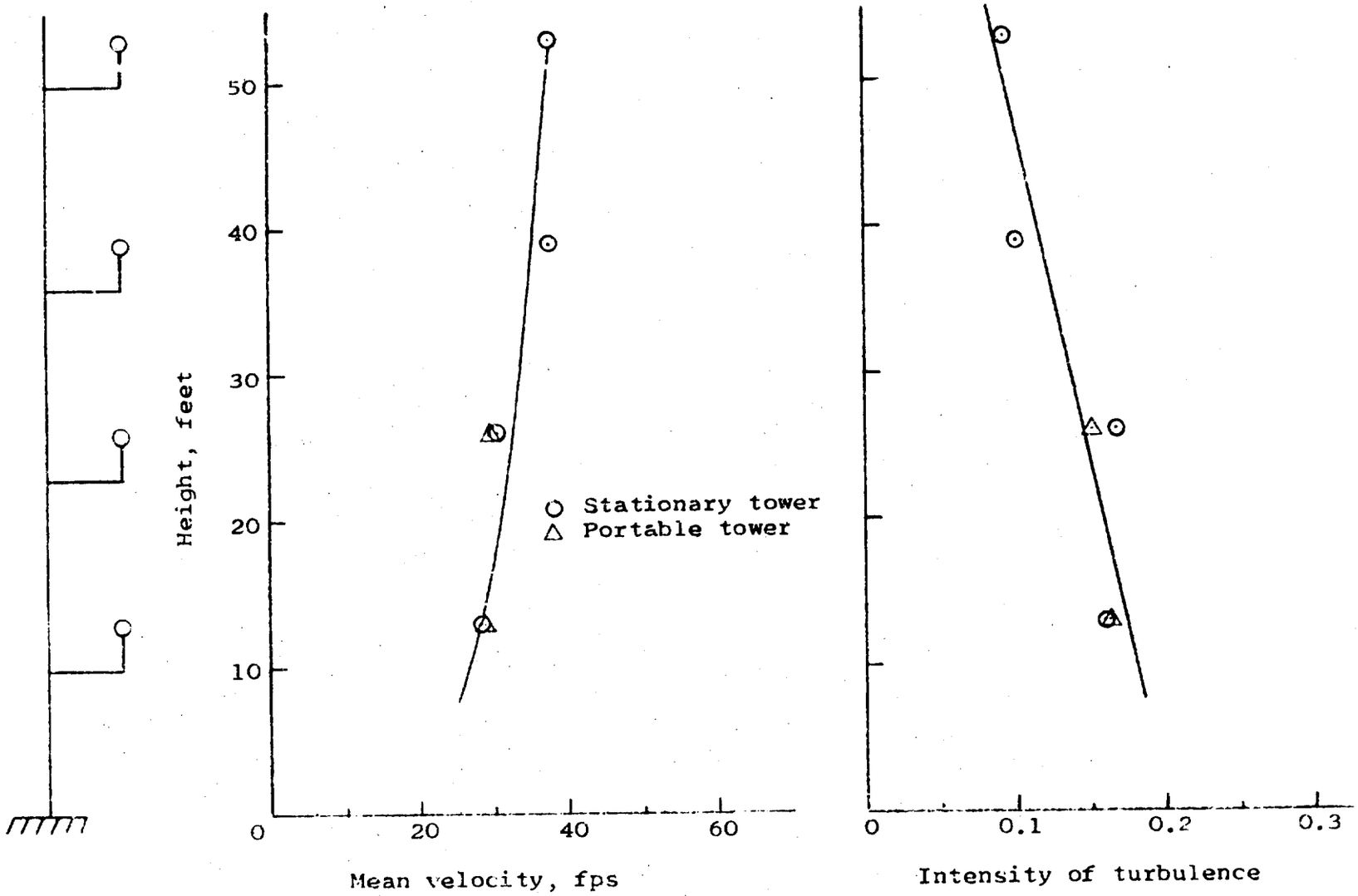

(e) Point 5.

Figure 7.- Continued.

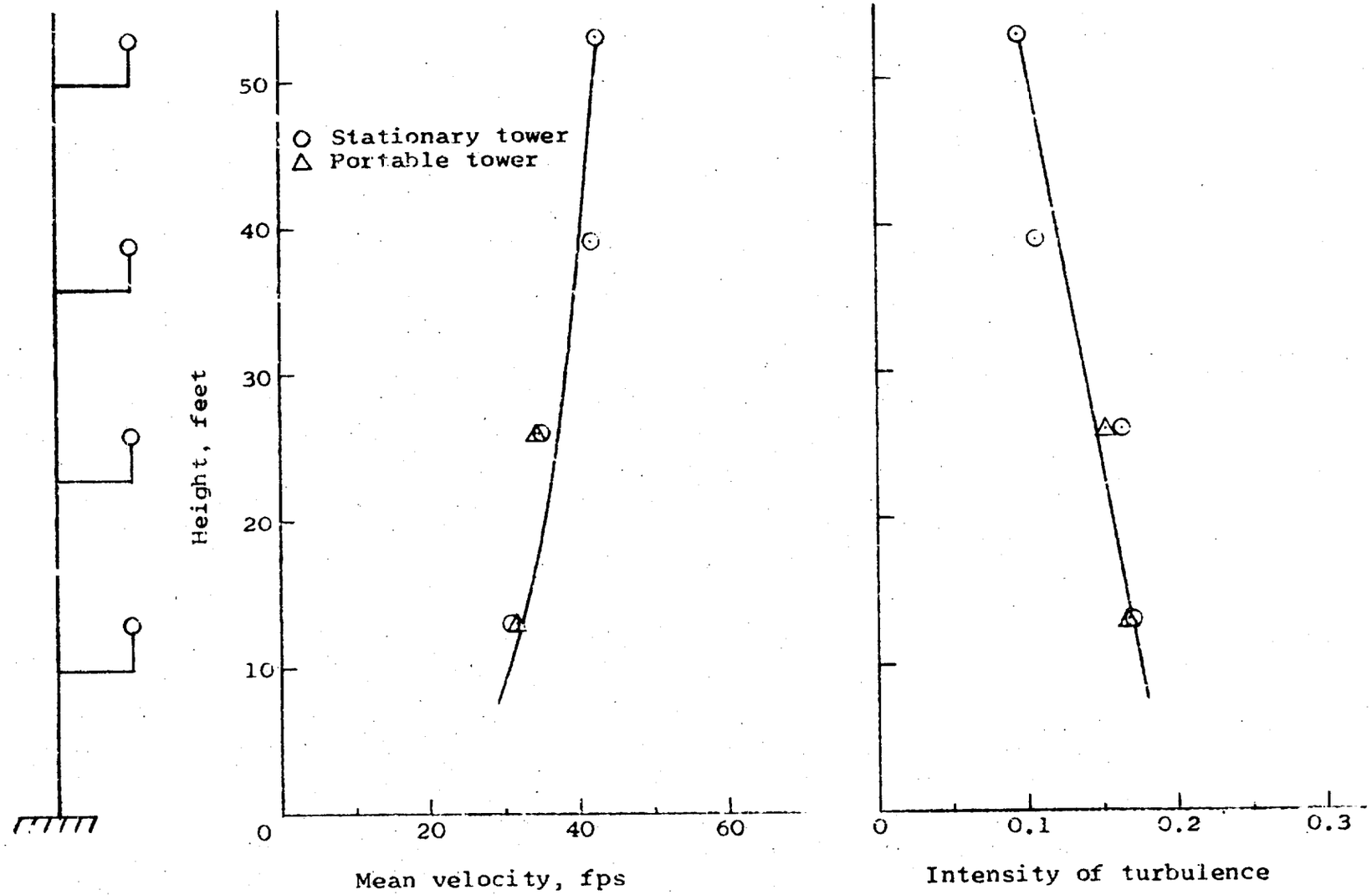

(f) Point 6.

Figure 7.- Continued.

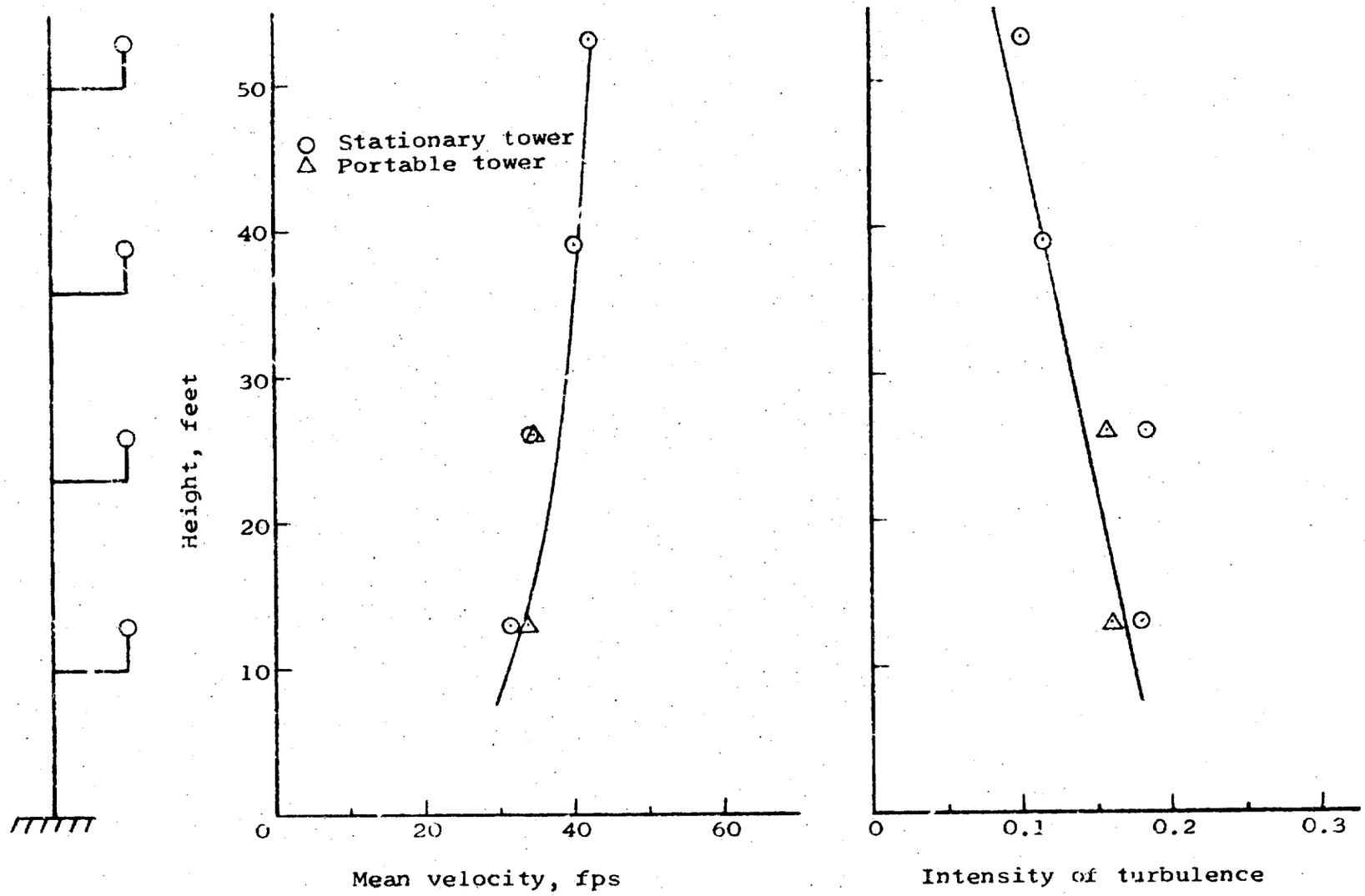

(g) Point 7.

Figure 7.- Concluded.

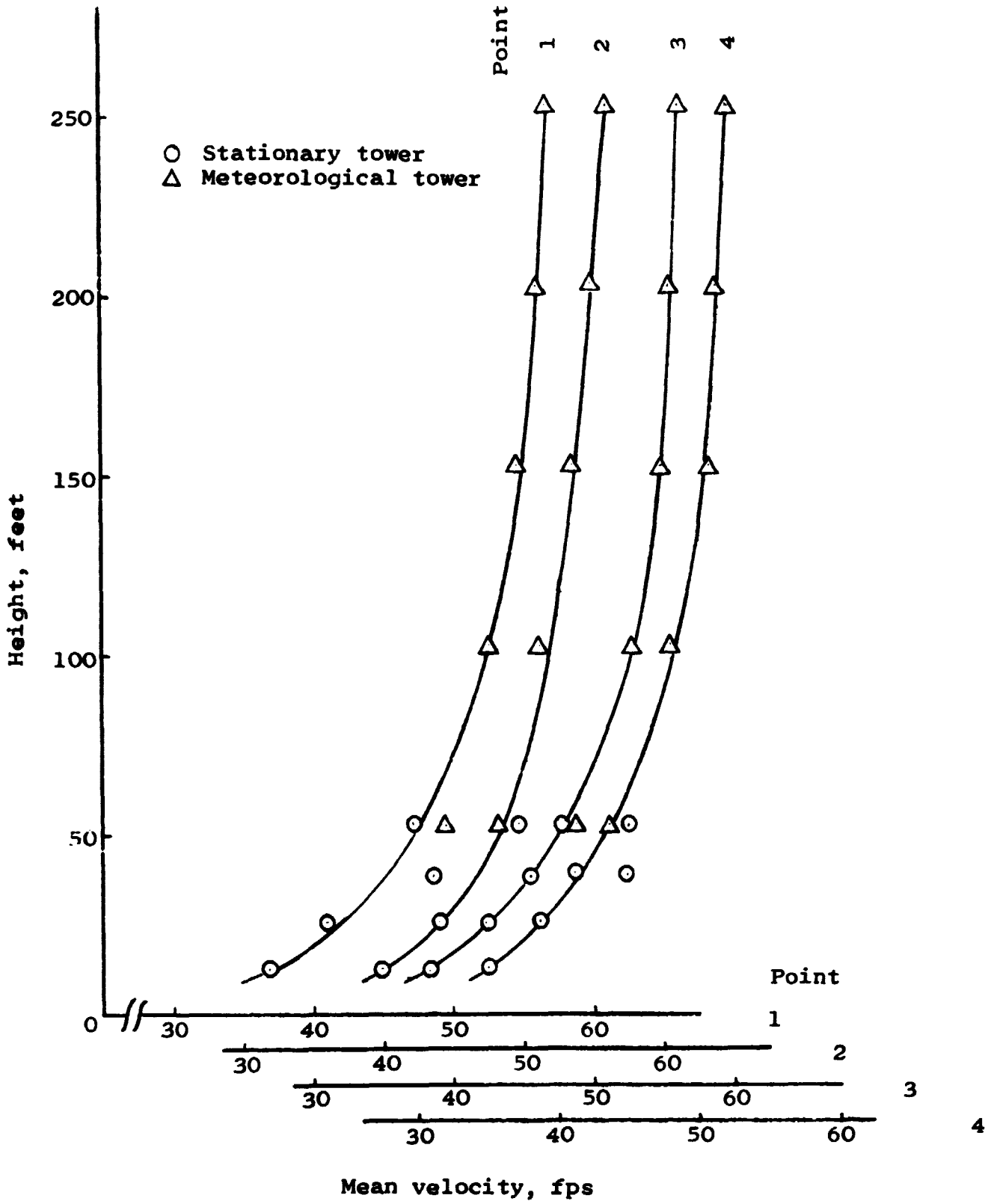

Figure 8.- Comparison of mean wind velocity profiles as measured on stationary tower and 250-foot meteorological tower.

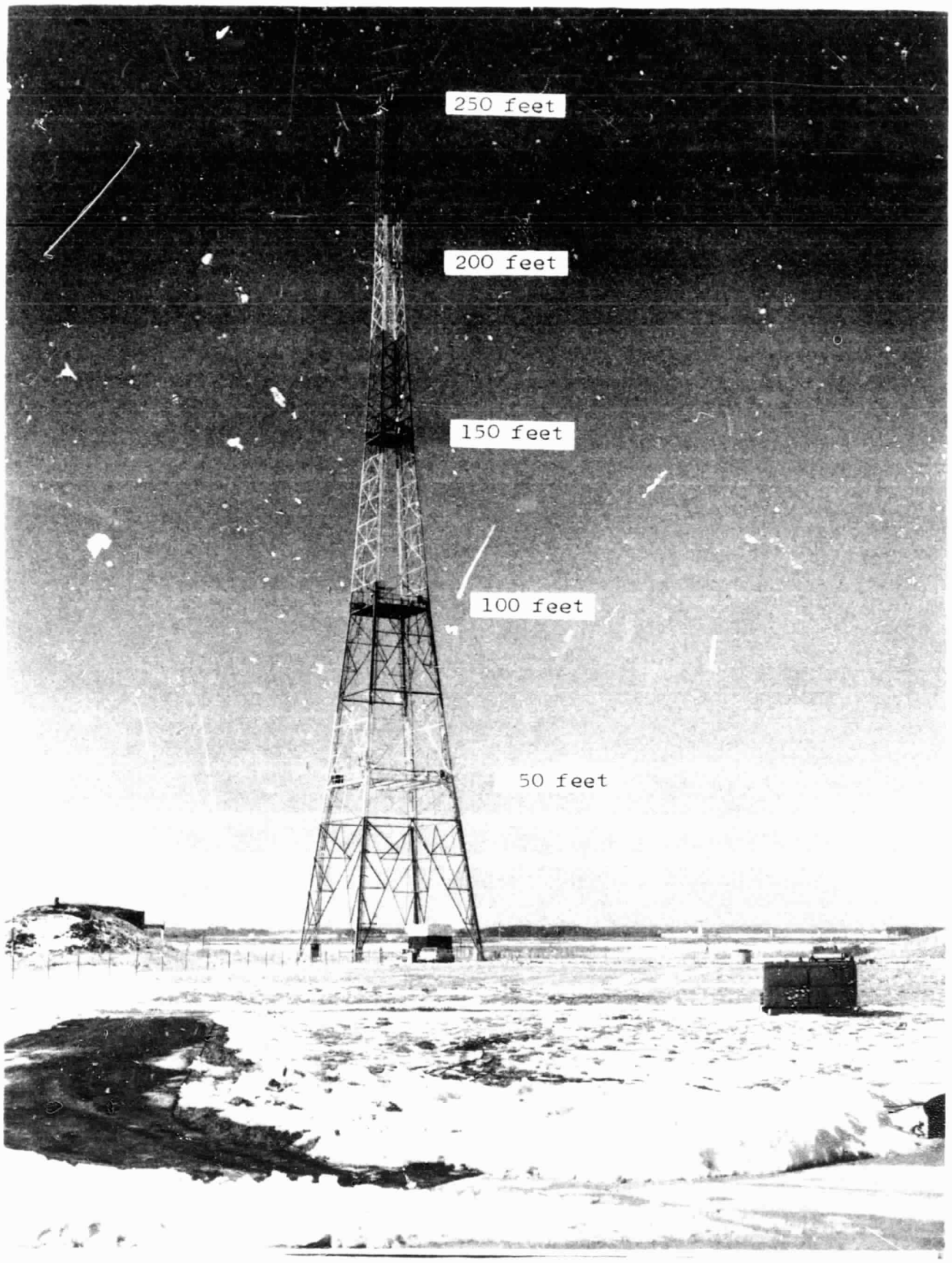

Figure 9.- Wallops Island 250-foot meteorological tower.

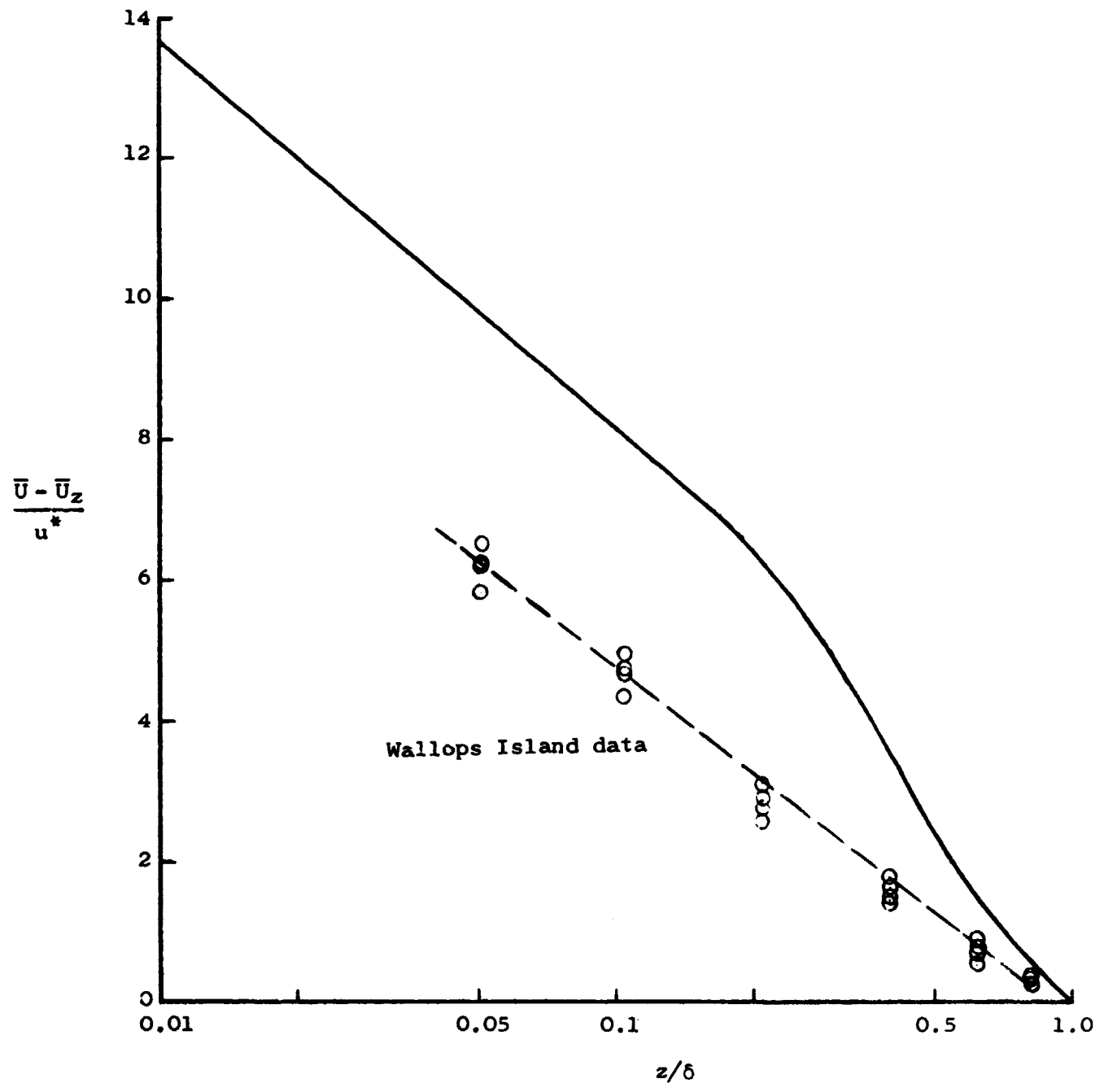

Figure 10.- Velocity defect in the boundary layer.

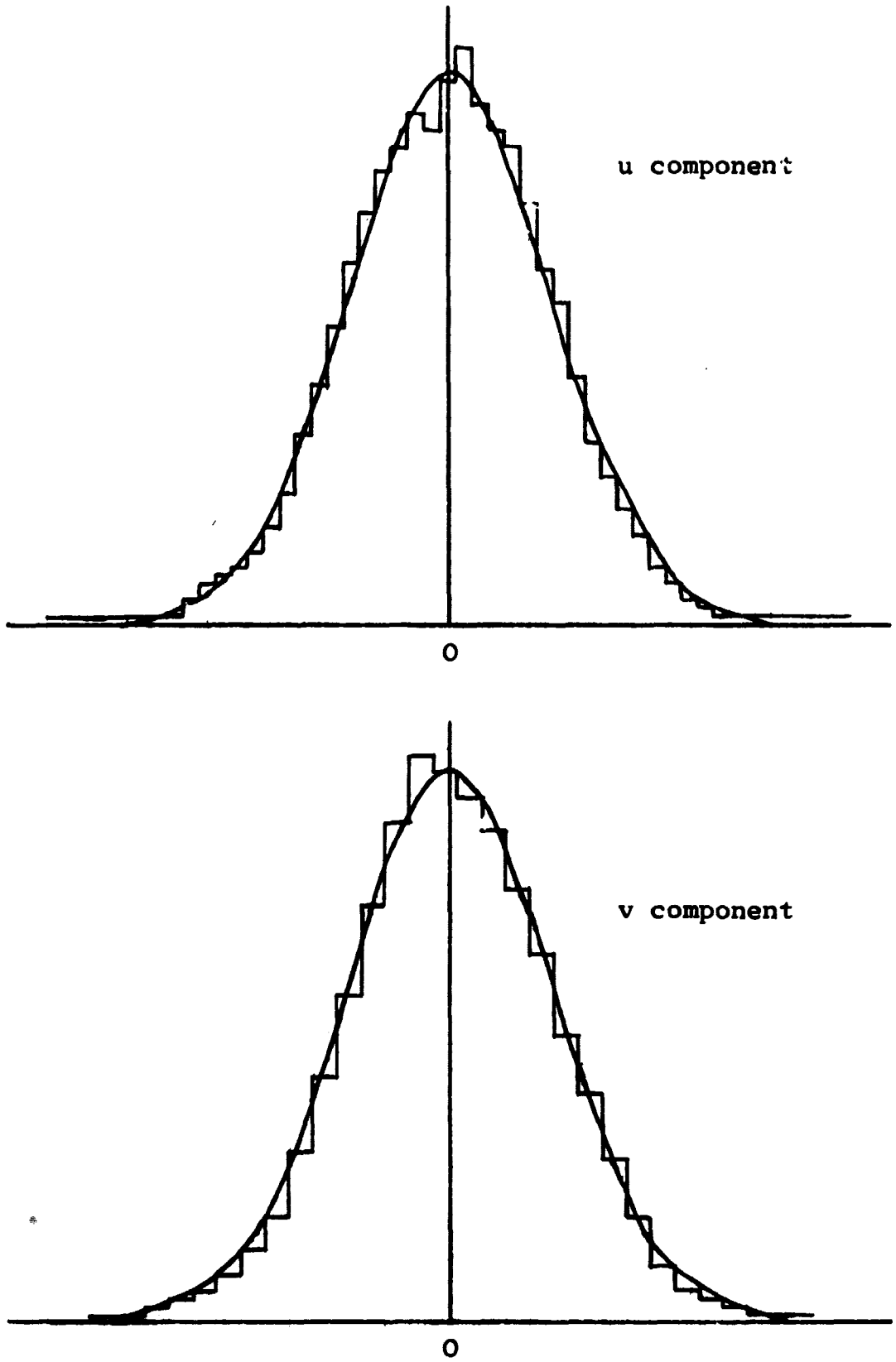

Figure 11.- Comparison of the measured probability distribution of the gust velocities with a Gaussian distribution.

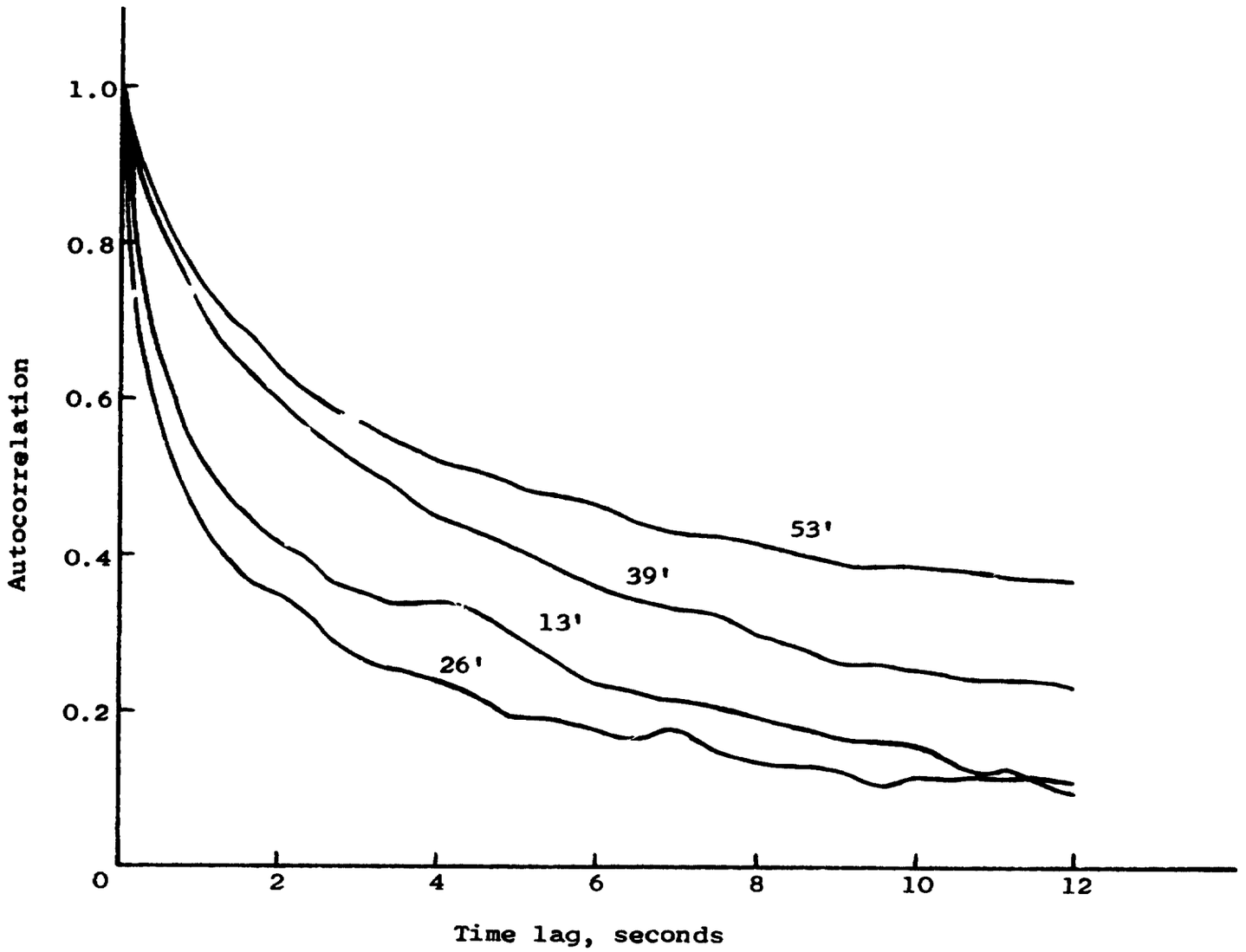

(a) Point 1.

Figure 12.- Autocorrelation function variation with height above the surface.

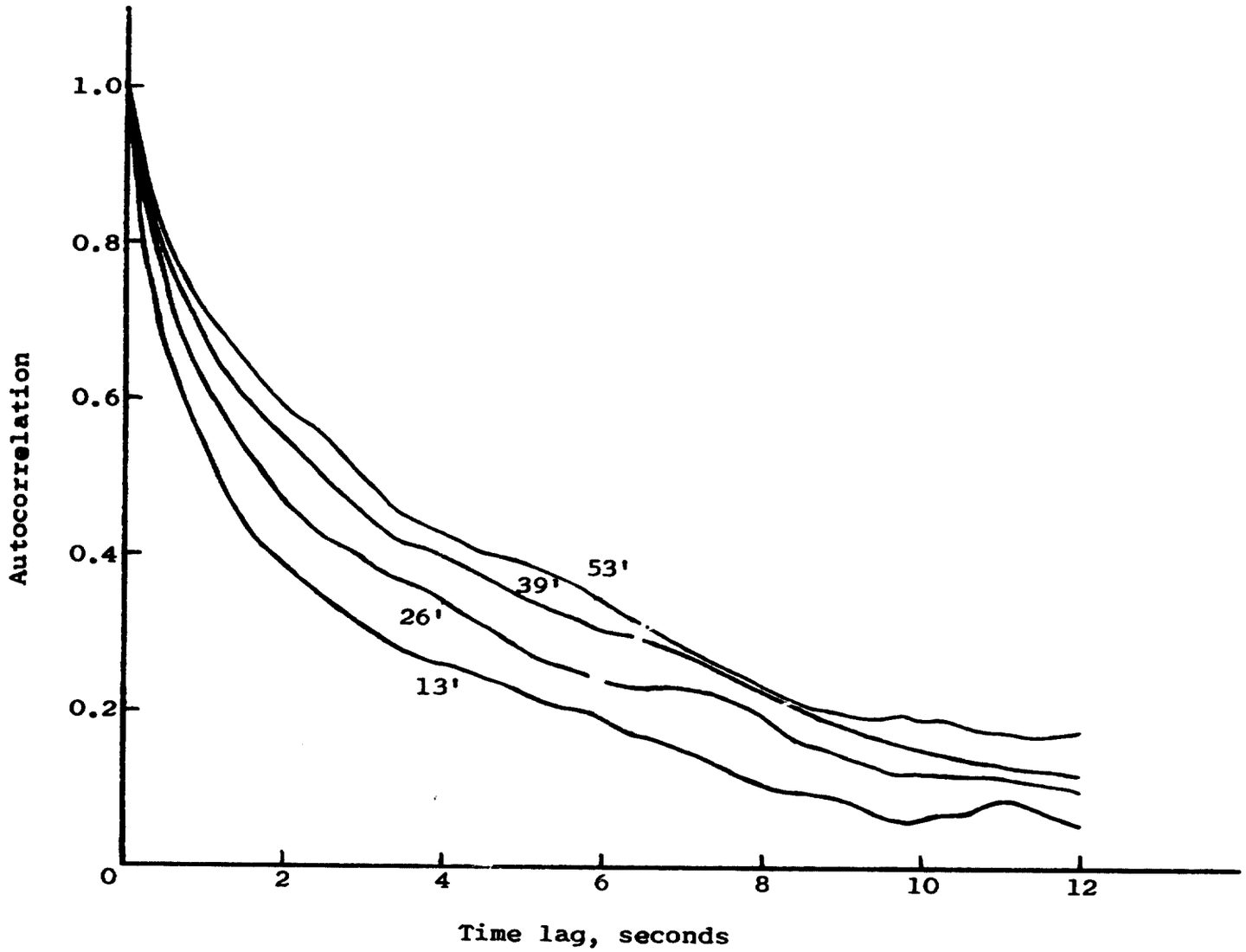

(b) Point 2.

Figure 12.- Continued.

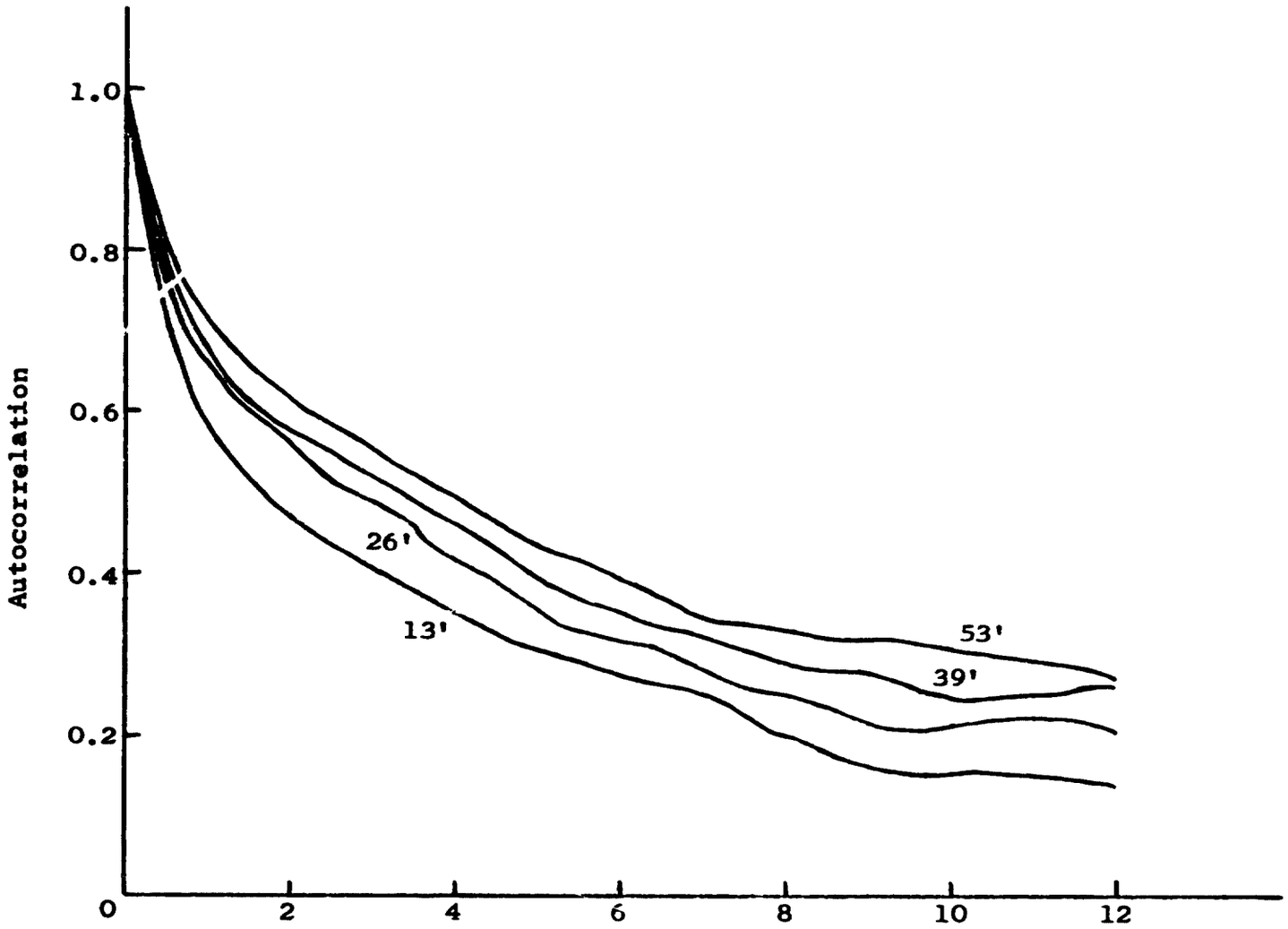

(c) Point 3.

Figure 12.- Continued.

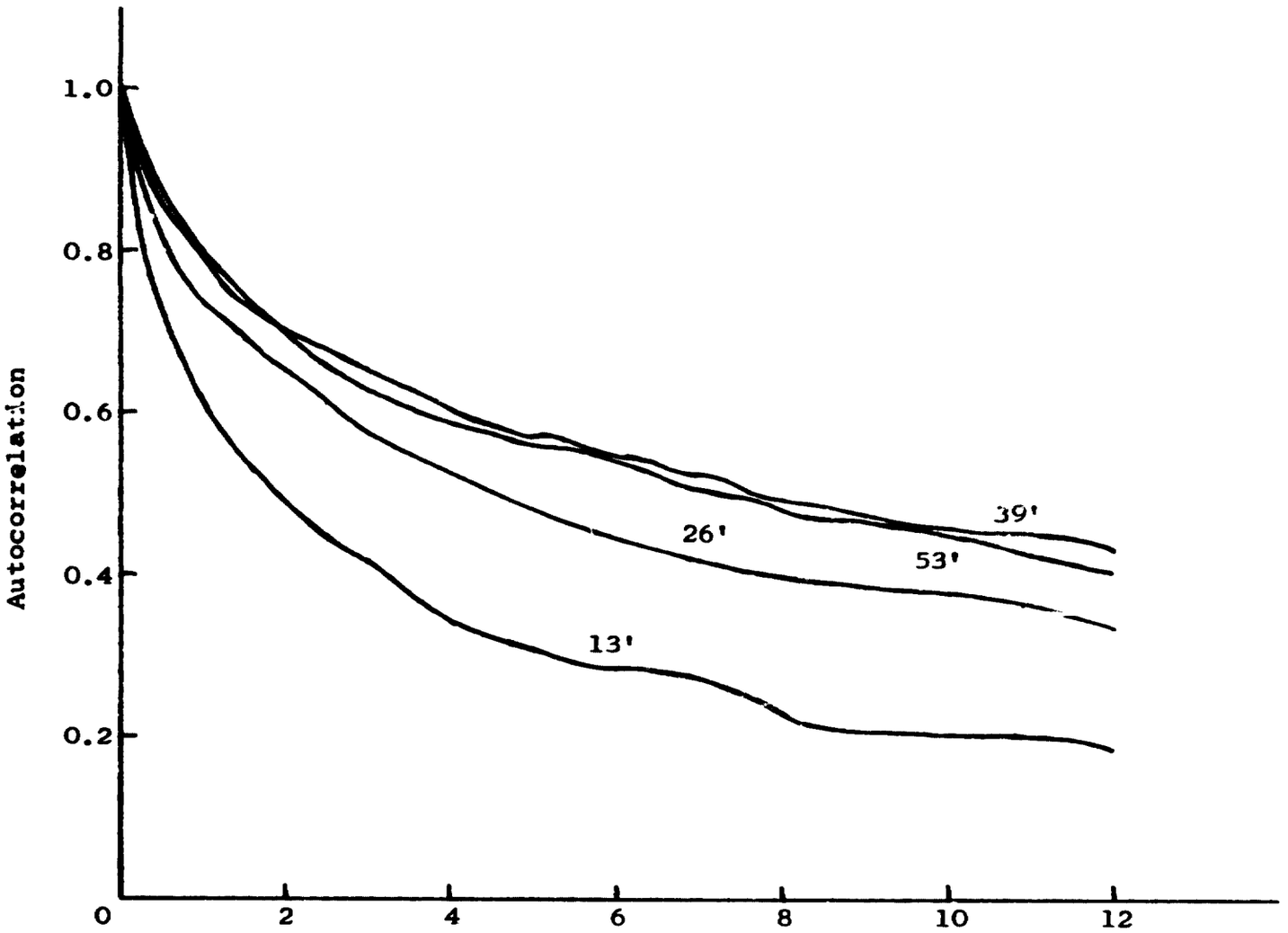

(d) Point 4.

Figure 12.- Continued.

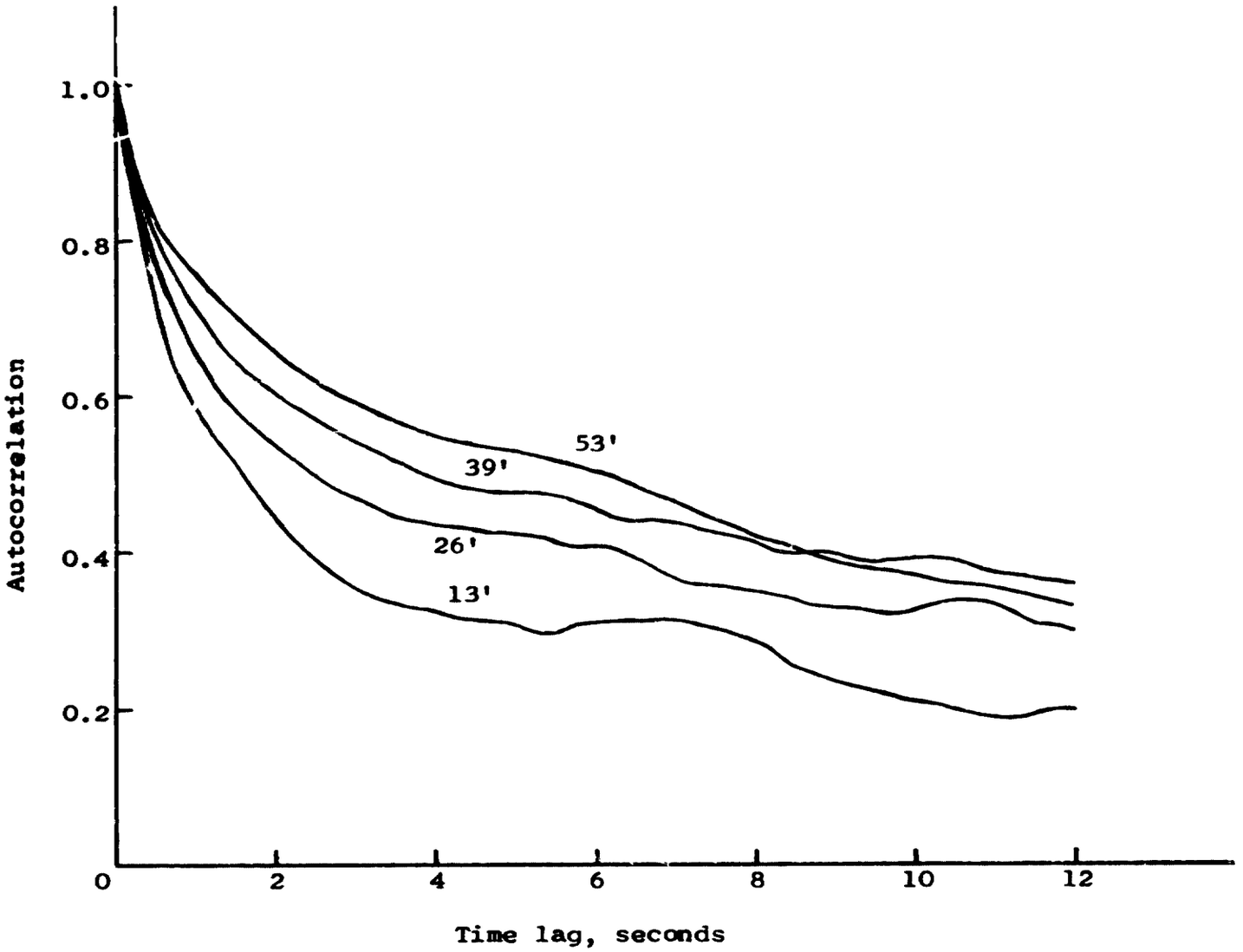

(e) Point 5.

Figure 12.- Continued.

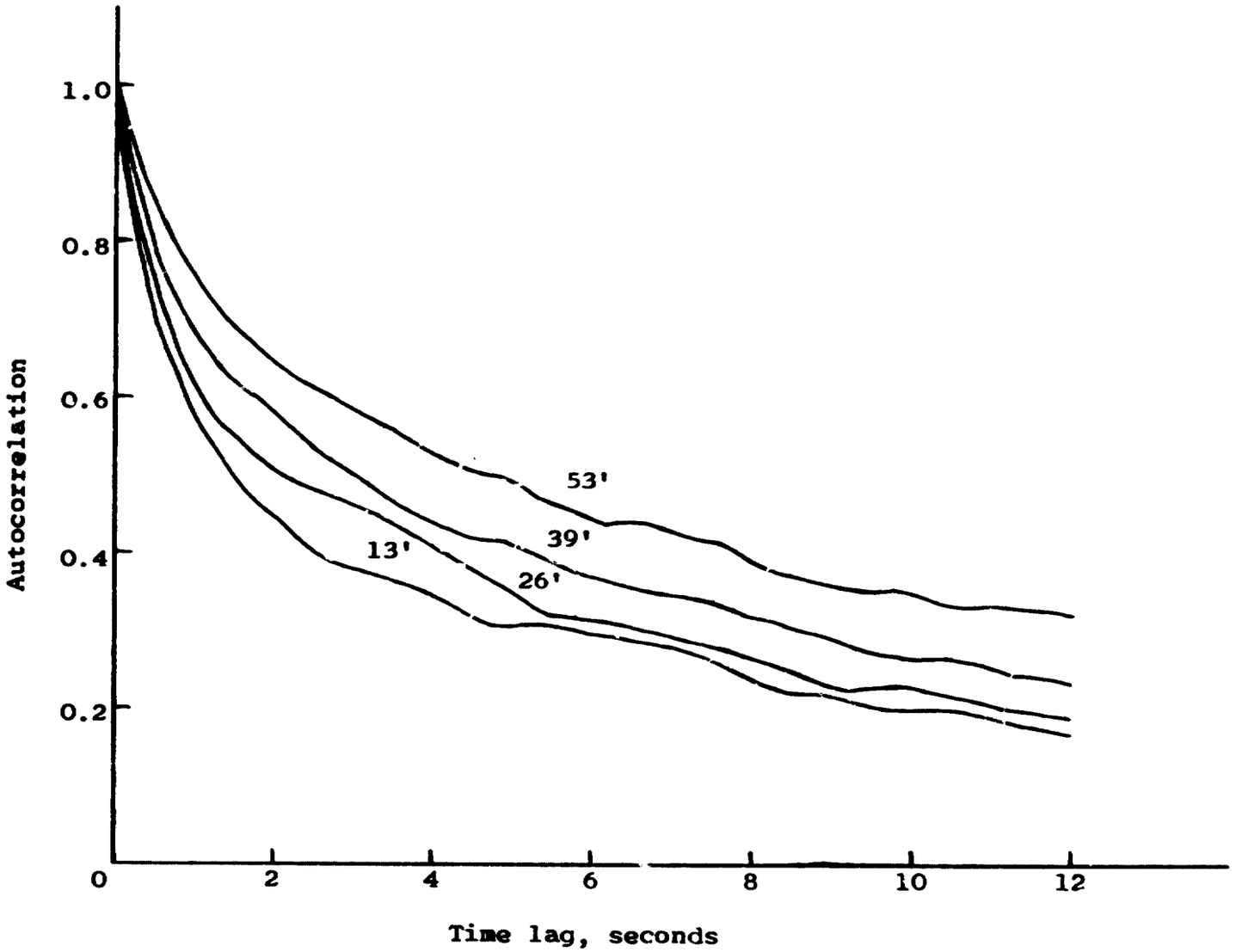

(f) Point 6.

Figure 12.- Continued.

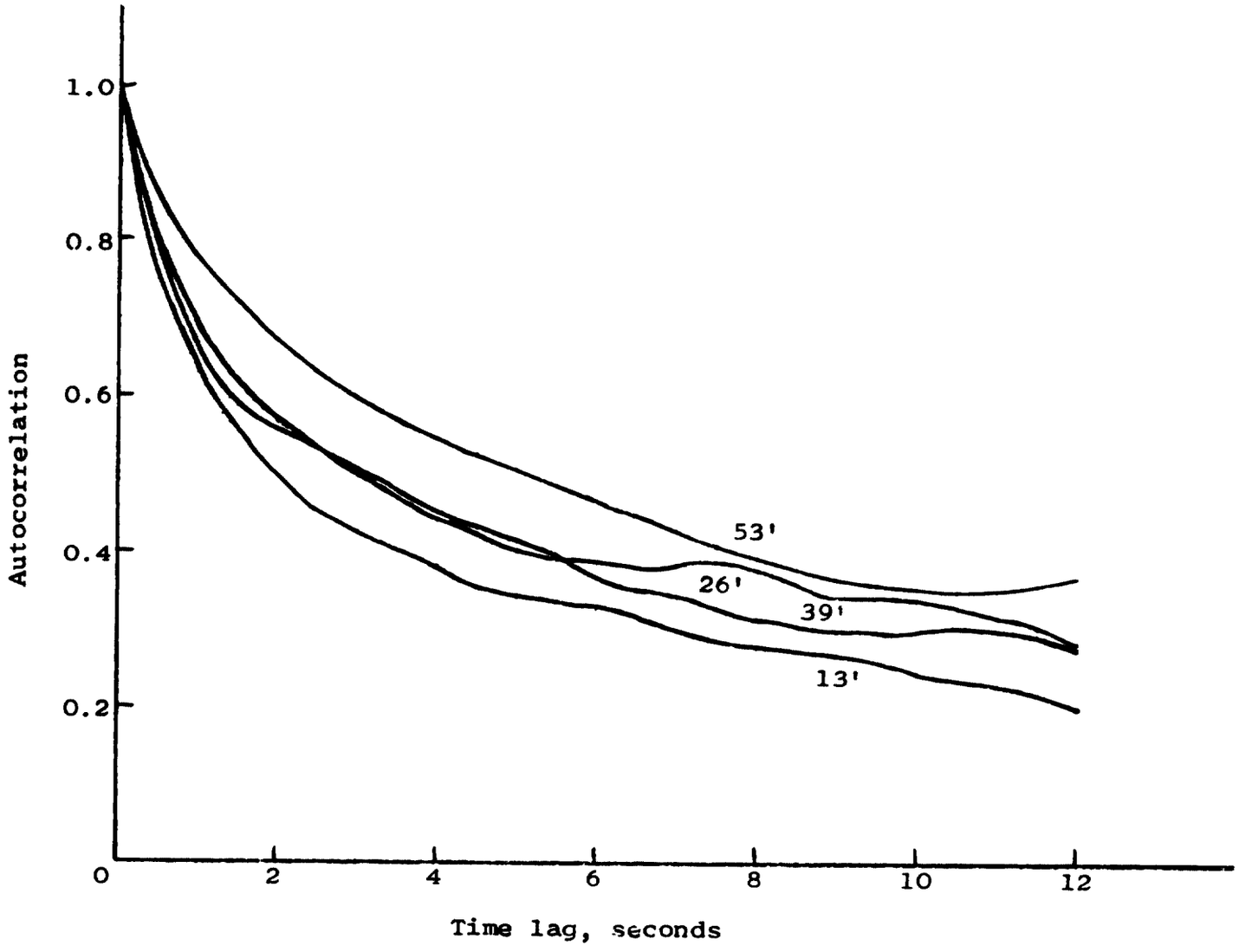

(g) Point 7.

Figure 12.- Concluded.

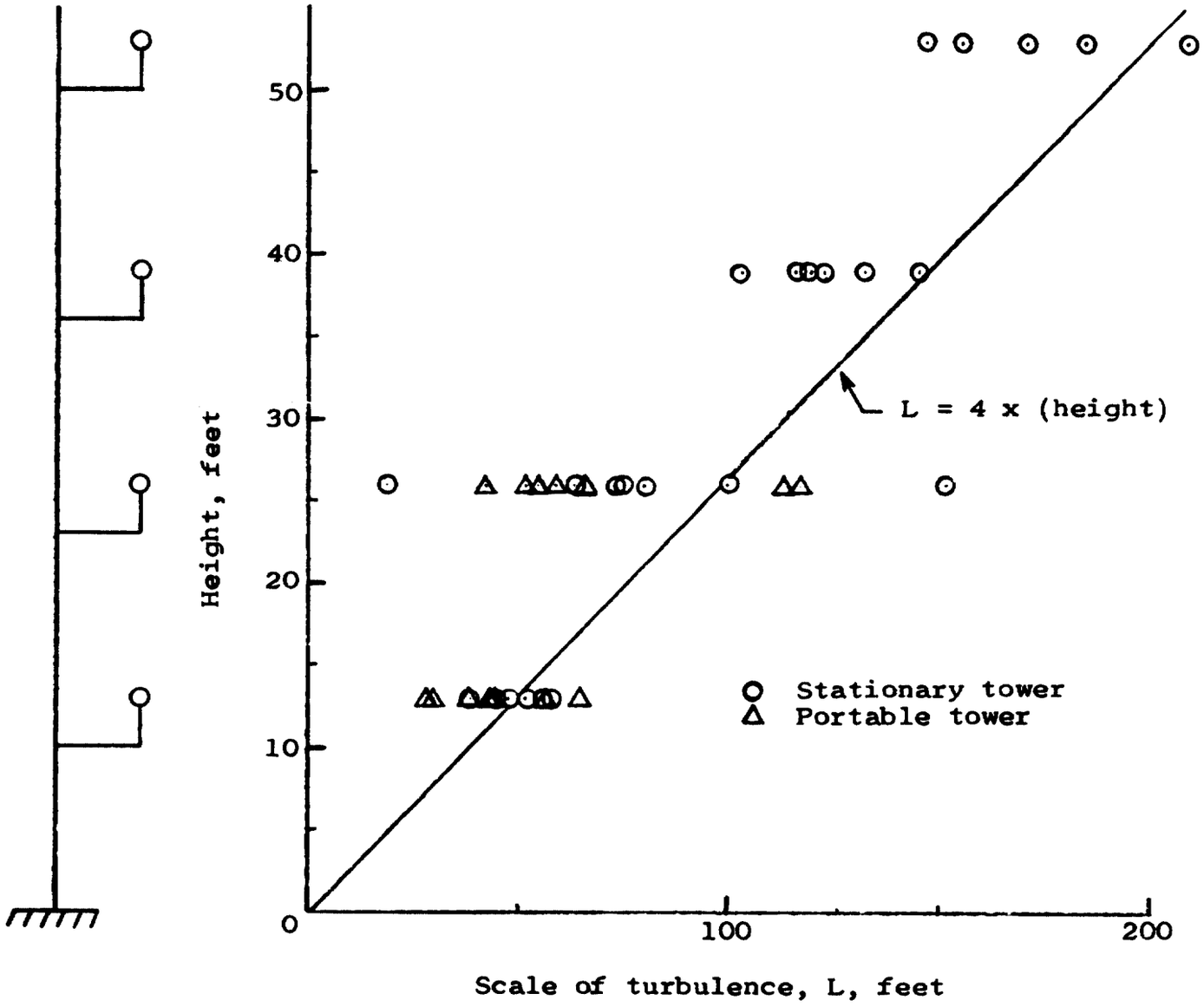

Figure 13.- Variation of turbulence scale with height.

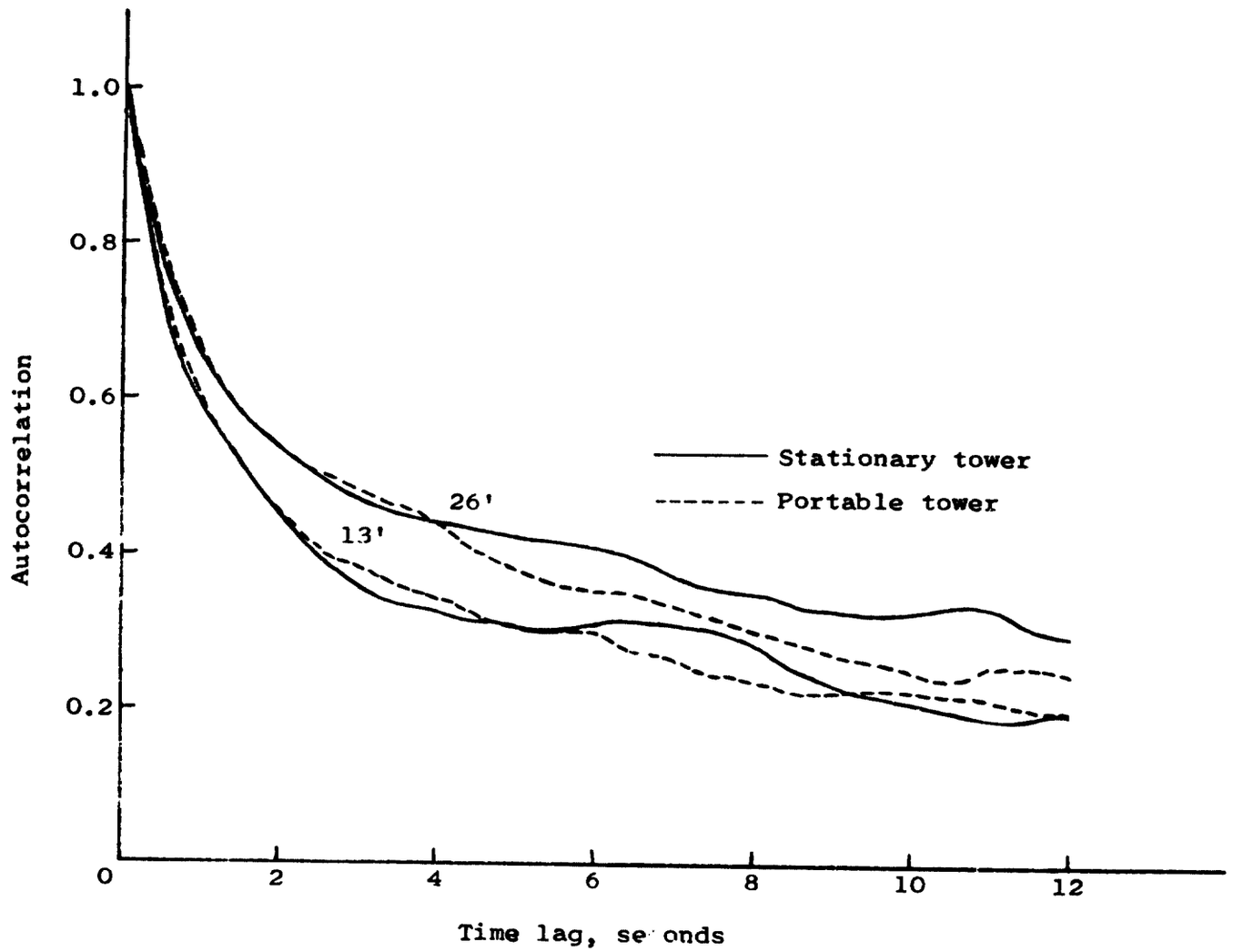

(a) Point 5.

Figure 14.- Comparison of autocorrelation function measured at the stationary tower and at the portable tower.

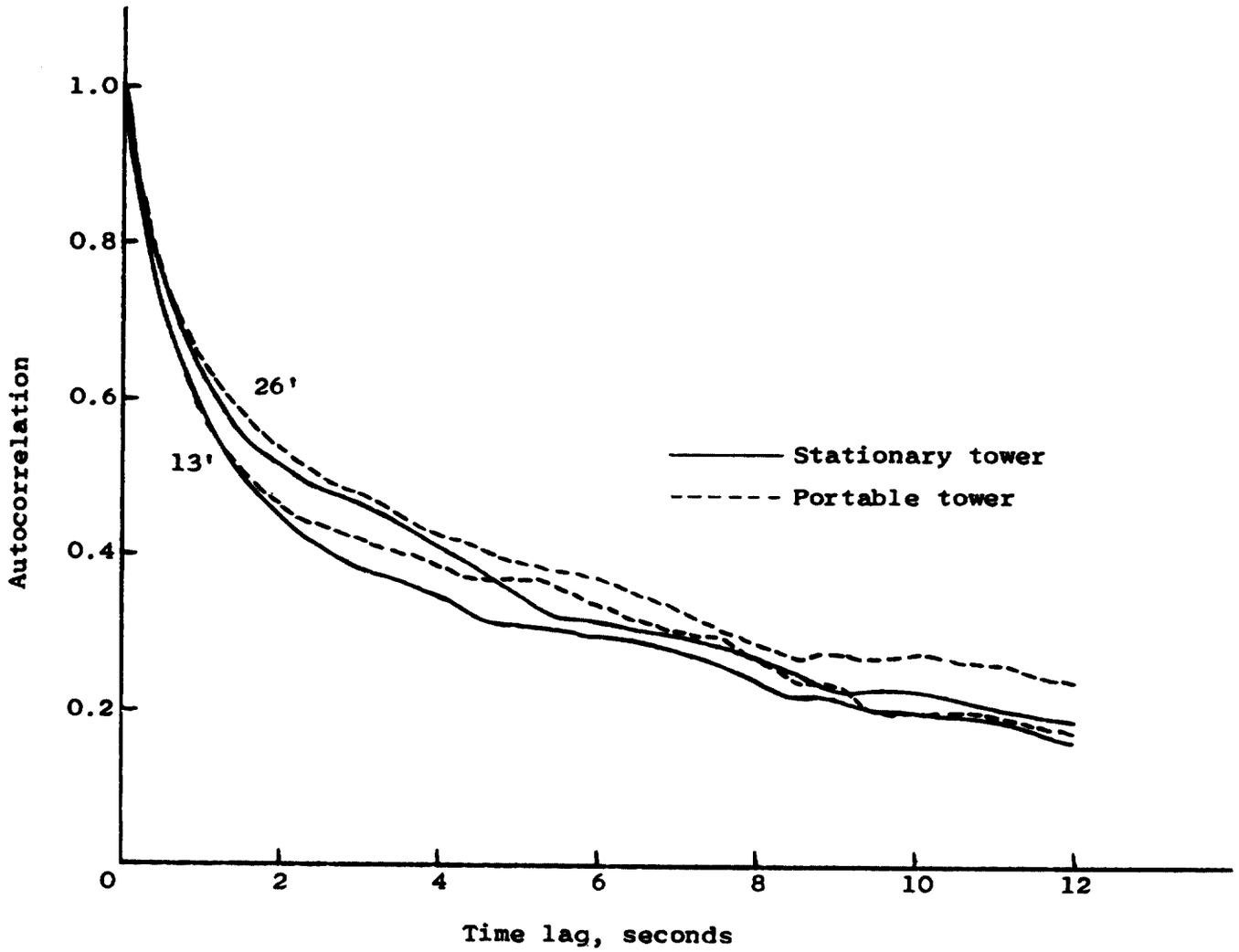

(b) Point 6.

Figure 14.- Concluded.

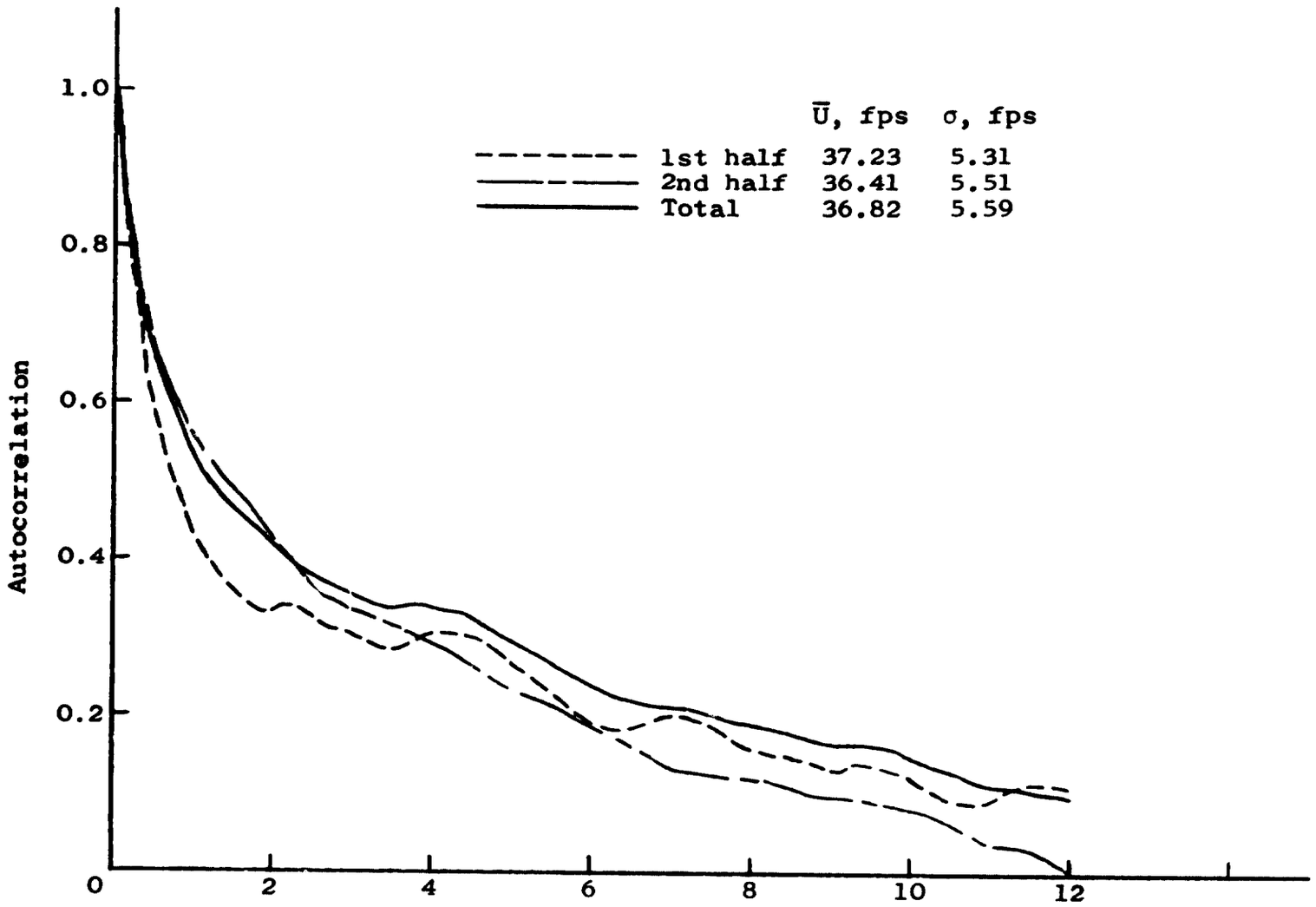

(a) 13 feet.

Figure 15.- Test for stationarity.

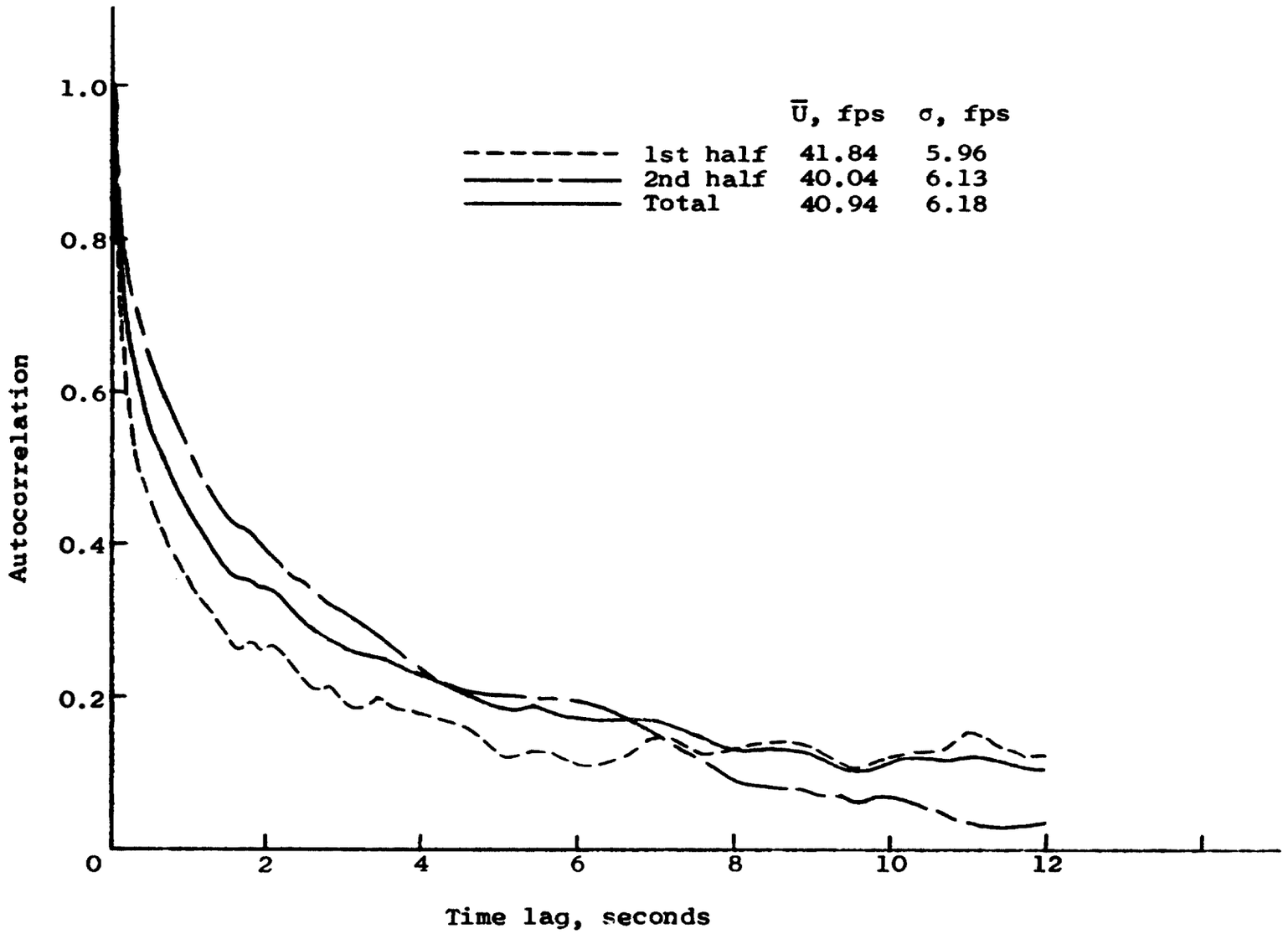

(b) 26 feet.

Figure 15.- Continued.

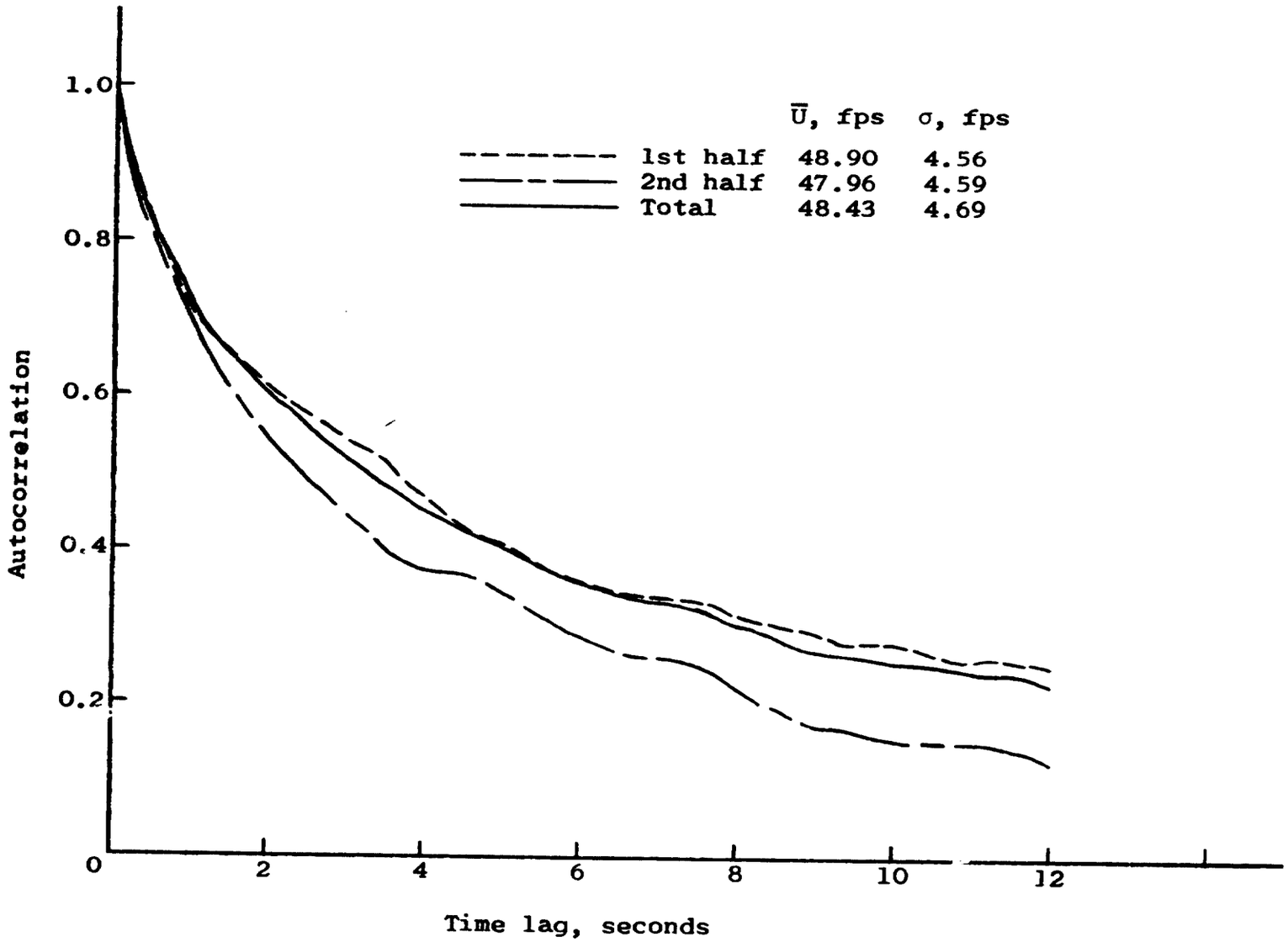

(c) 39 feet.

Figure 15.- Continued.

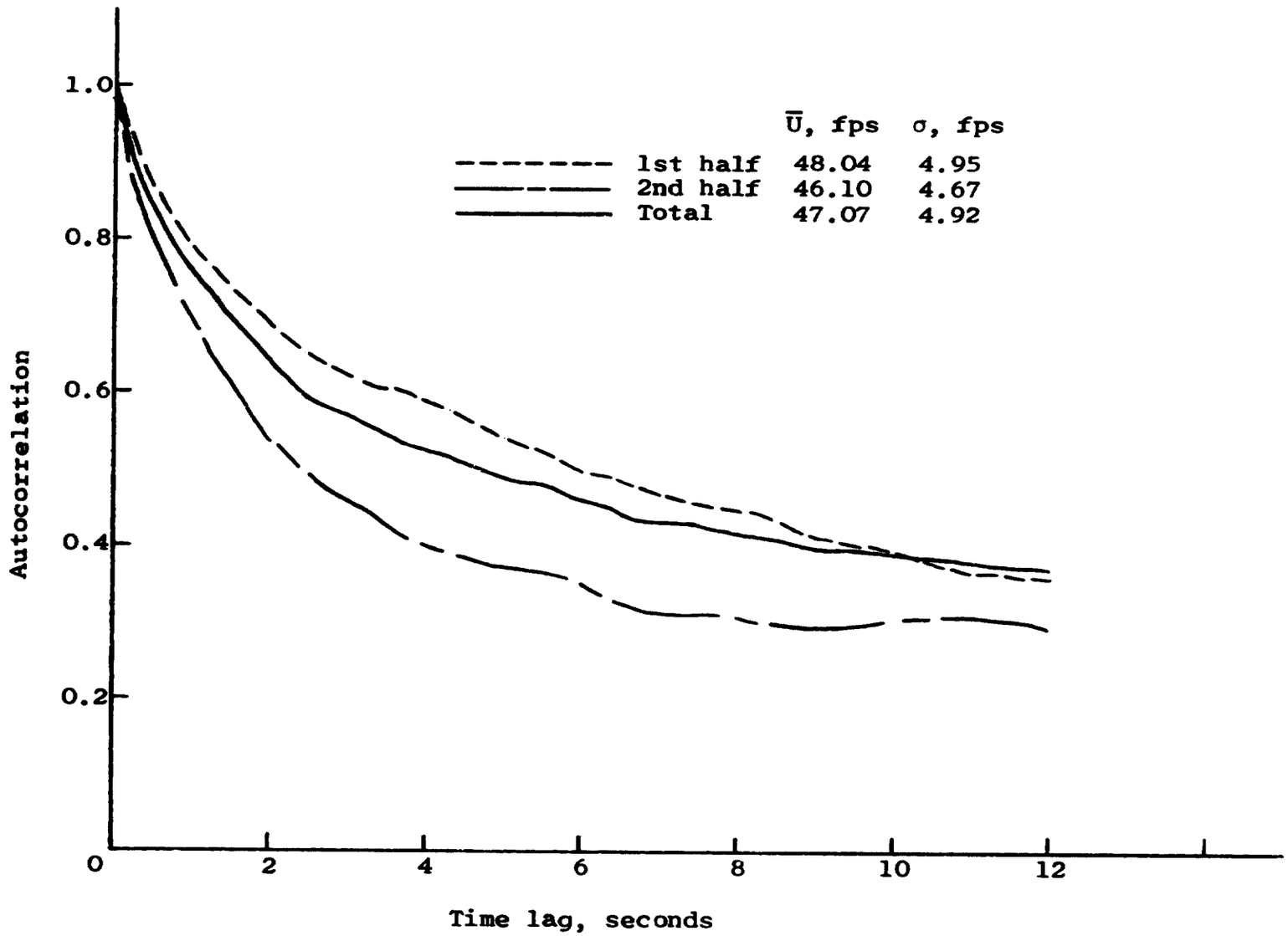

(d) 53 feet

Figure 15.- Continued.

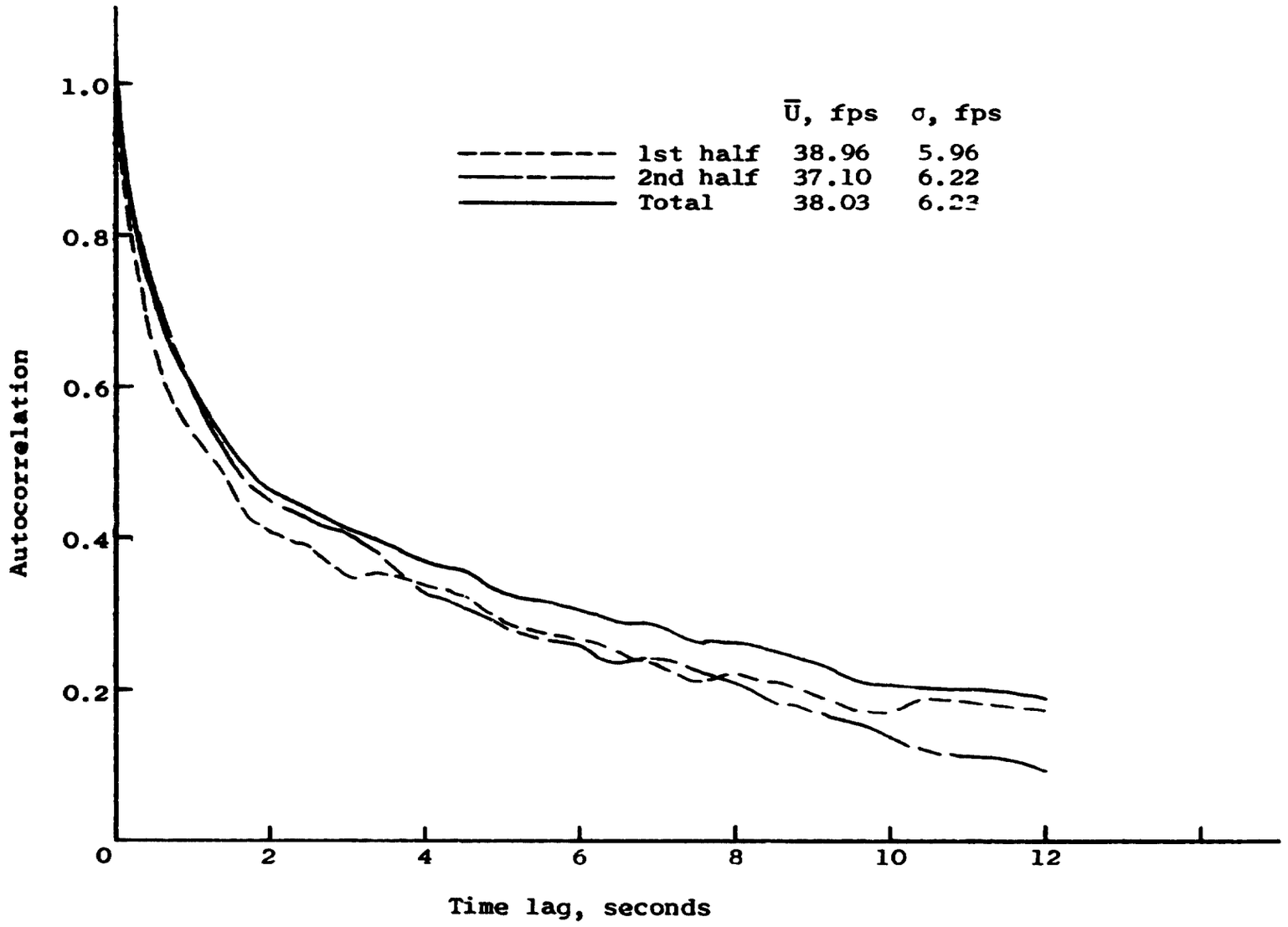

(e) 13 feet, portable tower.

Figure 15.- Continued.

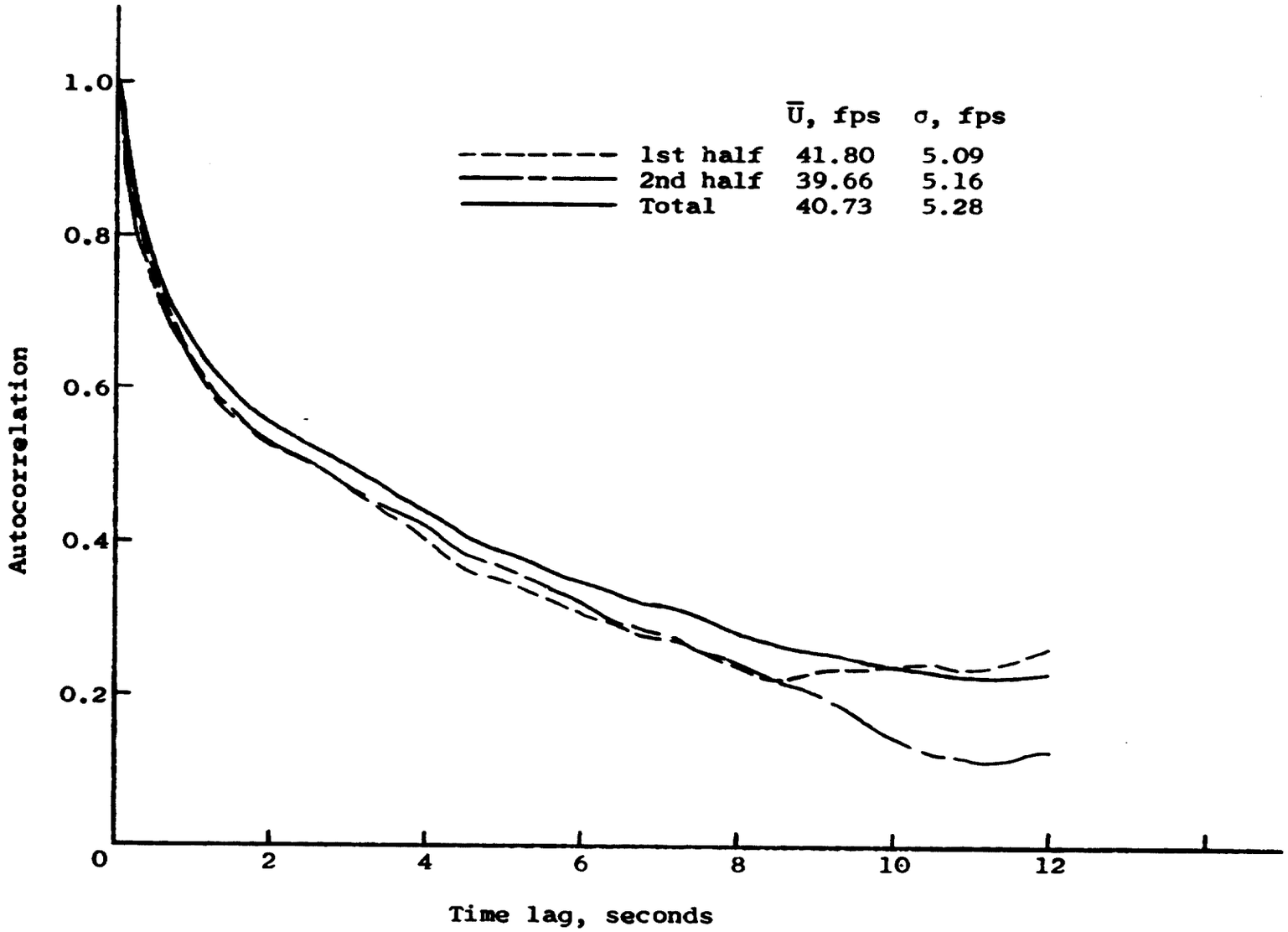

(f) 26 feet, portable tower.

Figure 15.- Concluded.

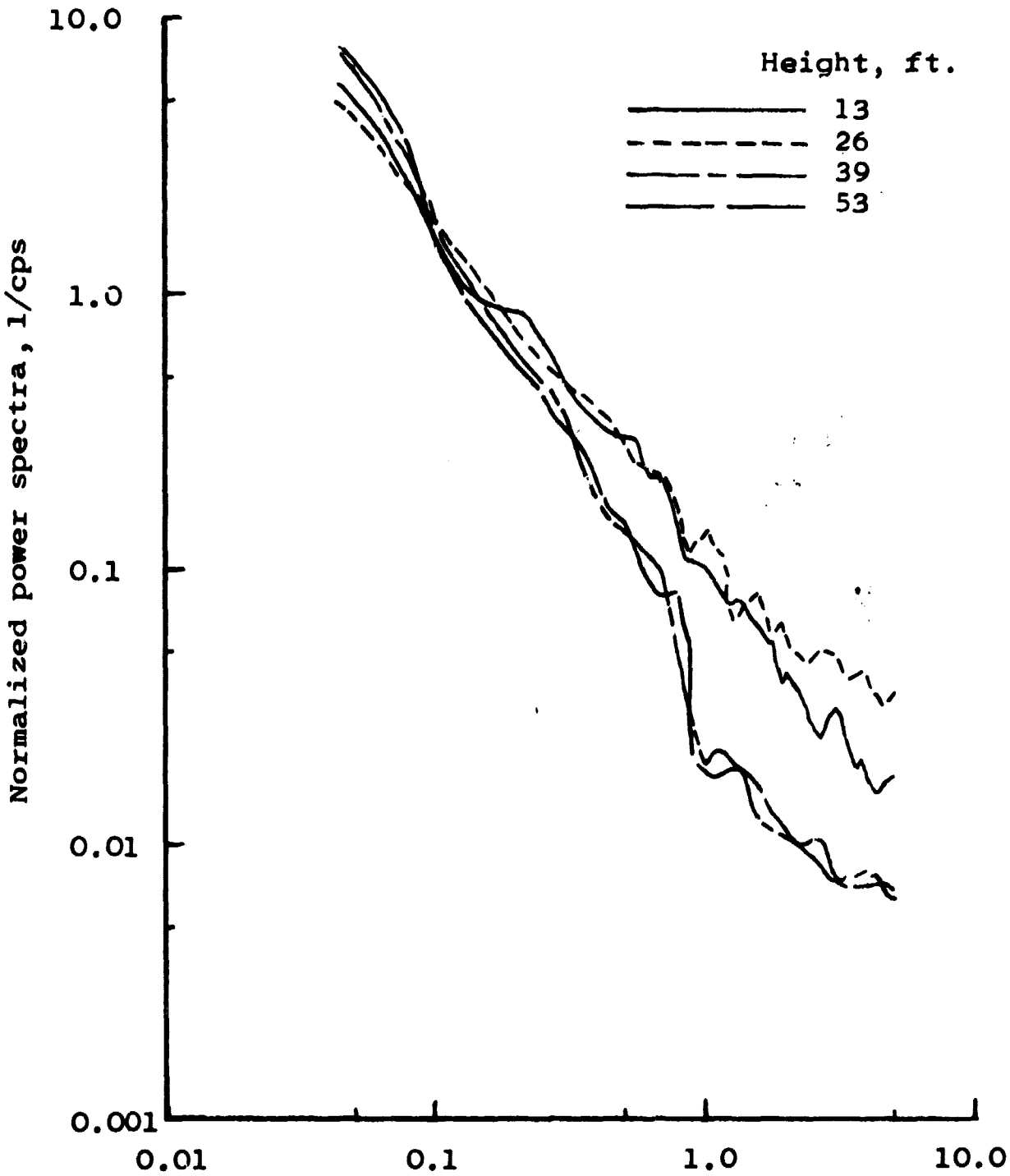

(a) Point 1.

Figure 16.- Power spectral density functions.

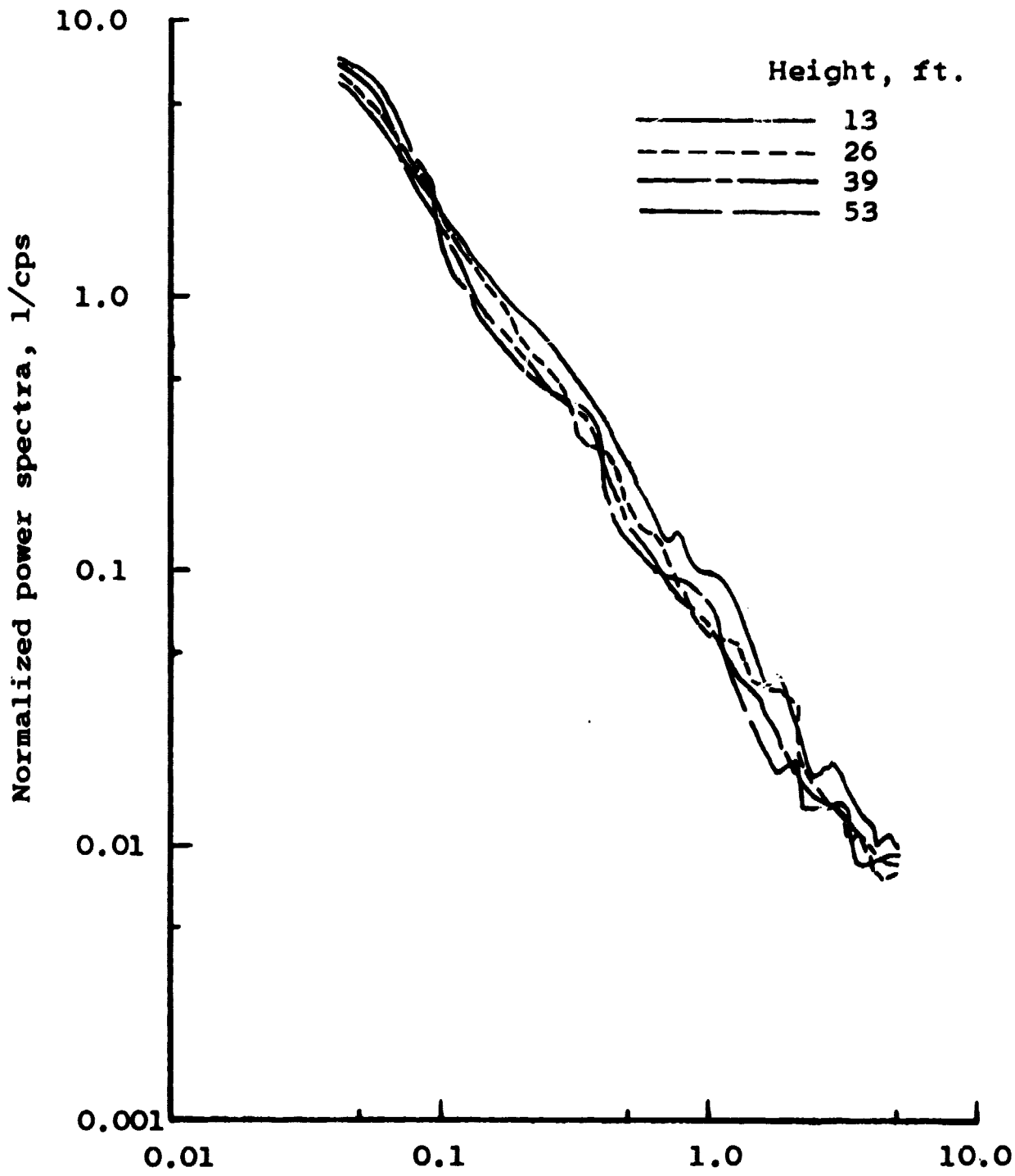

(b) Point 2.

Figure 16.- Continued.

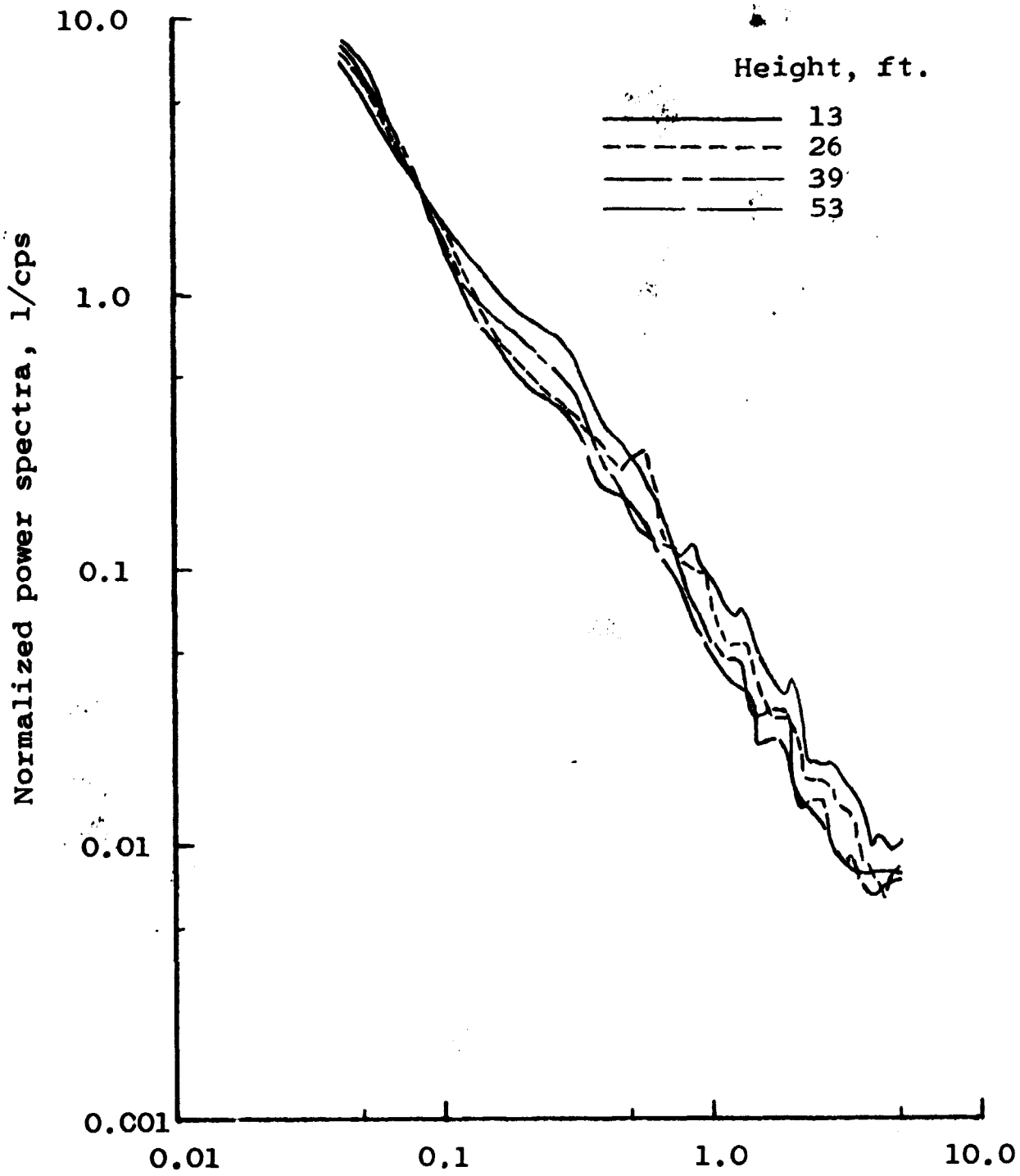

(c) Point 3.

Figure 16.- Continued.

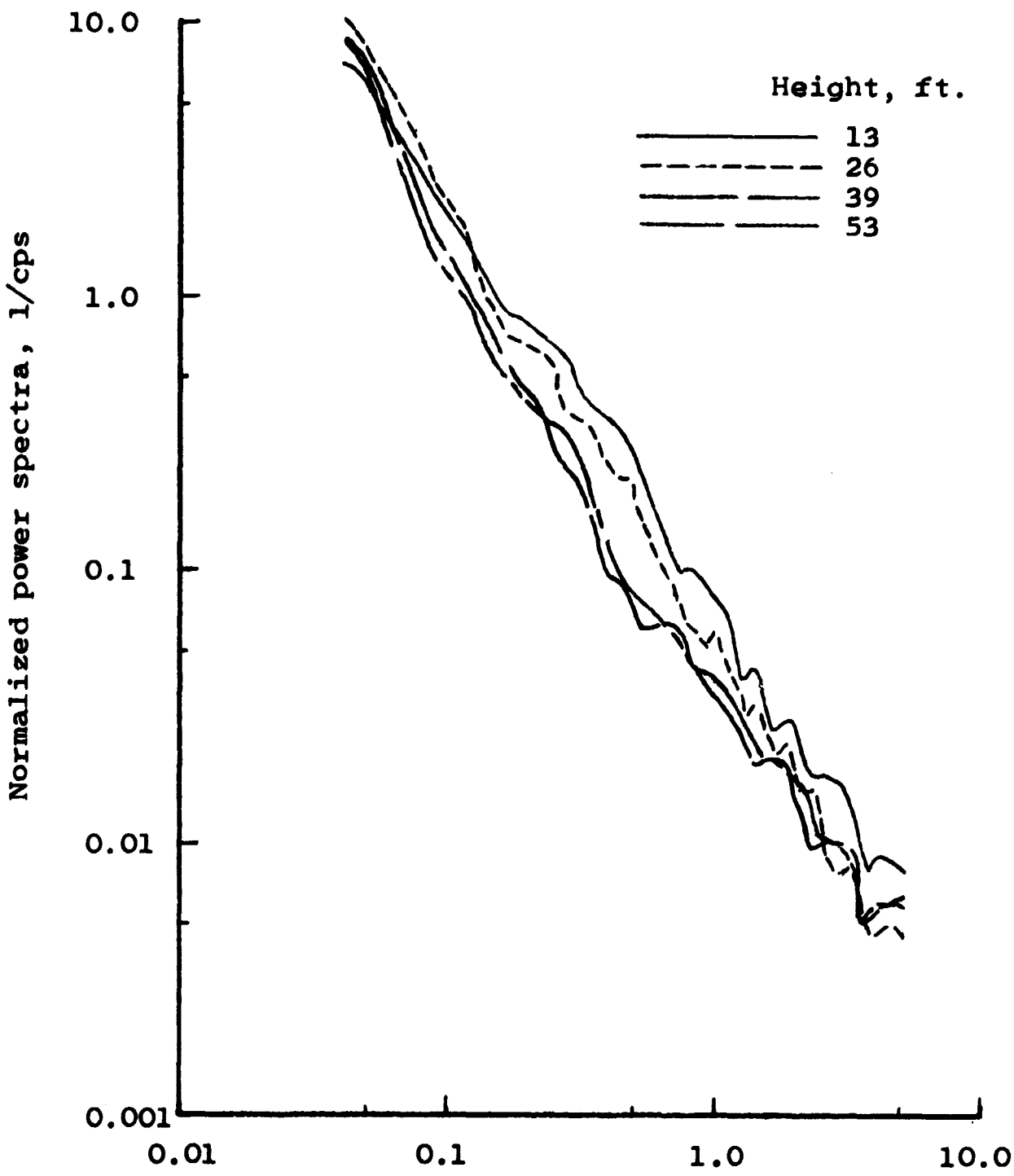

(d) Point 4.

Figure 16.- Continued.

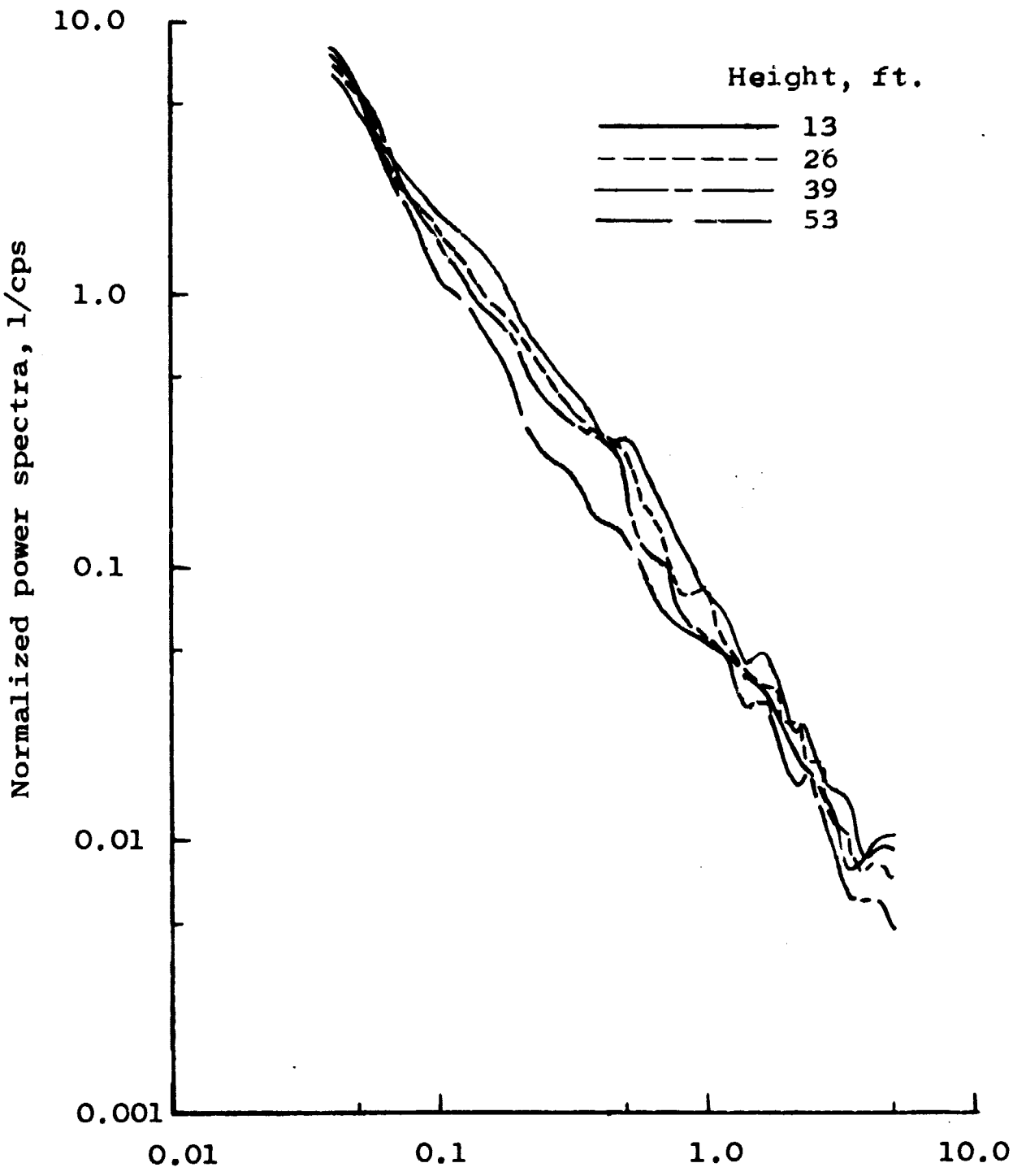

(e) Point 5.

Figure 16.- Continued.

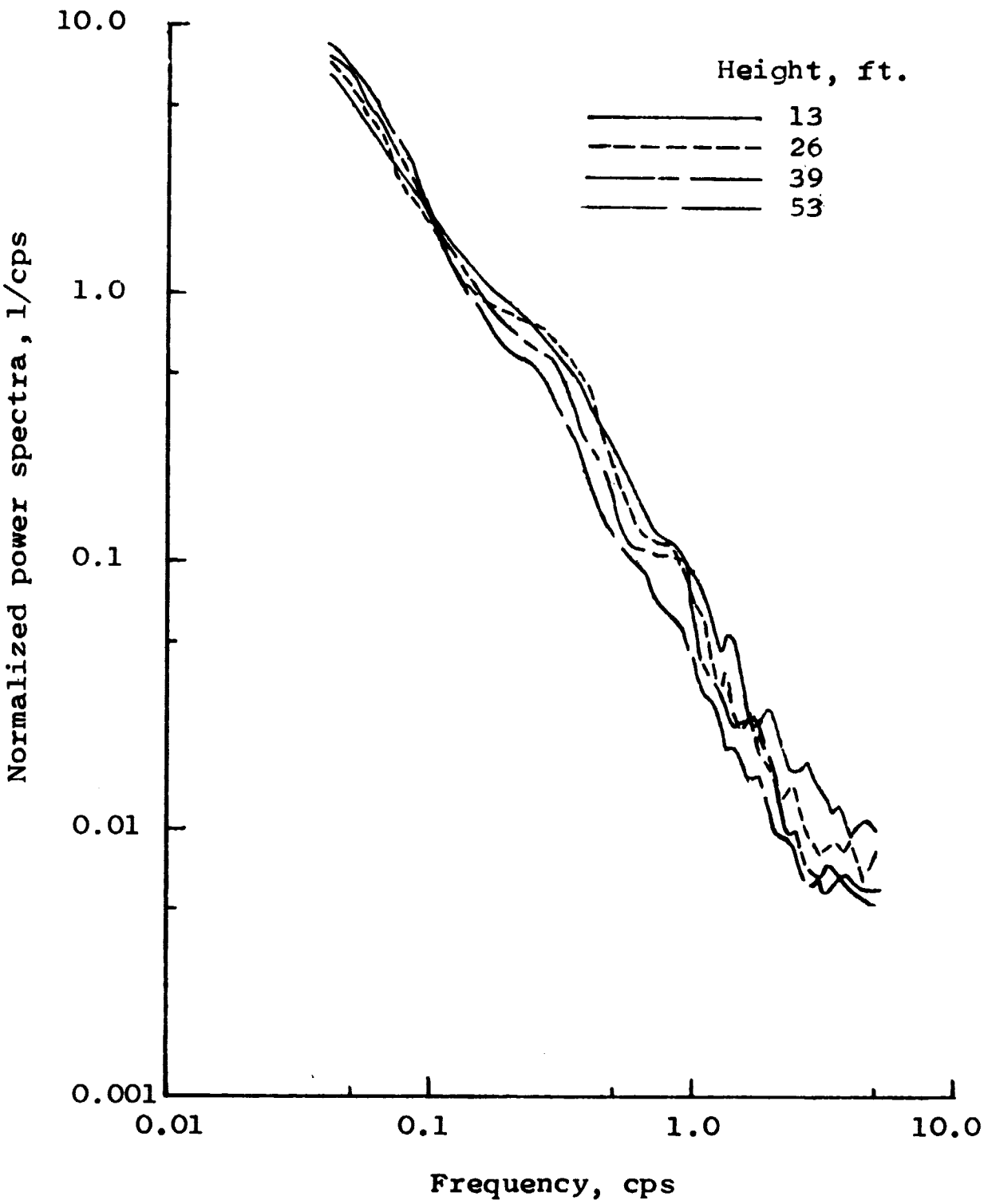

(f) Point 6.

Figure 16.- Continued.

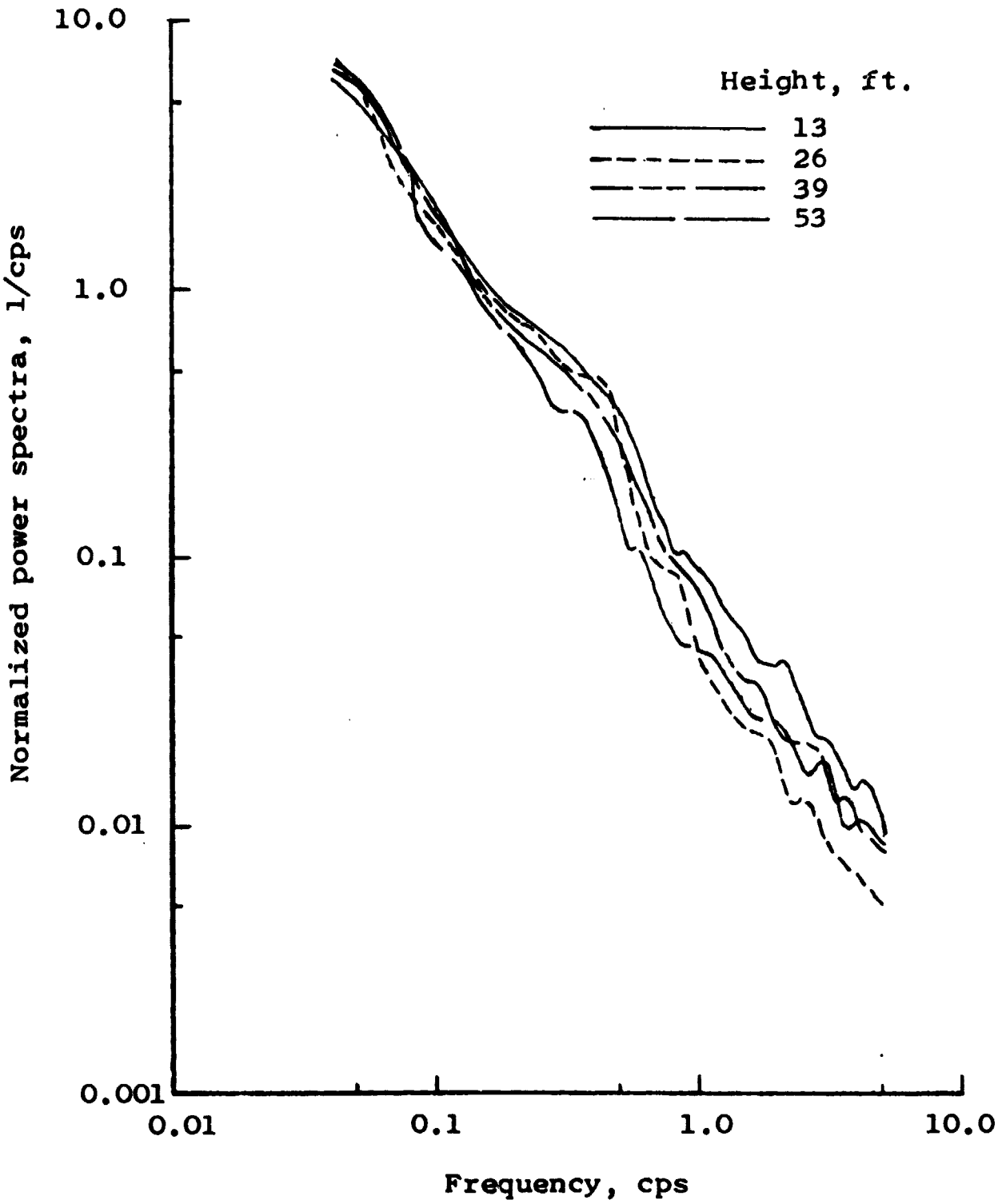

(g) Point 7.

Figure 16.- Concluded.

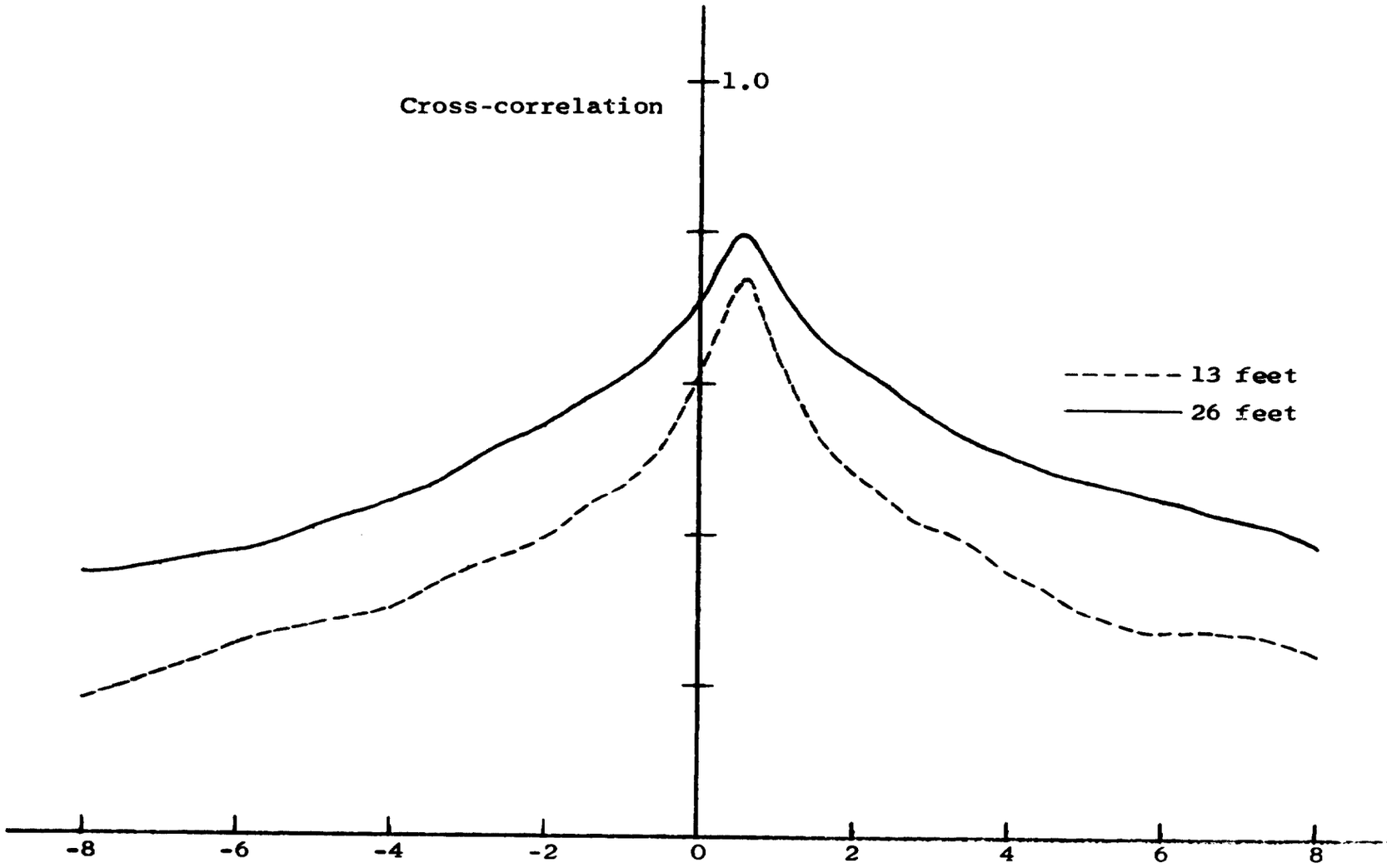

(a) d = 20 feet.

Figure 17.- Cross-correlation function.

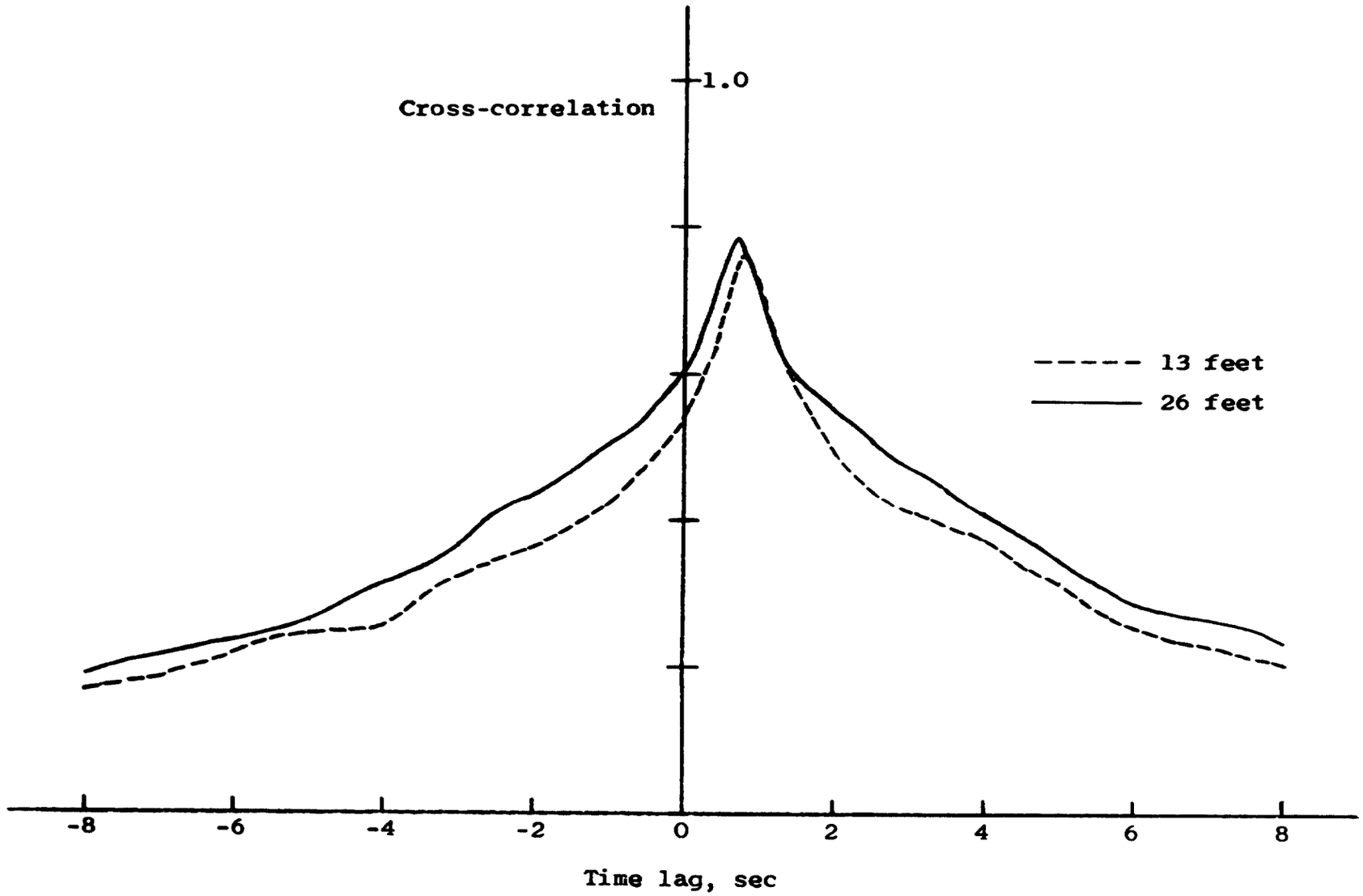

(b) d = 30 feet.

Figure 17.- Continued.

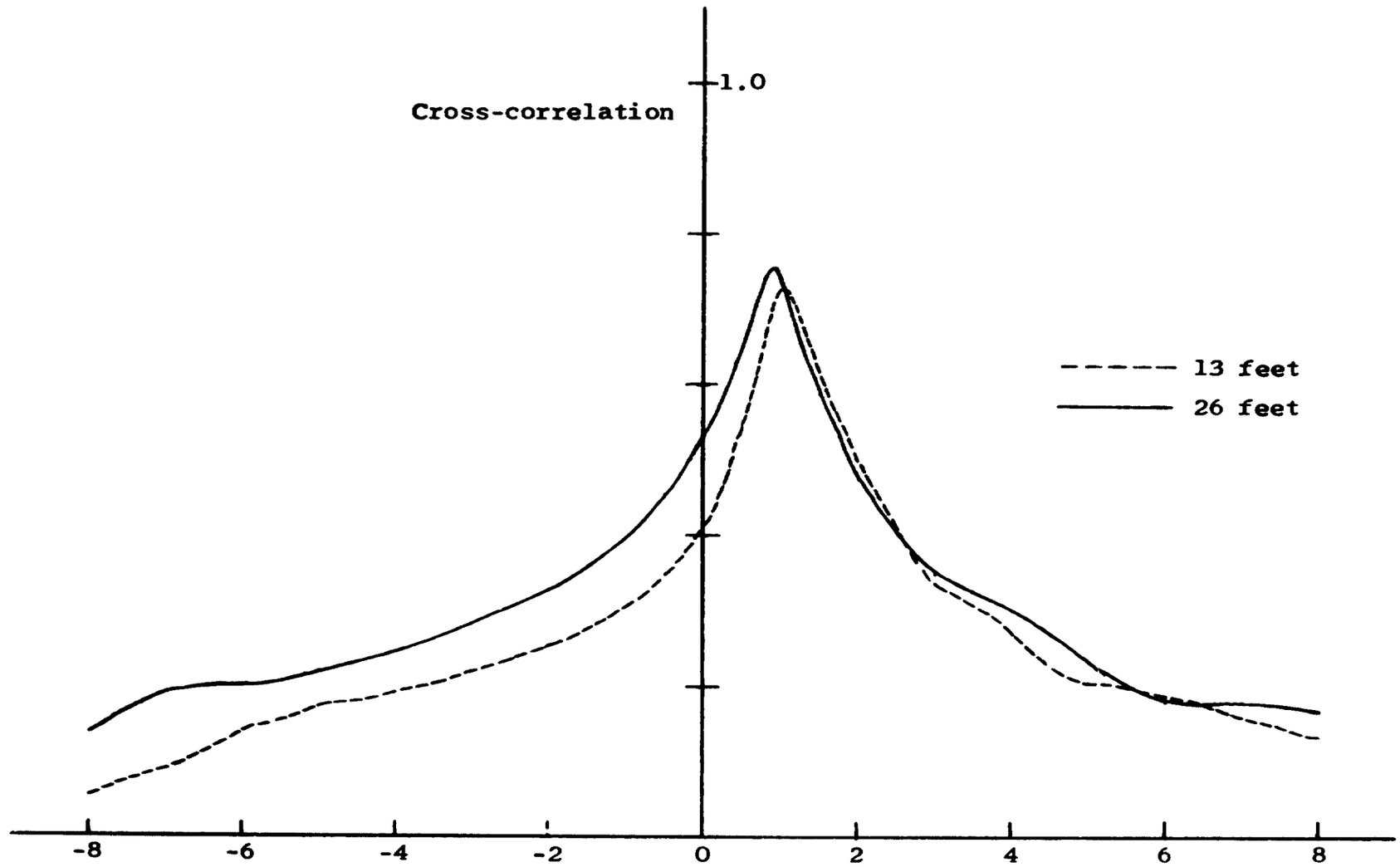

(c) d = 40 feet.

Figure 17.- Continued.

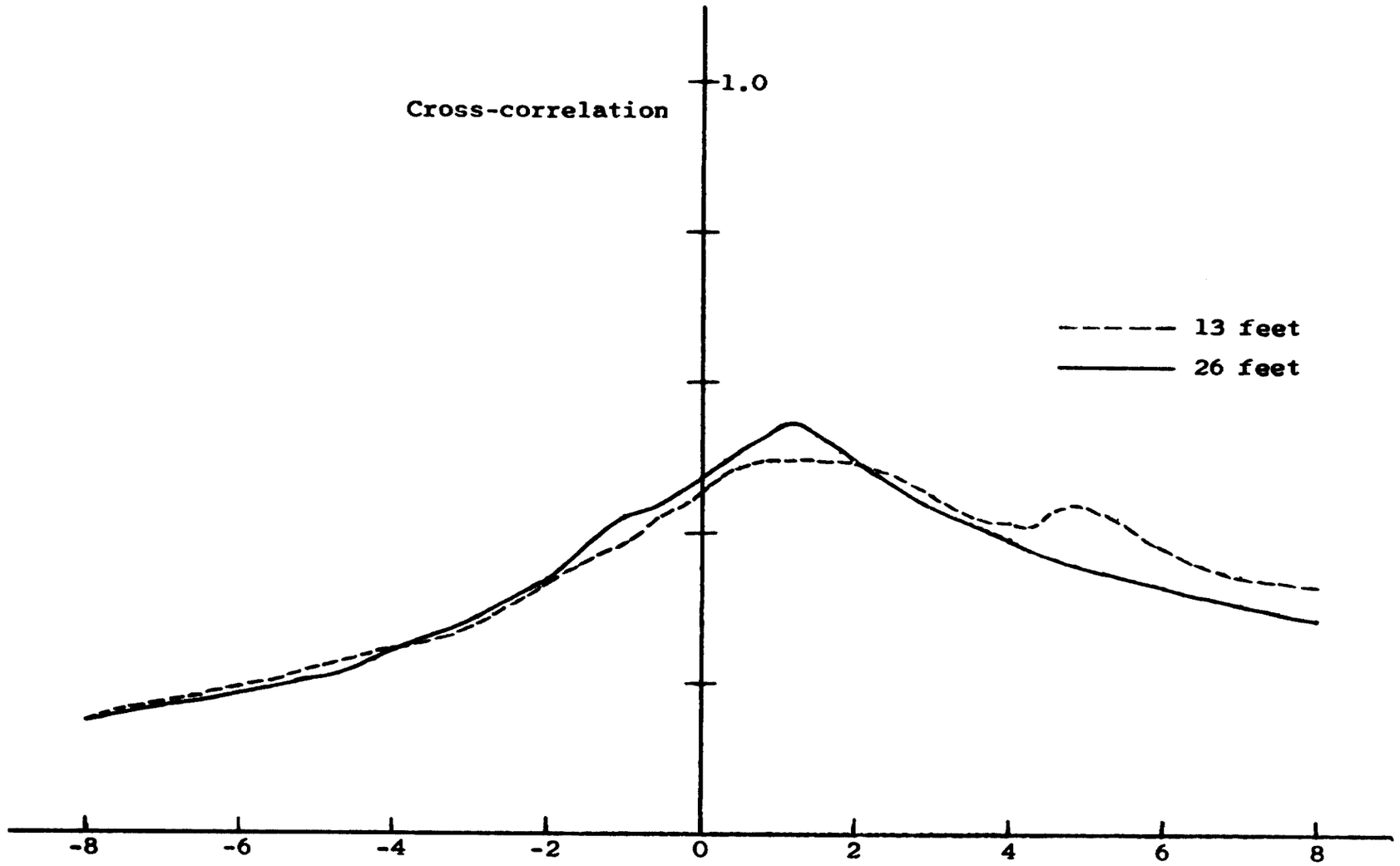

(d) d = 50 feet.

Figure 17.- Continued.

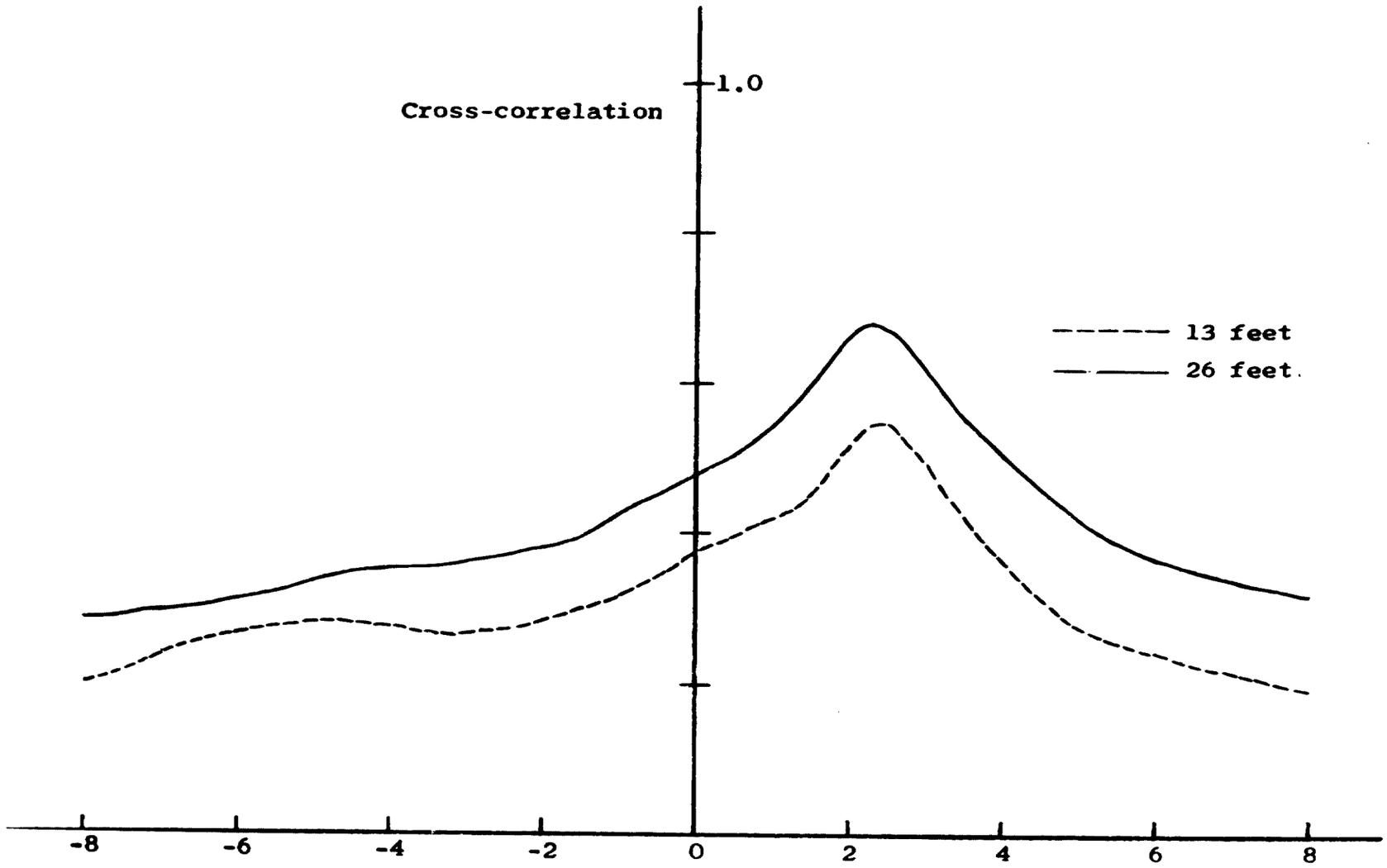

(e) d = 70 feet.

Figure 17.- Continued.

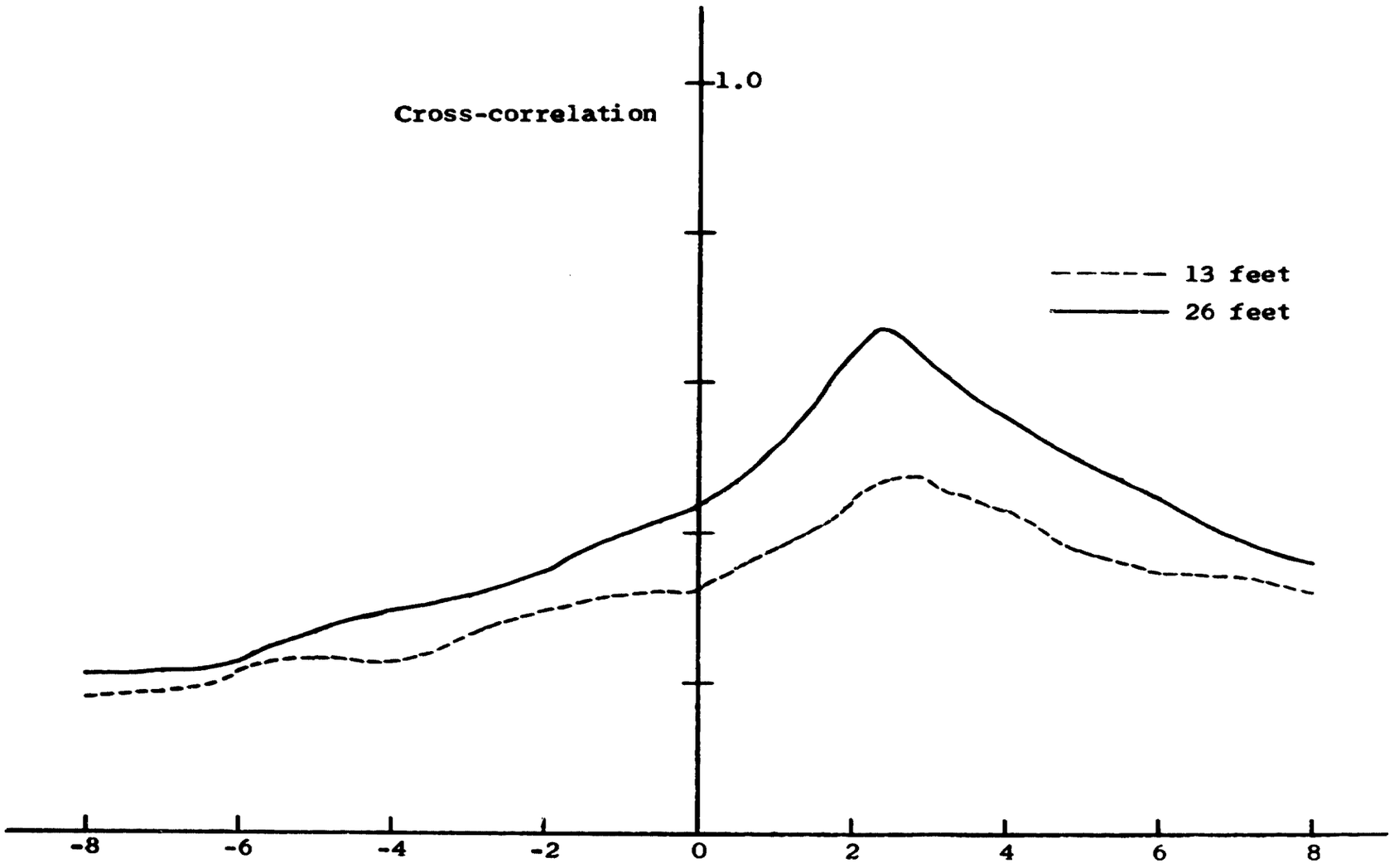

(f) d = 80 feet.

Figure 17.- Continued.

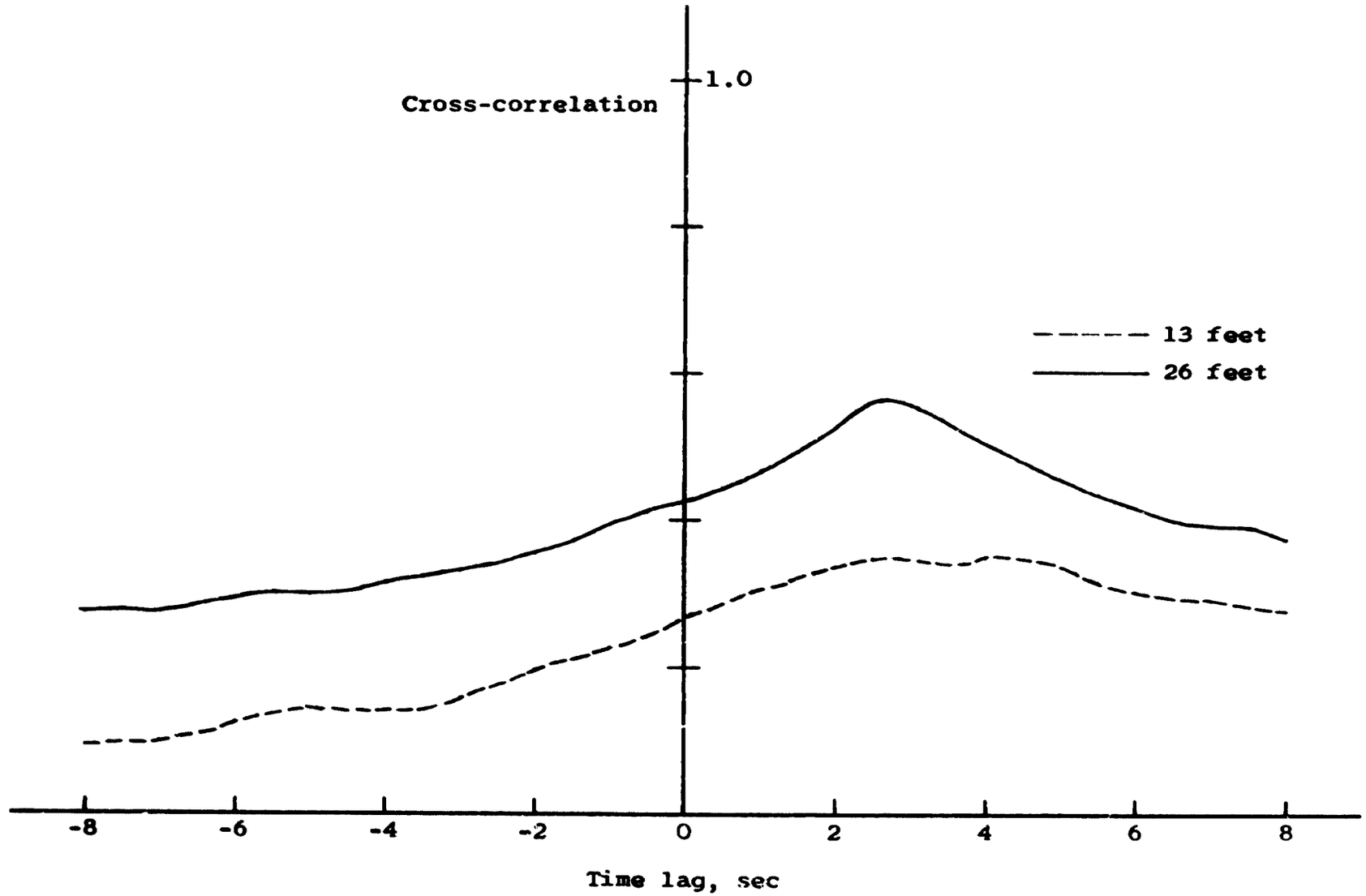

(g) d = 100 feet.

Figure 17.- Concluded.

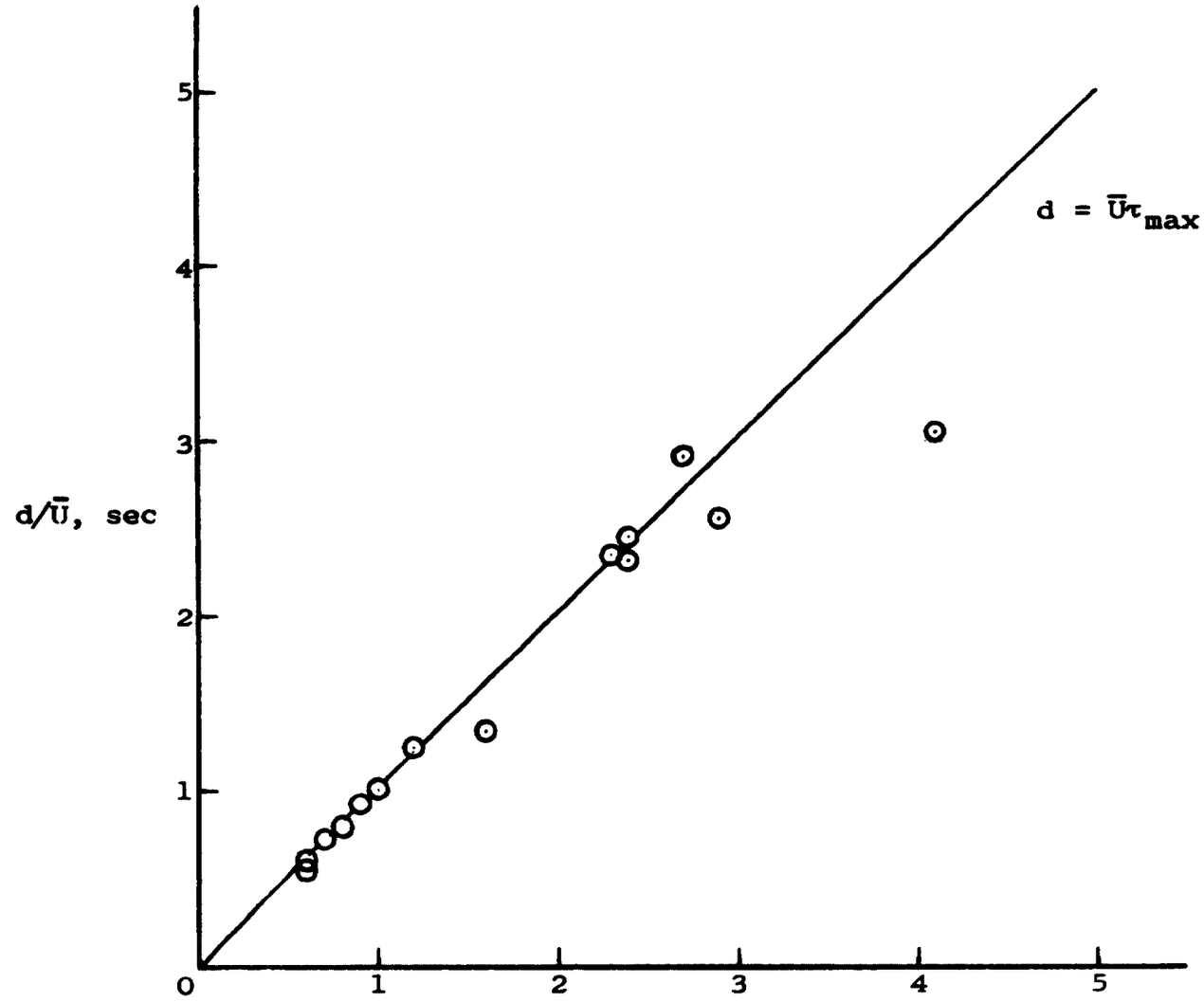

Figure 18.- Comparison of convection time delay, $d/\bar{U}$, with time to maximum correlation, τ_{max}.

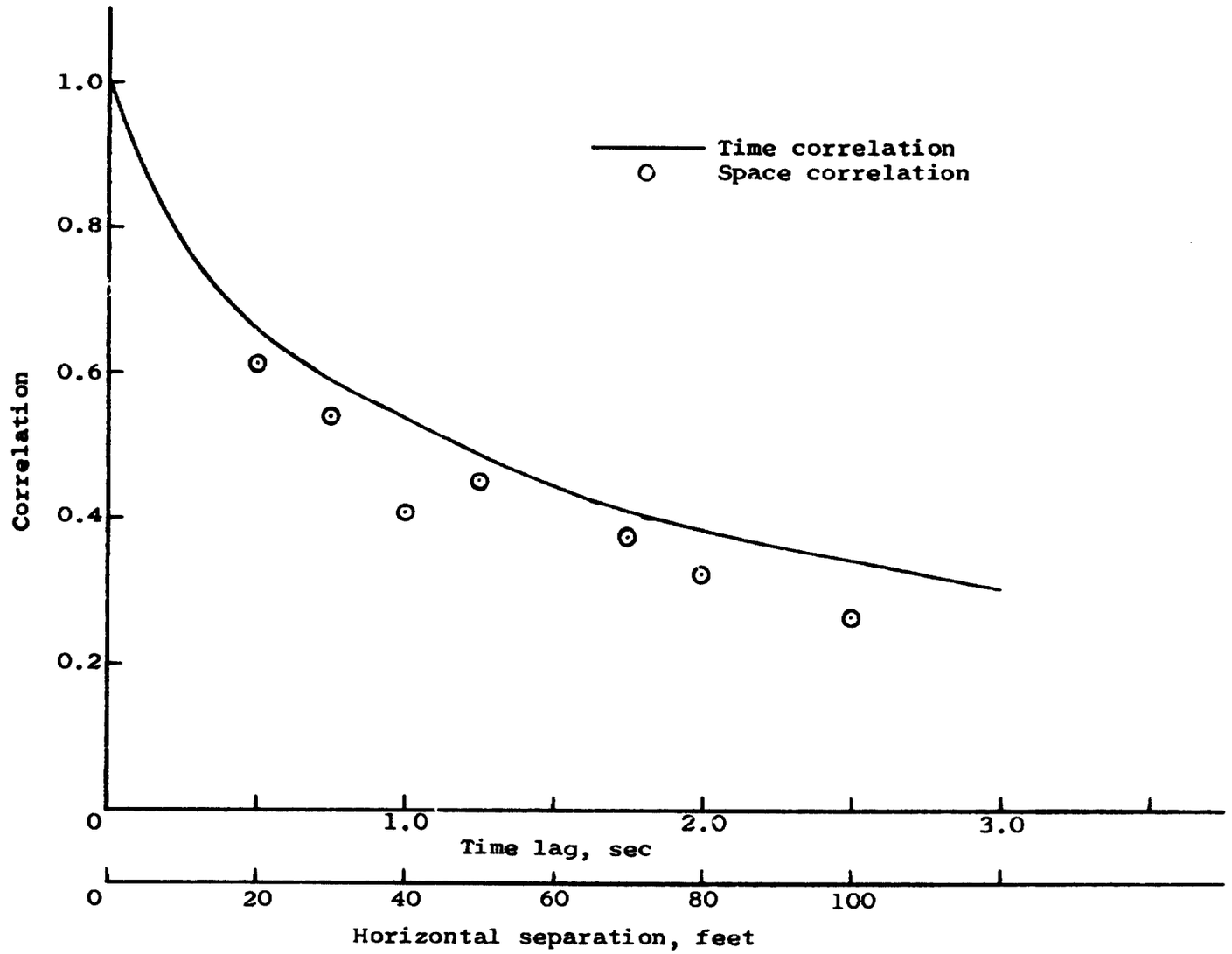

(a) Height = 13 feet.

Figure 19.- Comparison of time and space correlation

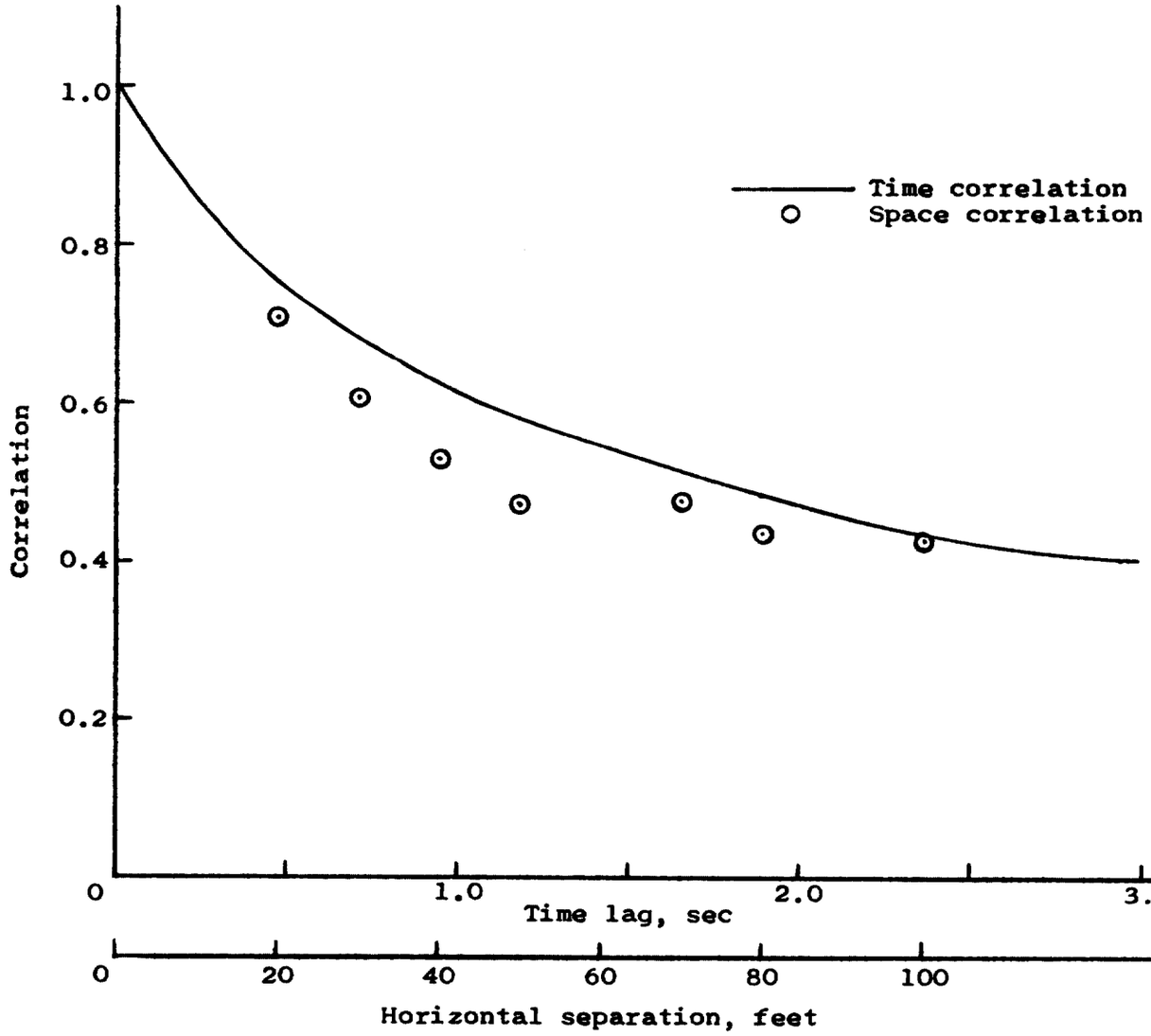

(b) Height = 26 feet.

Figure 19.- Concluded.

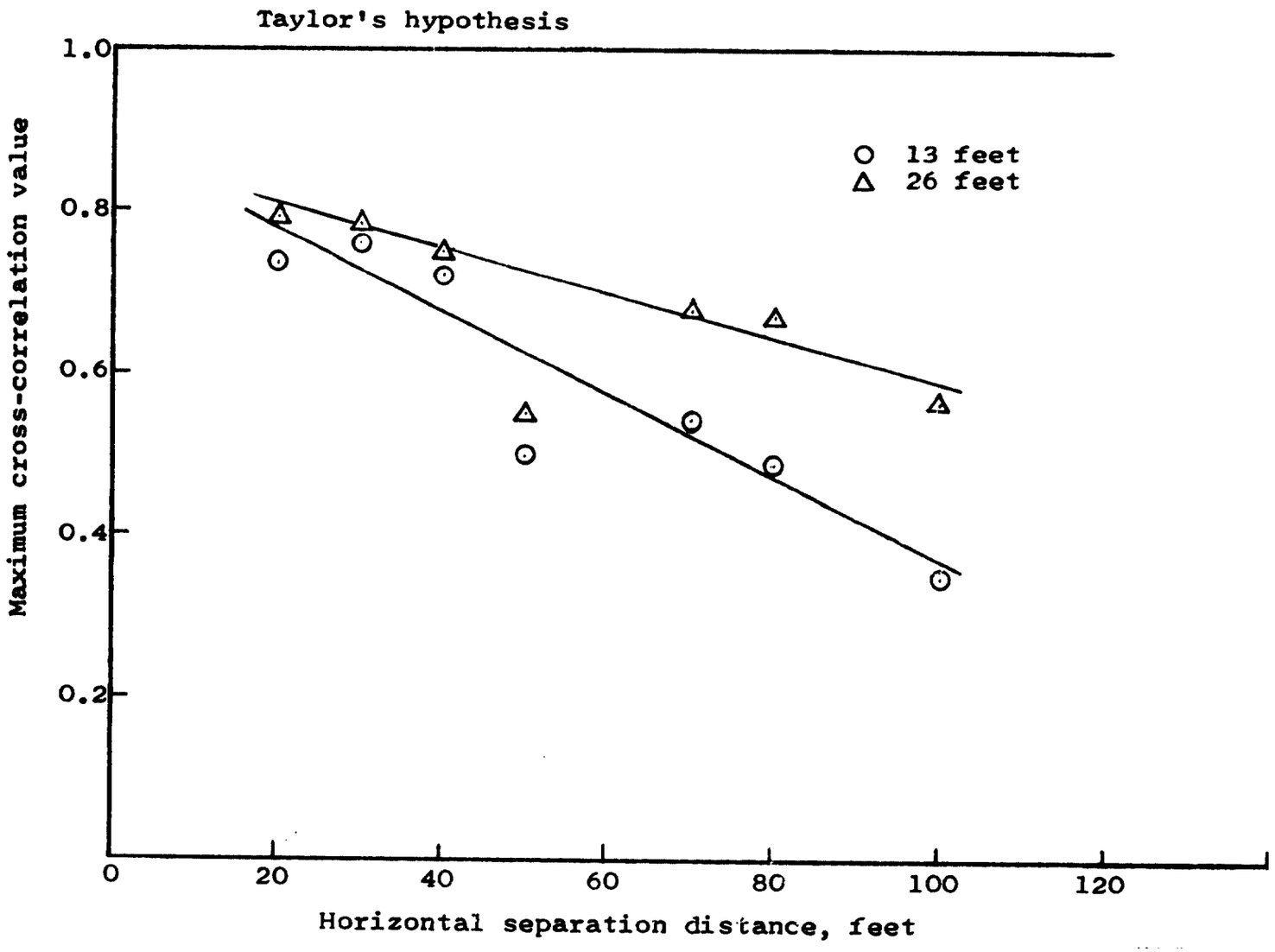

Figure 20.- Maximum cross-correlation value as a function of horizontal separation distance.

CONCLUSIONS

From the data presented in this thesis, a number of conclusions can be made concerning the wind environment at Wallops Island, Virginia. The data were recorded using fast response drag sphere anemometers and covered a range of heights up to 53 feet above the ground. These conclusions concern the horizontal components of turbulence only since no attempt was made to measure the vertical component. The data presented resulted from seven data samples recorded during an elapsed time of approximately four hours. The mean wind speeds measured at a height of 65 feet were between 37 and 48.5 fps. The meteorological conditions did not change significantly during this time interval.

The natural boundary layer studied was found to have the following characteristics:

1. The mean wind speed profiles are given by the power law approximation

$$\bar{U}_z = \bar{U}_{z_1} (z/z_1)^n$$

with the exponent n having a value of 0.16 or 0.17.

2. The intensity of turbulence decreases with height, and for the conditions of this investigation turbulence values were in the range of 0.084 to 0.183.

3. The roughness length, z_o, is equal to 5 cm. This value is in agreement with other values obtained over flat, grass-covered surfaces.

4. The probability distribution of both the u-component and v-component appear to be Gaussian.

5. The autocorrelation functions exhibit a dependence on height with the breakdown in correlation occurring more rapidly at the lower levels.

6. The "scale of turbulence" increases with height according to the linear approximation $L = (4 \times \text{height})$ for the range of heights covered.

7. The turbulence is homogeneous within bounds on distance of at least 80 feet.

8. The turbulence is reasonably stationary.

9. Atmospheric turbulence is a continuous random process. The normalized power spectra show a decrease in energy content with frequency at a slope of $-\frac{5}{3}$.

10. Horizontal isotropy was not established. The rms value of the u-component is greater than that of the v-component on the order of 20 percent, as is the case in wind-tunnel boundary layers.

From the cross-correlation data the following conclusions are made:

1. The cross-correlation between like components at two stations along the mean wind vector indicates a dependence on height; i.e., the correlation values are greater for the 26-foot height than for the 13-foot height.

2. The maximum cross-correlation value does occur at a time lag equal to the convection time delay, $d/\bar{U}$. This maximum correlation

value decreases with separation distance between the two measuring stations.

3. The comparison between time and space correlations indicates the validity of Taylor's hypothesis, $d = \bar{U}\tau$, for separation distances up to 100 feet.

4. A more stringent interpretation of Taylor's hypothesis — assuming equivalence of the time histories measured at the two stations along the mean wind — is not valid.

ACKNOWLEDGEMENTS

The author wishes to express his appreciation to everyone who has contributed to this study. The research was supported by his employer, the National Aeronautics and Space Administration. Gratitude is expressed to his supervisors in the Aeroelasticity Branch, Dynamic Loads Division, for making available time and support for this work.

The advice and counsel of Dr. J. B. Jones has been of special value in the preparation of this thesis. The author wishes to thank his colleagues in the Aeroelasticity Branch, particularly Jerome T. Foughner, Jr., and Robert M. Bennett, for their helpful suggestions.

Appreciation is expressed to Carol Jackson and Rossalyn Hampton for their care in typing the draft and final version of the manuscript.

REFERENCES

1. Foughner, J. T., Jr., and R. L. Duncan: A Full-Scale Ground Wind Loads Research Program. Presented at the Meeting on Ground Wind Load Problems in Relation to Launch Vehicles, Langley Research Center, Hampton, Virginia, June 7-8, 1966.
2. Taylor, G. I.: Diffusion by Continuous Movements. Proceedings of the London Mathematical Society, Ser. 2, 20, 196, 1921.
3. Taylor, G. I.: Statistical Theory of Turbulence. Proceedings of the Royal Society, A, 151, 421, 1935.
4. Taylor, G. I.: The Spectrum of Turbulence. Proceedings of the Royal Society, A, 164, 476, 1938.
5. Favre, A., J. Gaviglio and R. Dumas: Further Space-Time Correlations of Velocity in a Turbulent Boundary Layer. Journal of Fluid Mechanics, 3, 344, 1958.
6. Giblett, M. A., et al.: The Structure of Wind Over Level Country. Meteorological Office Geophysical Memoirs Number 54, 1932.
7. Lappe, U. O., B. Davidson and C. B. Notess: Analysis of Atmospheric Turbulence Spectra Obtained from Concurrent Airplane and Tower Measurements. Institute of the Aeronautical Sciences, Report Number 59-44, 1959.
8. Panofsky, H. A., H. E. Cramer and V. R. K. Rao: The Relation Between Eulerian Time and Space Spectra. Quarterly Journal of the Royal Meteorological Society, 84, no. 361, 270, 1958.

9. Laferty, J. D. and W. F. Hicks: An Investigation of the Aerodynamic Response of a Wind Anemometer. Thesis, United States Naval Postgraduate School, Monterey, California, 1967.

10. Duncan, R. L. and J. T. Foughner, Jr.: Wind Measurements Using a Vertical Array of Fast Response Anemometers. Presented at the Meeting on Ground Wind Load Problems in Relation to Launch Vehicles, Langley Research Center, Hampton, Virginia, June 7-8, 1966.

11. Duncan, R. L.: Measured Correlation of Turbulence in Ground Winds with an Indicated Application. Presented at the Meeting on Aircraft Response to Turbulence, Langley Research Center, Hampton, Virginia, September 24-25, 1968.

12. Sutton, O. G.: Micrometeorology. McGraw-Hill Book Company, Inc., New York, 1953.

13. Panofsky, H. A., A. K. Blackadar and G. E. McVehil: The Diabatic Wind Profile. Quarterly Journal of the Royal Meteorological Society, 86, 1960.

14. Singer, I. A. and C. M. Nagle: A Study of the Wind Profile in the Lowest 400 Feet of the Atmosphere. Brookhaven National Laboratory, Upton, N. Y., BNL 718(T-254), 1962.

15. Knudsen, J. G. and D. L. Katz: Fluid Dynamics and Heat Transfer. McGraw-Hill Book Company, Inc., New York, 1958.

16. Hinze, J. O.: Turbulence. McGraw-Hill Book Company, Inc., New York, 1959.

17. Lumley, J. L. and H. A. Panofsky: The Structure of Atmospheric Turbulence. John Wiley and Sons, New York, 1964.

18. Pasquill, F.: Atmospheric Diffusion. D. Van Nostrand Company, London, 1962.

19. Batchelor, G. K.: The Theory of Homogeneous Turbulence. The University Press, Cambridge, England, 1956.

20. Houbolt, J. C., R. Steiner and K. G. Pratt: Dynamic Response of Airplanes to Atmospheric Turbulence Including Flight Data on Input and Response. NASA TR R-199, 1964.

21. Clauser, F. H.: Advances in Applied Mechanics, Vol. 4, 1, 1956.

22. Davenport, A. G.: Dependence of Wind Loading on Meteorological Parameters. International Symposium on Wind Effects on Buildings and Structures, Ottawa, Sept. 1967.

VITA

The author was born [redacted] in [redacted]. He received his elementary education in Covington and graduated from Handley High School in Winchester, Virginia. He attended Virginia Polytechnic Institute and received a B. S. degree in mechanical engineering in 1963. He is a member of Tau Beta Pi, Pi Tau Sigma, Phi Kappa Phi, and Omicron Delta Kappa.

In 1963 the author was employed by the National Aeronautics and Space Administration at the Langley Research Center in Hampton, Virginia. He spent the winter and spring quarters of 1965 at V.P.I. completing the course requirements for a M. S. degree in mechanical engineering.

He is married to the former Sandra Smith of Covington, Virginia, and they have one daughter, Karen.

APPENDIX

DRAG SPHERE CALIBRATION FOR FIELD OPERATION

The following steps are followed for each strain gage on the two-component balance to determine the gage sensitivity for use of the drag sphere instrument.

1. Static calibration:

Statically load the balance with incremental weights and record output voltage of obtained static calibration curve.

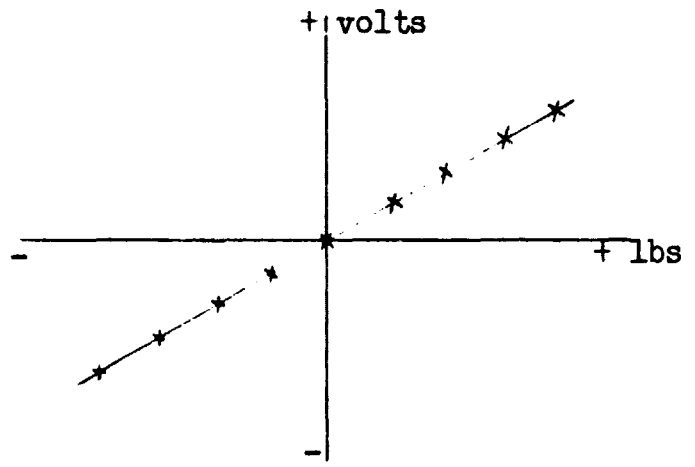

The curve should be linear with a slope, A_1. A_1 has units of lb/volt.

2. Dynamic calibration:

Place the instrument in a wind tunnel and record output voltages for various values of tunnel dynamic pressure. Multiply output voltages by A_1 to obtain the measured force in pounds and plot this force against the tunnel dynamic pressure.

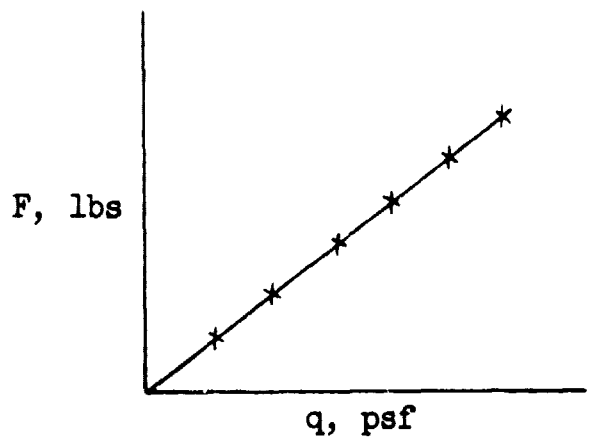

This plot should also be linear with a slope, A_2. (The linearity of this curve indicates a constant drag coefficient, C_D, in the Reynolds number range of calibration.)

$$F = (C_D)(\text{drag area})(q)$$

$$\text{drag area} = \text{constant}$$

The product A_1A_2 gives another constant, A_3, with units of psf/volt.

3. Calibrate resistor:

With a known resistance, R_1, in the circuit and no external load on the gage, the output voltage, V_1, should be recorded:

$$V_1(\text{volts}) \times A_3(\text{psf/volt}) = q_1(\text{psf})$$

R_1 is equivalent to a dynamic pressure of q_1.

4. Field operation:

With the drag sphere in place for field use and no wind on the instrument, insert the calibrate resistor, R_1, in line and record the voltage output, V_F. Since R_1 is equivalent to q_1, it follows that the sensitivity of the recordings will be

$$A_4 = q_1/V_F, \text{ psf/volt}$$

R_1 is then removed from the circuit and the instrument is ready for field operation.